

AD-A073 920

NORTH TEXAS STATE UNIV DENTON DEPT OF PHYSICS
OPTICALLY INDUCED HOT ELECTRON EFFECTS IN SEMICONDUCTORS. (U)
JUN 78 A L SMIRL

F/G 20/12

N00014-76-C-1077

UNCLASSIFIED

1 OF 3
AD
A073920



AD
A073920



ADA073920

LEVEL *III*

(12)

Summary Report

***—Optically Induced Hot Electron
Effects in Semiconductors***



prepared by
Arthur L. Smirl
Department of Physics
North Texas State University
Denton, TX 76203

This document has been approved
for public release and sale; its
distribution is unlimited.

Prepared for the Office of Naval Research
Electronic and Solid State Sciences Program
Under Contract NR 318-048

ENC FILE COPY

79 09 17 004

REPORT DOCUMENTATION PAGE		READ INSTRUCTIONS BEFORE COMPLETING FORM
1. REPORT NUMBER	2. GOVT ACCESSION NO.	3. RECIPIENT'S CATALOG NUMBER
4. TITLE (and Subtitle) Optically Induced Hot Electron Effects in Semiconductors. <i>8060310</i>		5. TYPE OF REPORT & PERIOD COVERED <i>Summary rept.</i> 1 Sept 1978 - 31 Aug. 1979
7. AUTHOR(s) Arthur L. Smirl <i>10</i>		6. PERFORMING ORG. REPORT NUMBER
9. PERFORMING ORGANIZATION NAME AND ADDRESS Department of Physics North Texas State University Denton, Texas 76203		8. CONTRACT OR GRANT NUMBER(s) N00014-76-C-1077 <i>15</i>
11. CONTROLLING OFFICE NAME AND ADDRESS ONR, Electronic and Solid State Sciences Program Office of Naval Research Arlington, VA 22217 <i>11</i>		10. PROGRAM ELEMENT, PROJECT, TASK AREA & WORK UNIT NUMBERS <i>12 174 P.</i>
14. MONITORING AGENCY NAME & ADDRESS (if different from Controlling Office) ONR Resident Representative 528 Federal Building 300 East 8th Street Austin, TX 78701		12. REPORT DATE June 1978 1978
16. DISTRIBUTION STATEMENT (of this Report) <div style="border: 1px solid black; padding: 5px; display: inline-block;">This document has been approved for public release and sale; its distribution is unlimited.</div>		13. NUMBER OF PAGES
17. DISTRIBUTION STATEMENT (of the abstract entered in Block 20, if different from Report) Approved for public release; distribution unlimited		15. SECURITY CLASS. (of this report) Unclassified
18. SUPPLEMENTARY NOTES		15a. DECLASSIFICATION/DOWNGRADING SCHEDULE
19. KEY WORDS (Continue on reverse side if necessary and identify by block number) Photoexcited Carriers Germanium Ultrafast Phenomena		
20. ABSTRACT (Continue on reverse side if necessary and identify by block number) We report here , our progress in using the high electric fields and ultra-short pulses from mode-locked lasers to study the temporal evolution of the saturable optical properties of semiconductors on a picosecond time scale. In these studies, the excite and probe technique is employed to obtain information concerning the ultrafast dynamics of photogenerated electron-hole plasmas. Germanium has been chosen for the initial investigations since its bandgap energy is comparable to but less than the photon energy of the Nd: glass laser.		

DDC
RECEIVED
SEP 19 1979
REGISTERED
C

409923

FOREWARD

This Summary Report by Arthur L. Smirl, Department of Physics, North Texas State University, Denton, Texas, covers research progress for the period 1 September 1978 to 31 August 1979, under Office of Naval Research Contract NR 318-048.

The use of trade names in this report does not constitute an official endorsement or approval of the use of such hardware or software. This report may not be cited for purposes of advertisement, and its publication does not constitute Navy approval of findings or conclusions.

Arthur L. Smirl

Arthur L. Smirl
Principal Investigator

Accession For	
ASIS	<input checked="checked" type="checkbox"/>
DDO TAB	
Unannounced	
Justification	
By _____	
Distribution/	
Availability Codes	
Dist	Avail and/or special
A	

TABLE OF CONTENTS

	Page
Summary.	iii
I. Introduction and Review	1
II. Record of Activities	14
A. Free-Carrier, Intervalence-Band, and Indirect Absorption and Auger Recombination	16
B. Parametric Scattering or State-Filling	24
C. Measurement of Carrier Recombination Times and Diffusion at High Carrier Densities.	31
D. NATO Lecture and Seminar	33
E. Summary of Activity.	33
III. Professional Publications and Activities	35
IV. Vita	38
V. References	44
Appendix A: Picosecond Optical Measurement of Free- Carrier, Intervalence-Band, and Indirect Absorption in Germanium at High Optically Created Carrier Densities	45
Appendix B: The Effects of Parametric Scattering, and Energy-Gap Narrowing, and State Filling on the Optical Response of Germanium	56
Appendix C: The Physics of Nonlinear Absorption and Ultra- fast Carrier Relaxation in Semiconductors	82
Appendix D: High Intensity Picosecond Photoexcitation of Semiconductors	136

SUMMARY

Here, we report on our progress in understanding the ultrafast kinetics of high-density, hot electron-hole plasmas generated in semiconductors by intense picosecond pulses from mode-locked lasers. This report covers the contract period 1 September 1978 to 31 August 1979. Previous contract periods (1 September 1976 to 30 August 1978) are covered in detail in previous annual summary reports.

Intense ultrashort optical pulses having durations of a few picoseconds and peak powers of 10^8 watts can be readily generated by mode-locking Nd-glass lasers. The extremely high power and short duration of pulses from these lasers make possible the study of the saturable optical transmission properties and hot electron dynamics of semiconductors on a picosecond time scale. Generally, we have employed the excite and probe technique in these studies. The studies have provided direct information, concerning ultrafast electronic processes.

Specifically, in the studies of interest here, the sample is first irradiated by an 11 psec excite pulse at $1.06 \mu\text{m}$. The absorption of the excite pulse creates a large, rapidly evolving, nonequilibrium carrier distribution that changes the transmission properties of the sample. This initial pulse is then followed at various time delays by a weak probe pulse of the same wavelength that monitors the evolution of the enhanced germanium transmission with time. A graph of the probe pulse transmission versus time exhibits two distinct features. The first is a rapid rise and fall in the probe transmission. This narrow spike in probe transmission is approximately two picoseconds wide and is centered about zero delay. This spike is followed by a gradual rise and fall of the probe transmission lasting hundreds of picoseconds.

At the beginning of this contract period there were at least two possible explanations for the narrow spike in probe transmission and three explanations for the slower rise and fall in probe transmission lasting hundreds of picoseconds. The narrow spike in probe transmission centered about zero delay had been attributed (1) to a parametric scattering of the excite beam into the probe beam path by a grating formed in the germanium by the interference of the two pulses near zero delay and (2) to state-filling and band-gap narrowing. The slow rise in probe transmission had been attributed (1) to band-filling, (2) to a cooling of a hot carrier distribution created by direct absorption of the excite pulse, or (3) to Auger recombination combined with an absorption versus carrier density relationship containing a minimum. In our last renewal proposal, we suggested experiments designed to determine the origins of the narrow spike and the broad structure in probe transmission.

In this report, we summarize the results of these separate studies that (1) demonstrate that the slow rise in probe transmission at 100 K is not an integration effect caused by band-filling, (2) indicate that this slow rise is not caused by carrier recombination combined with an absorption vs. density curve containing a minimum, (3) provide evidence that the narrow spike at zero delay is a correlation effect, and (4) use laser-induced grating techniques to separate and measure the effects of carrier diffusion and carrier recombination at high carrier densities.

I. INTRODUCTION AND REVIEW

In the past half decade, studies of the optical properties of high-density electron-hole plasmas generated in undoped semiconductors by the direct absorption of intense, ultrashort pulses from mode-locked lasers have provided direct information concerning ultrafast electronic processes.¹⁻¹⁸ Generally, early experimental studies in this area employed mode-locked pulses from a Nd-glass laser as an excitation source to generate the electron-hole plasma. This source produces optical pulses that are approximately 10 psec in duration and that often have peak powers in excess of 10^8 watts at a wavelength of $1.06 \mu\text{m}$. These pulses when focused on the surface of a thin semiconductor sample can produce a measured irradiance of 10^{-2} J/cm^2 . Direct absorption of such an optical pulse can create carrier densities of approximately 10^{20} cm^{-3} . Germanium was chosen as a candidate for study in many of these early investigations primarily because it is a readily-available, well-characterized semiconductor with a bandgap that is comparable to but less than the energy of a photon at a wavelength of $1.06 \mu\text{m}$ (1.17 eV).

Among these early studies, are the measurement of the enhanced transmission of single ultrashort optical pulses through germanium^{1,5} and the measurement of the temporal evolution of this enhanced transmission on a picosecond time scale using the excite and probe technique.^{1,3,5} In the first of these experiments, the nonlinear transmission of a single picosecond $1.06 \mu\text{m}$ pulse is measured as a function of incident optical pulse

energy, as shown in Fig. 1. Notice that our excite pulse can be made energetic enough to alter the optical properties of the germanium. In the second study, the sample is first irradiated by an 11 psec excite pulse at $1.06 \mu\text{m}$. The absorption of the excite pulse creates a large, rapidly evolving, nonequilibrium carrier density that changes the transmission properties of the sample. This initial pulse is then followed at various time delays by a weak probe pulse of the same wavelength that monitors the evolution of the enhanced germanium transmission with time. A graph of the probe pulse transmission versus time (Fig. 2) exhibits two distinct features. The first is a rapid rise and fall in probe transmission. This narrow spike in probe transmission is approximately two picoseconds wide and is centered about zero delay. This spike is followed by a gradual rise and fall of the probe transmission lasting hundreds of picoseconds.

The narrow spike in probe transmission was first observed by Kennedy *et al.*¹ and was attributed by them to a saturation and relaxation of the direct absorption. Subsequently, Shank and Auston³ observed, in addition to the narrow spike near zero delay, the slower structure at longer delays. In light of this additional structure, they reinterpreted the narrow spike in probe transmission near zero delay as a parametric coupling between excite and probe beams caused by an index grating produced by the interference of the two beams in the germanium sample. While recognizing that some parametric scattering is bound to occur during such measurements, Ferry¹⁵ has recently presented numerical studies that account for the spike in germanium transmission in terms of

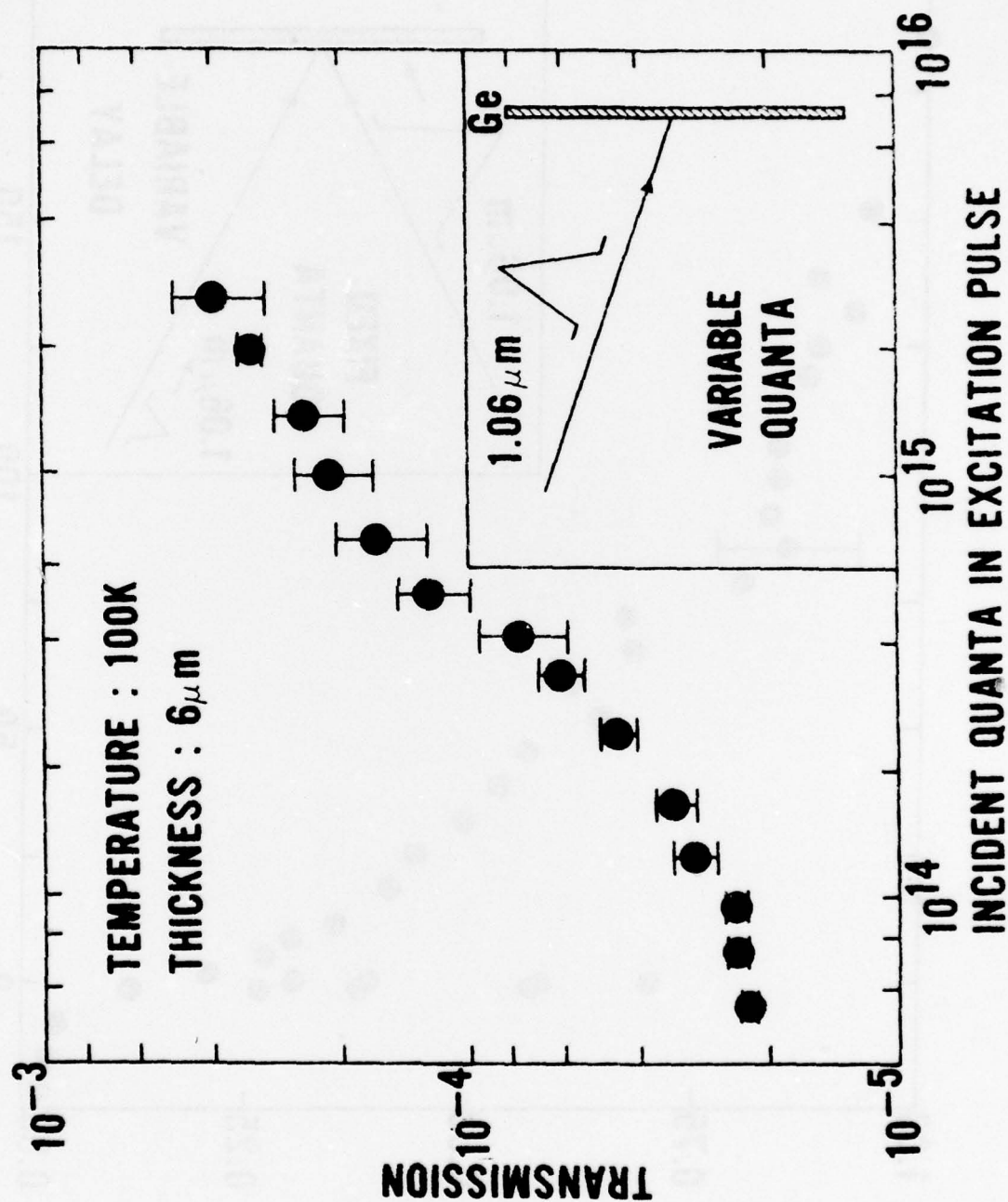


Figure 1. Change in transmission of a 6 μm -thick germanium sample as a function of incident excite pulse energy at 1.06 μm . Note a pulse energy of 2×10^{15} quanta corresponds to a surface irradiance of approximately 10^{-2} J/cm².

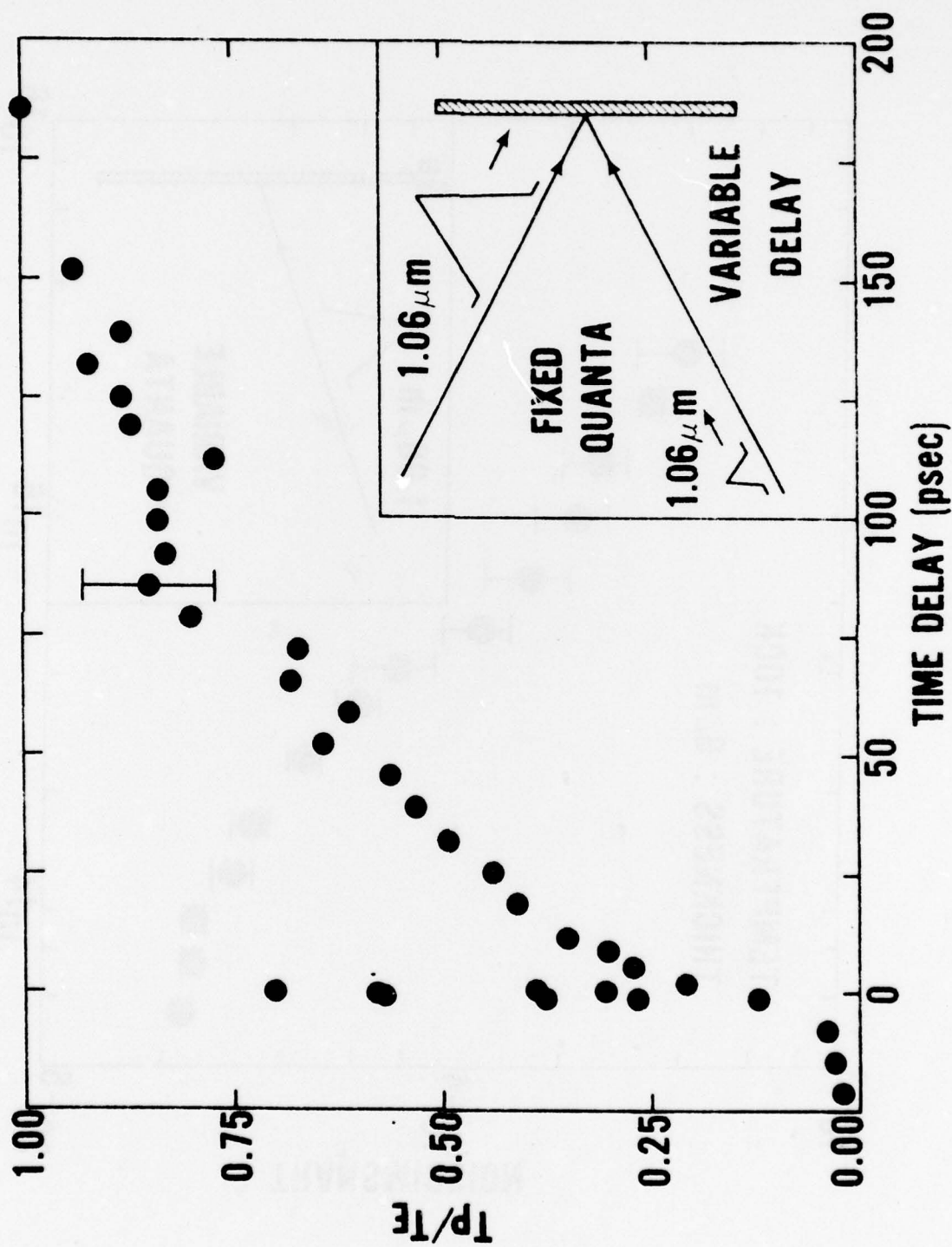


Figure 2. Probe pulse transmission vs delay between the excite pulse at $1.06 \mu\text{m}$ and the probe pulse at $1.06 \mu\text{m}$ for a sample temperature of 100 K. The data are plotted as the normalized ratio of probe pulse transmission to excite pulse transmission, T_p/T_e , in arbitrary units. The error bar represents one typical statistical standard deviation.

state filling and band-gap narrowing. If, indeed, these processes are responsible for the narrow rise and fall in probe transmission, a careful study of this structure should yield information concerning carrier scattering rates from the optically-coupled states.

The slow rise in probe transmission with delay, as depicted in Fig. 2, was first observed by Shank and Auston.³ They attributed this slower structure in probe transmission to band-filling. That is, they attributed this rise to a saturation of the direct absorption caused by a filling of the conduction (valence) band states by optically-created electrons (holes) up to and including the optically-coupled states needed for absorption. As a result, the buildup of this effect should be proportional to the total number of carriers created, i.e. it should follow the integrated optical pulse energy. Notice that this interpretation does not involve hot electron effects. According to this interpretation, the rise in probe transmission contains little semiconductor physics. It is merely an artifact of the measurement technique: the integral of the intensity correlation function. These conclusions were based on observations performed only at room temperature.

Later, Smirl *et al.*⁵ independently extended the 1.06 μm excite and probe measurements of Kennedy *et al.*¹ to include probe structure at longer delays. In addition, they determined the dependence of the excite and probe measurements on sample temperature and excite pulse energy levels. Specifically, the nonlinear transmission was measured as a function of incident optical pulse energy at sample temperatures of 100 K and 297 K (Fig. 3). In addition, the normalized transmission of the probe pulse as a function of time delay after an excite pulse was measured for the

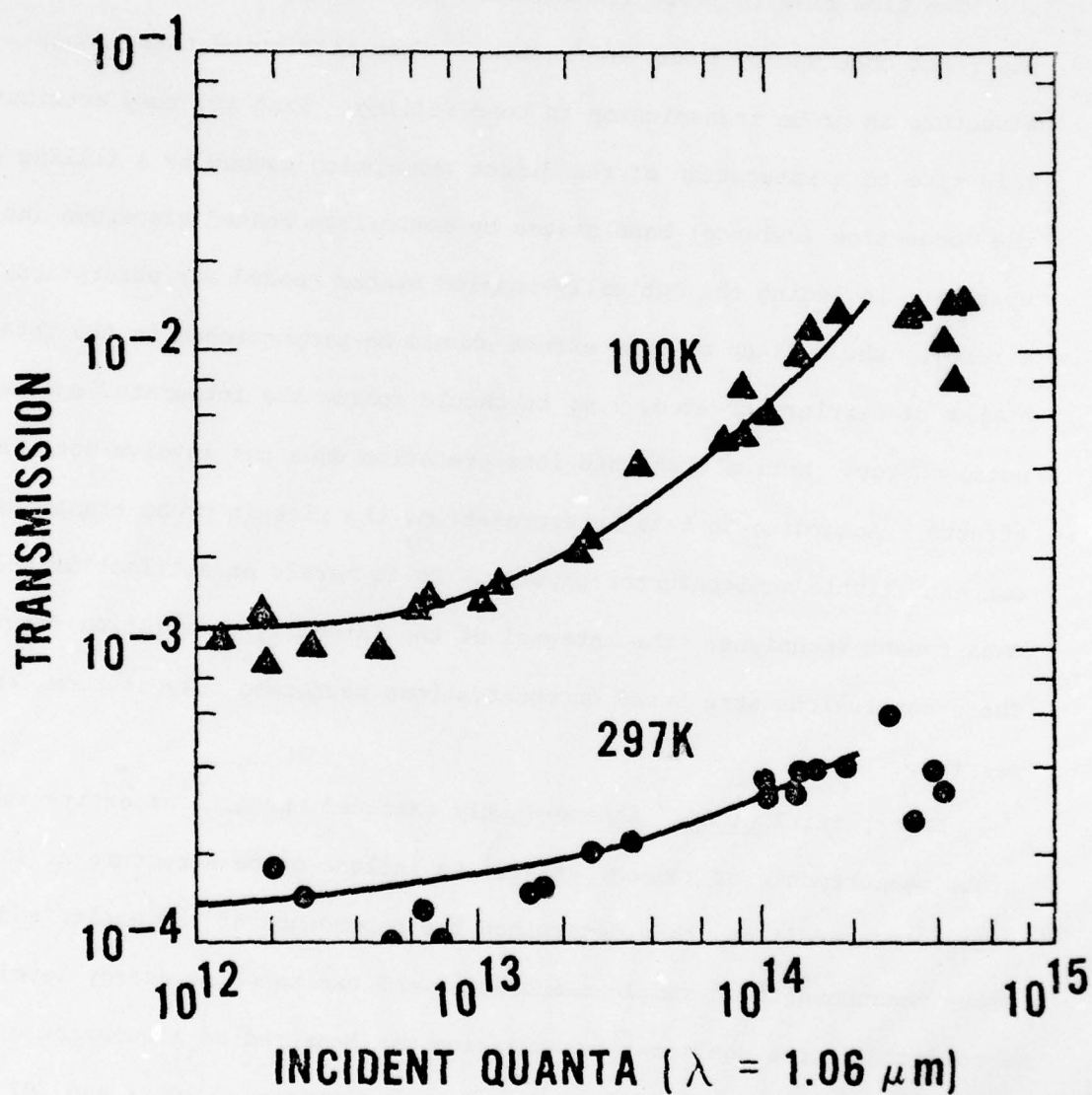


Figure 3. Transmission of a 5.2- μm -thick germanium sample as a function of incident quanta at 1.06 μm for sample temperatures of 100 K and, 297 K. The solid lines are theoretical curves from Elci *et al.* The data are from Smirl *et al.*⁵

same two temperatures (Fig. 4) and for three different excite pulse energy levels (not shown). The temperature dependence of the probe transmission measurements contained surprising new information: the rise in probe transmission at 100 K was too slow (~ 100 psec) to be attributed to an integration effect (i.e. it did not appear to follow the integrated optical energy of the excite pulse). The authors suggested that this slow rise in probe transmission might be attributed to a cooling of the energetic electrons (holes) created in the conduction (valence) band by the direct absorption of the excite pulse. Thus, the rise in probe transmission was taken to be an indication of the carrier relaxation time.

At this point, Elci et al.⁷ presented the first detailed theoretical treatment of these problems. Their model (hereafter referred to as the ESSM model) attempts to account for the nonlinear transmission and the excite and probe response of germanium in terms of: (1) direct band-to-band absorption, (2) free-carrier absorption, (3) long wavevector phonon-assisted intervalley carrier scattering, (4) phonon-assisted carrier relaxation, (5) carrier-carrier Coulomb collisions, and (6) plasmon-assisted recombination. In short, the authors attributed the rise in the probe transmission with the delay after an intense excite pulse to a cooling of the hot electron-hole plasma created by the absorption of the excite pulse. The results of these calculations are presented as solid lines in Fig. 3 and Fig. 4; the theoretical fit to the nonlinear transmission data and the probe transmission data can be regarded as satisfactory, given the complexity of the problem. Subsequently, van Driel et al.⁸ conducted further nonlinear transmission studies, in which the energy band gap of the germanium sample was tuned by hydrostatic pressure, that seemed to corroborate the proposed model.

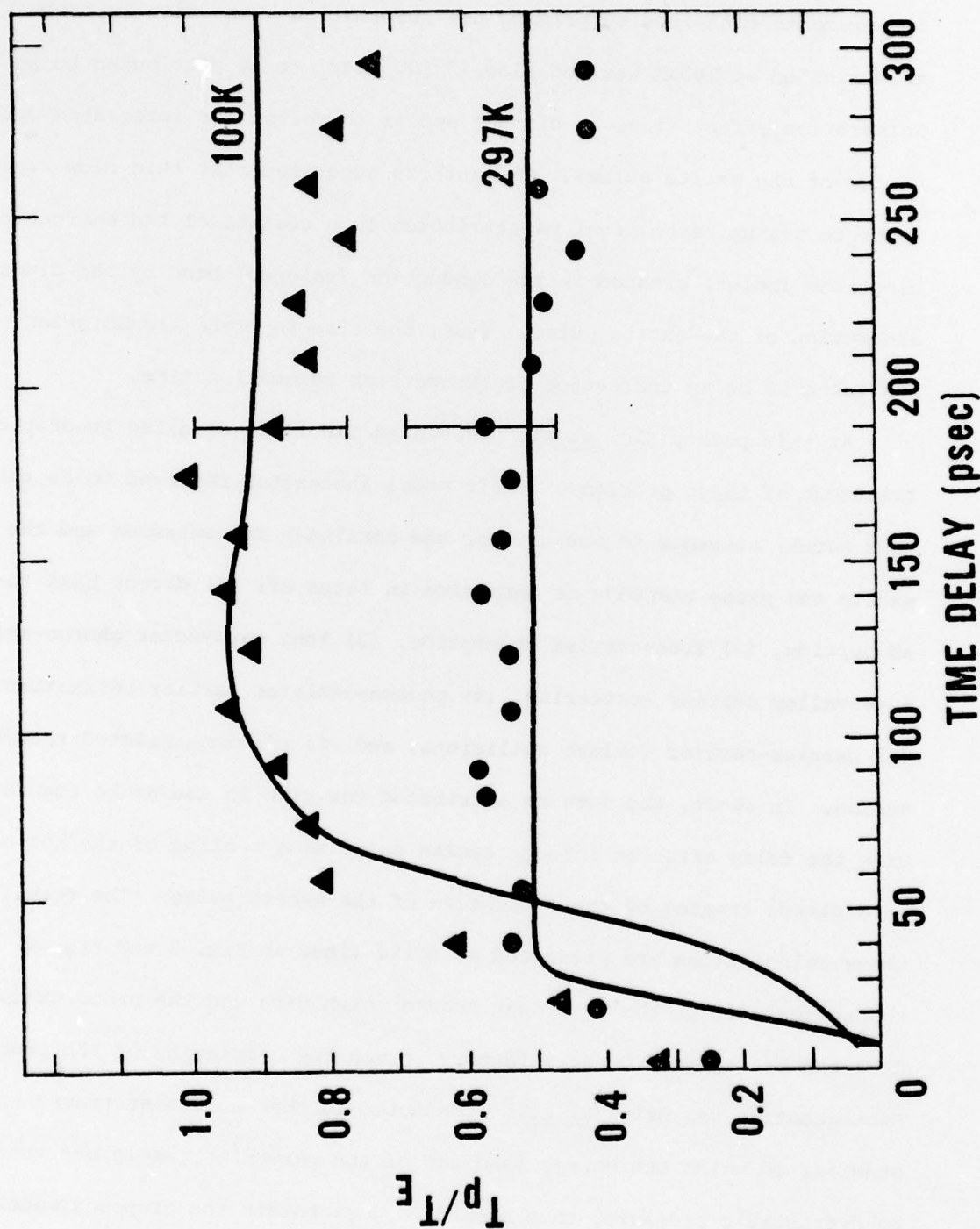


Figure 4. Probe pulse transmission versus delay between the excite pulse at 1.06 μm and the probe pulse at 1.06 μm for sample temperatures of 100 and 297 K. The data are plotted as the normalized ratio of probe pulse transmission to excite pulse transmission, T_p/T_e , in arbitrary units. The solid lines are theoretical curves from Elci et al.⁷ The experimental data are from Smirl et al.⁵

Despite the apparent successes of this model, some basic questions remain concerning the roles of the various physical processes in determining the saturation and temporal evolution of the optical transmission of thin germanium samples under intense optical excitations. Elci *et al.*⁷ noted that their calculations contained serious assumptions that warranted further theoretical and experimental investigation. The major assumptions were the following: (i) The carrier-carrier collision rate was assumed to be high enough to justify taking the carrier distributions to be Fermi-Dirac. Ferry¹⁵ has recently re-examined this approximation by calculating the time and energy dependence of the distribution function at the high carrier photogeneration rates encountered here. He concludes that on a time scale of tens of picoseconds the distribution function does indeed approximate a Fermi distribution; however, on shorter time scales it contains a δ -function-like spike located at the optically coupled states. Thus, for purposes of calculating the probe-pulse transmission, one may reasonably assume the distribution is Fermi-like. (ii) Carrier Fermi energies and temperatures were taken to depend only on time, rather than on both space and time, thus ignoring the pulse-propagation and carrier-diffusion problems within the optical interaction region of the sample. Therefore, parameters describing the electron-hole plasma, such as the electron number, must be viewed as spatial averages throughout the sample volume.

Elci *et al.*⁷ also noted at the outset that their work contained only a few of the many possible electronic interactions. Recent studies^{4,12,15} indicate that processes other than those named above may be important. Most of these effects, such as bandgap narrowing,¹⁵ intervalence-band absorption,¹⁴ Auger recombination⁴ and Coulomb-assisted indirect absorption,¹²

are only observed at large carrier densities. The possible importance of including these processes in any interpretation of the rise in probe transmission is demonstrated in the following section.

In the previous two paragraphs, we have outlined the assumptions and omissions of the initial ESSM model; however, there is another problem associated with the original calculations that is of importance to the present work. The physical constants for germanium, specifically the electron-phonon coupling constants, are not well-known enough to allow a precise calculation of the energy relaxation rate. Latham *et al.*¹⁰ have previously discussed this point in detail. For the theoretical fits shown in Fig. 4, the electron-phonon coupling constants are chosen as 6×10^{-4} erg cm⁻¹ for a lattice temperature of 297 K and 2×10^{-4} erg cm⁻¹ at 100 K. These values are within the range of the accepted theoretically and experimentally determined values listed by Latham *et al.*¹⁰; however, they are much lower than the mean value of 1×10^{-3} erg cm⁻¹ as obtained from an average of the eight values listed. Since the carrier cooling rate is proportional to the square of the electron-phonon coupling constant, the fitted values result in carrier cooling rates that are 3 and 25 times slower than that obtained by using the average value. In fact, a repetition of the original calculations substituting the average electron-phonon coupling constant shows (see Latham *et al.*¹⁰, Fig. 8) that carrier cooling is too rapid to account for the rise in probe transmission.

At this point, perhaps we should pause to summarize the state of our understanding of the origin of the slow rise in probe transmission observed in the early excite and probe studies as discussed in the previous few paragraphs and displayed in Fig. 4. Originally, Shank and Auston³, attributed this rise in probe transmission to a saturation of the direct

absorption as a result of band filling. We remind the reader, again, that this interpretation was based on measurements performed only at room temperature. Subsequently, Elci et al.⁷ attributed this rise in probe transmission to a cooling of a hot electron-hole plasma created by direct absorption of the excite pulse. Although the original calculations by Elci et al.⁷ are sound, time has shown that the proposed model (ESSM model) has several objectionable features as detailed in the last three paragraphs: (1) uncertainties in the optical phonon-electron coupling constant, (2) neglect of the spatially inhomogeneous nature of the parameters that characterize the carrier distributions, and (3) the omission of important processes such as diffusion and Auger recombination from the model. The authors realized and stated at the outset that their model contained serious assumptions and approximations that warranted further study and that the model contained only a few of the many possible processes. It was hoped, however, that the model would serve as a basis for further study and development.

In sharp contrast to the interpretation by Elci et al.⁷, Auston et al.¹² have stated that they expect the energy relaxation time in germanium to be too short to account for the rise in probe transmission shown in Fig. 4. This suggestion is, of course, consistent with the more detailed numerical studies presented by Latham et al.¹⁰, as discussed above. More importantly, in the spirit of suggesting plausible alternative models for evaluation, Auston et al.¹² stated that enhanced intervalence-band and Coulomb-assisted indirect absorption effects might be important at the high photogenerated carrier densities encountered in these excite and probe experiments. Furthermore, they suggested that these processes might introduce

a minimum in the absorption versus carrier density curve in germanium in the following way: The direct absorption coefficient will remain approximately constant as a function of photogenerated carrier density until the density reaches the point where the electrons (holes) clog the states needed for direct electronic transitions in the conduction (valence) band. At this point, the direct absorption coefficient rapidly decreases. On the other hand, Coulomb-assisted indirect, intervalence-band, and free-carrier absorption coefficients monotonically increase with carrier density. Thus, the absorption coefficient could initially decrease with increasing density, as the direct absorption coefficient saturates, then increase with increasing density as the free-carrier, intervalence-band and indirect absorption coefficients become large enough to dominate. In a private communication, S. McAfee and D. H. Auston further explained how an absorption curve containing a minimum could be combined with Auger recombination to account for the rise in probe transmission of Fig. 4. Briefly, the absorption of the excite pulse creates an initial carrier density greater than n_{\min}' where n_{\min} denotes the density at which the minimum total absorption coefficient occurs. As the initial photogenerated carrier density is decreased in time by Auger recombination, the absorption coefficient of the germanium will decrease in time until the carrier density reaches n_{\min}' , then increase. Thus, the probe transmission will increase then decrease, if the initial optically-created carrier density is greater than n_{\min}' . In direct contrast to the ESSM model, this interpretation does not require hot electron effects. This model does, however, require a minimum in the absorption versus carrier density curve.

Consequently, we summarize and emphasize that there were at the beginning of this contract period at least two possible explanations for the narrow spike in probe transmission and three explanations for the slower rise and fall in probe transmission lasting hundreds of picoseconds (see Fig. 2). The narrow spike in probe transmission centered about zero delay had been attributed (1) by Shank and Auston³ to a parametric scattering of the excite beam into the probe beam path by a grating formed in the germanium by the interference of the two pulses near zero delay and (2) by Ferry¹⁵ to state-filling and band-gap narrowing. The slow rise in probe transmission had been attributed (1) to band-filling, (2) to a cooling of a hot carrier distribution created by direct absorption of the excite pulse, or (3) to Auger recombination combined with an absorption versus carrier density relationship containing a minimum. In our last renewal proposal, we suggested experiments designed to determine the origins of the narrow spike and broad structure in probe transmission. In Sec. II, we give a record of our achievements and progress during this contract period in achieving these goals. Next, we provide a list of professional publications and activities (Sec. III) during the past year, and in Sec. IV, we provide the reader with an updated vita. Finally, in Appendices A, B, C, and D, we provide reprints and preprints of our work from 1 September 1978 to the present. Reprints for the contract years 1 September 1976 to 1 September 1977 and 1 September 1977 to 1 September 1978 are contained in previous summary reports.

For a more detailed review of the above areas, the reader is referred to Appendix D.

II. RECORD OF ACTIVITIES

To appreciate our work during this period, the reader must understand the state of our knowledge concerning the picosecond excite and probe response of germanium in August 1978. A brief review of these studies is presented in the previous section. A more detailed, tutorial review is provided in Appendix C and Appendix D. Briefly, we now summarize the state of affairs. We had previously measured the enhanced transmission of single optical pulses at $1.06\text{ }\mu\text{m}$ through germanium as a function of incident pulse energy (Fig. 1), and we had measured the temporal evolution of this enhanced transmission on a picosecond time scale using the $1.06\text{-}\mu\text{m}$ -excite and $1.06\text{-}\mu\text{m}$ -probe technique (Fig. 2). The latter measurements reveal a sharp rise and fall in probe transmission center about zero delay and lasting approximately 2 psec. This spike is followed by a slower rise and fall in probe transmission lasting hundreds of picoseconds. Auston and Shank² had originally attributed the narrow spike in probe transmission to a parametric scattering of the excite beam into the probe beam. More recently, Ferry¹⁵ has suggested that this spike may be caused by state-filling combined with energy band-gap narrowing. Auston and Shank² also initially interpreted the slow rise in probe transmission as an excite-pulse integration effect caused by band-filling (not to be confused with state-filling). We (Smirl et al.⁵) later performed measurements (Fig. 3 and Fig. 4) that revealed that the probe transmission increases for approximately 100 psec following excitation for a sample temperature of 100 K; however, the rise in probe transmission is less than 40 psec at 300 K. As a result of the measurements at liquid nitrogen temperature, we had initially^{5,7} attributed the slower rise in probe transmission at 100 K to a cooling of a hot plasma created by absorption of the excite pulse. Thus, the rise in probe transmission

measures the energy relaxation rate and should be a sensitive measure of the electron-phonon coupling constants. The investigations that we reported and discussed previously (see Latham *et al.*¹⁰) had subsequently shown that uncertainties in the electron-phonon coupling constants cast doubt on this interpretation. In contrast, Auston *et al.*¹² had stated that they expected the energy relaxation rate to be too short to account for this rise in probe transmission. They had also suggested¹² that processes omitted from our model, specifically intervalence-band and Coulomb-assisted indirect absorption, might be important. Indeed, they suggested¹² that these processes might introduce a minimum in the absorption versus carrier density curve and, through a private communication, explained that this curve might be combined with Auger recombination to account for the rise in probe transmission. Thus, there were at least three possible explanations for the slow rise in probe transmission:

- (1) the rise, like the "correlation" spike, is an artifact of the experimental technique (an integration effect)
- (2) the rise is caused by a cooling of a dense "hot" carrier distribution
- (3) the rise is due to Auger recombination combined with a absorption vs. density curve containing a minimum, caused by intervalence-band and Coulomb-assisted indirect absorption.

And two possible explanations for the sharp spike in probe transmission:

- (1) the spike is a correlation effect (i.e. a parametric scattering of excite beam into the probe beam by a laser-induced grating).
- (2) the spike is a result of state-filling combined with band-gap narrowing.

In the remainder of this section, we summarize the results of three separate studies that (1) demonstrate that the slow rise in probe transmission at 100 K is not an integration effect caused by band-filling, (2) indicate that this slow rise is not caused by carrier recombination combined with an absorption vs. density curve containing a minimum, (3) provide evidence that the narrow spike at zero delay is a correlation effect, and (4) use laser-induced grating techniques to separate and measure the effects of carrier diffusion and carrier recombination at high carrier densities.

Free-Carrier, Intervalence-Band, and Indirect

Absorption and Auger Recombination

Here, we have attempted to test the first and third possibilities for the rise in probe transmission listed above and have attempted to ascertain the importance of free-carrier, intervalence-band, and indirect absorption effects in excite and probe experiments at 1.06 μm . The experimental configuration used in these studies is similar to that used by Auston et al.⁴ and is shown in Fig. 5. The excite pulses used here were approximately 10 psec in duration and had peak powers of approximately 10^8 W at a wavelength of 1.06 μm , and they produced a measured irradiance of approximately 10^{-2} J/cm² when focused on the crystal surface. The plasma produced by the absorption of the excite pulse was probed using weak pulses of two types: one at 1.06 μm had a photon energy greater than the direct band-gap energy for germanium, and the other at 1.55 μm had an energy less than the direct gap but greater than the indirect gap. The latter probe, at a wavelength of 1.55 μm , was generated by stimulated Raman scattering in benzene. We emphasize that the energy of a quanta at 1.06 (1.17 eV) is sufficient to excite direct band-to-band transitions in germanium as well as free-carrier, intervalence-band, and indirect transitions, whereas, the energy of a quanta

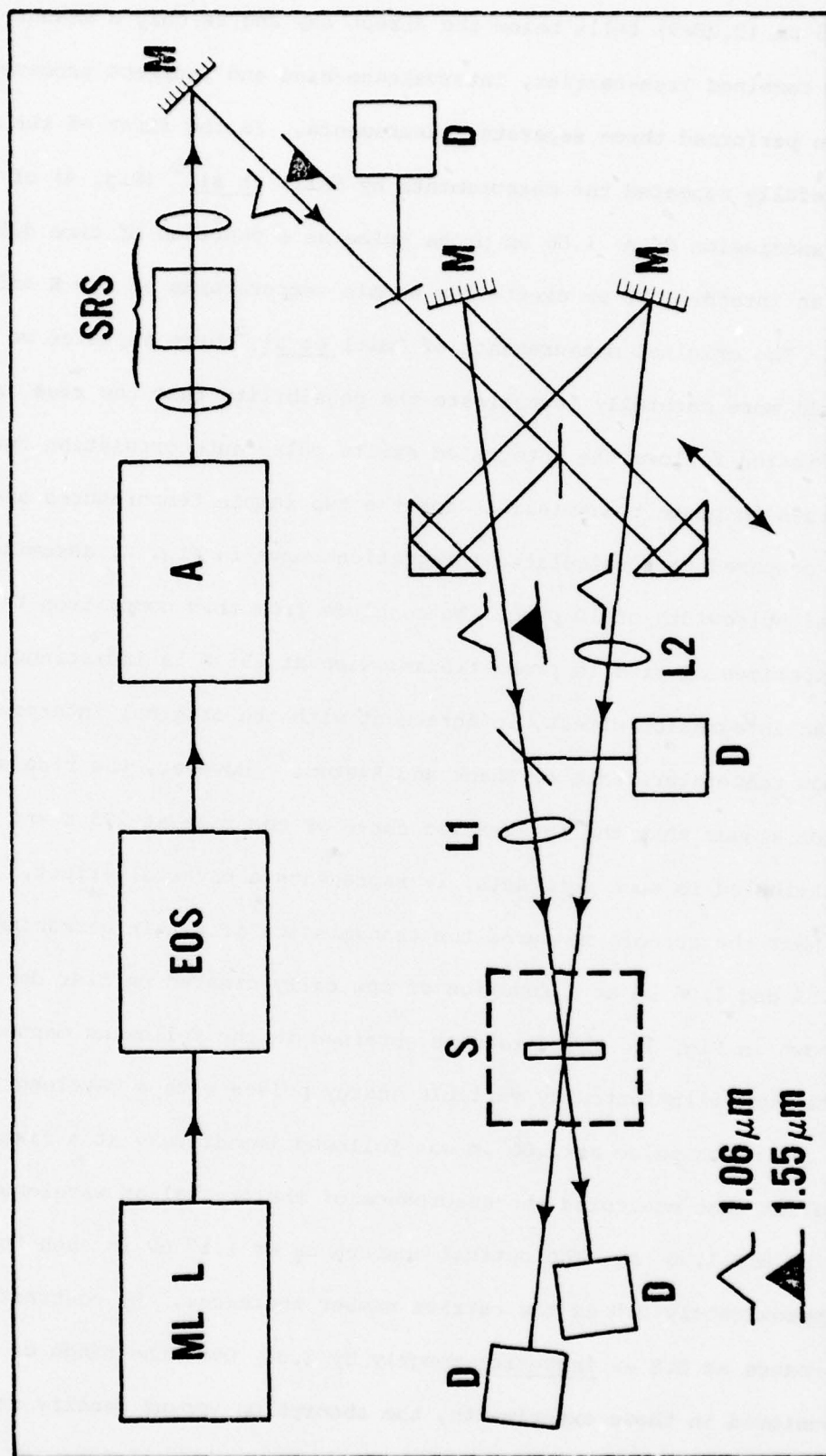


Figure 5. Block diagram of the experimental configuration for excite and probe measurements at 1.06 and 1.55 μm , where MLL denotes the mode-locked laser, EOS the electro-optical switch, A the laser amplifier, SRS the stimulated-Raman-scattering cell, M a mirror, D a detector, L1 and L2 lens, and S the sample (from Smirl et al.¹⁴).

at $1.55 \mu\text{m}$ (0.08eV) falls below the direct gap and is only a measure of the combined free-carrier, intervalence-band and indirect processes.

We performed three separate measurements. In the first of these, we carefully repeated the measurements by Smirl *et al.*⁵ (Fig. 4) of the transmission of a $1.06 \mu\text{m}$ probe pulse as a function of time delay after an intense $1.06 \mu\text{m}$ excite for sample temperatures of 100 K and 295 K. The original measurements of Smirl *et al.*⁵ were repeated so that we could more carefully investigate the possibility that the rise in probe transmission follows the integrated excite pulse autocorrelation function. The rises in probe transmissions for the two sample temperatures are carefully compared to a calculated integration curve in Fig. 6, assuming an optical pulsewidth of 10 psec. We conclude from this comparison that the experimental rise in probe transmission at 295 K is indistinguishable from an integration effect, in agreement with the original interpretation of room temperature data by Shank and Auston.³ However, the rise at 100 K is much slower than the integration curve or the rise at 295 K and cannot be attributed to such artifacts; it represents a physical effect.

Next the authors measured the transmission of a thin germanium sample at 1.55 and $1.06 \mu\text{m}$ as a function of optically-created carrier densities as shown in Fig. 7. The data were obtained in the following manner. The crystal was illuminated by variable energy pulses with a wavelength of $1.06 \mu\text{m}$. Each pulse at $1.06 \mu\text{m}$ was followed immediately at a fixed delay by pulses that monitored the absorbance of the crystal at wavelengths of $1.55 \mu\text{m}$ and $1.06 \mu\text{m}$. The optical absorbance at 1.17eV is seen to decrease by approximately 3.5 as the carrier number increases. By contrast the absorbance at 0.8eV increases roughly by 2.3. Over the range of densities encountered in these experiments, the absorption versus density relationship at 1.17eV does not exhibit a minimum. Thus, a temporal decay of the

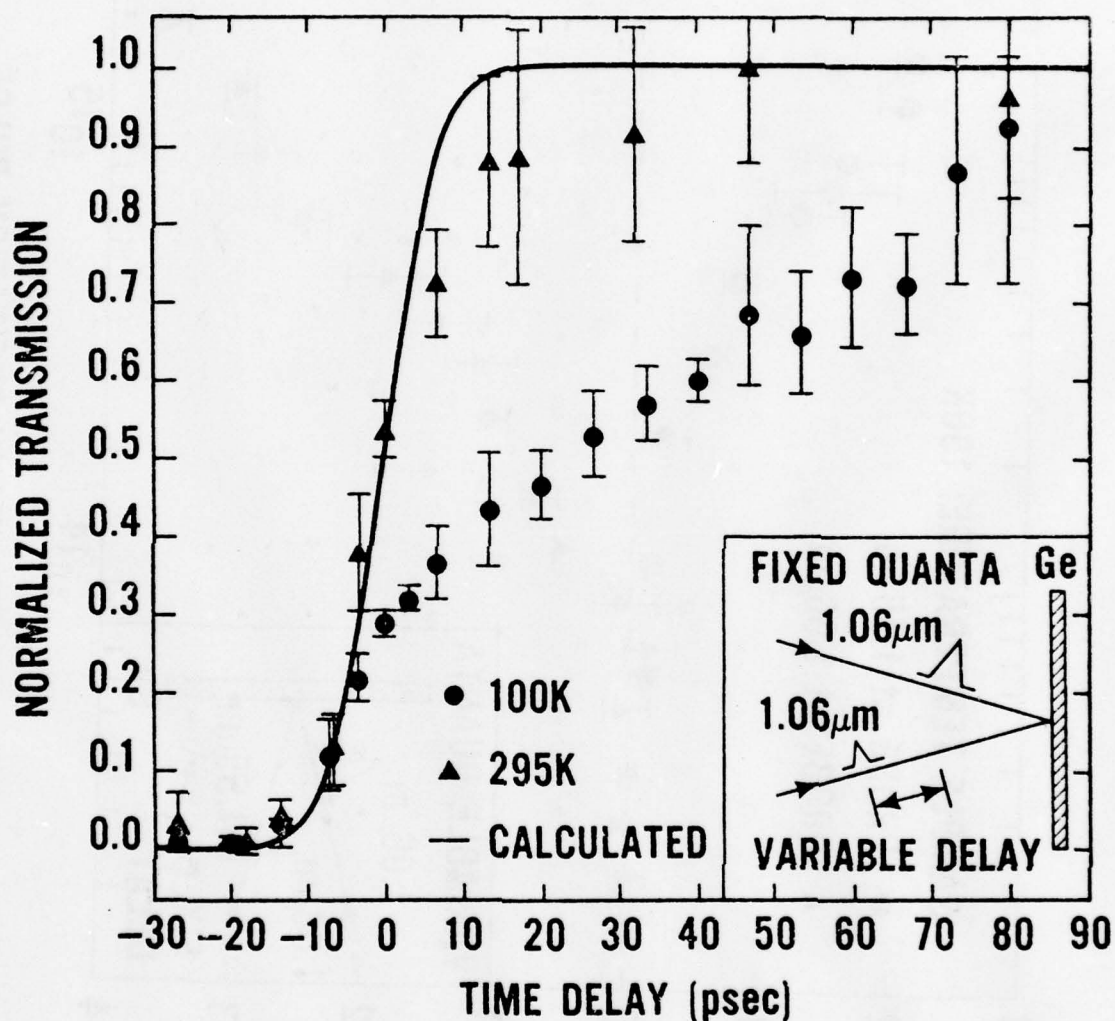
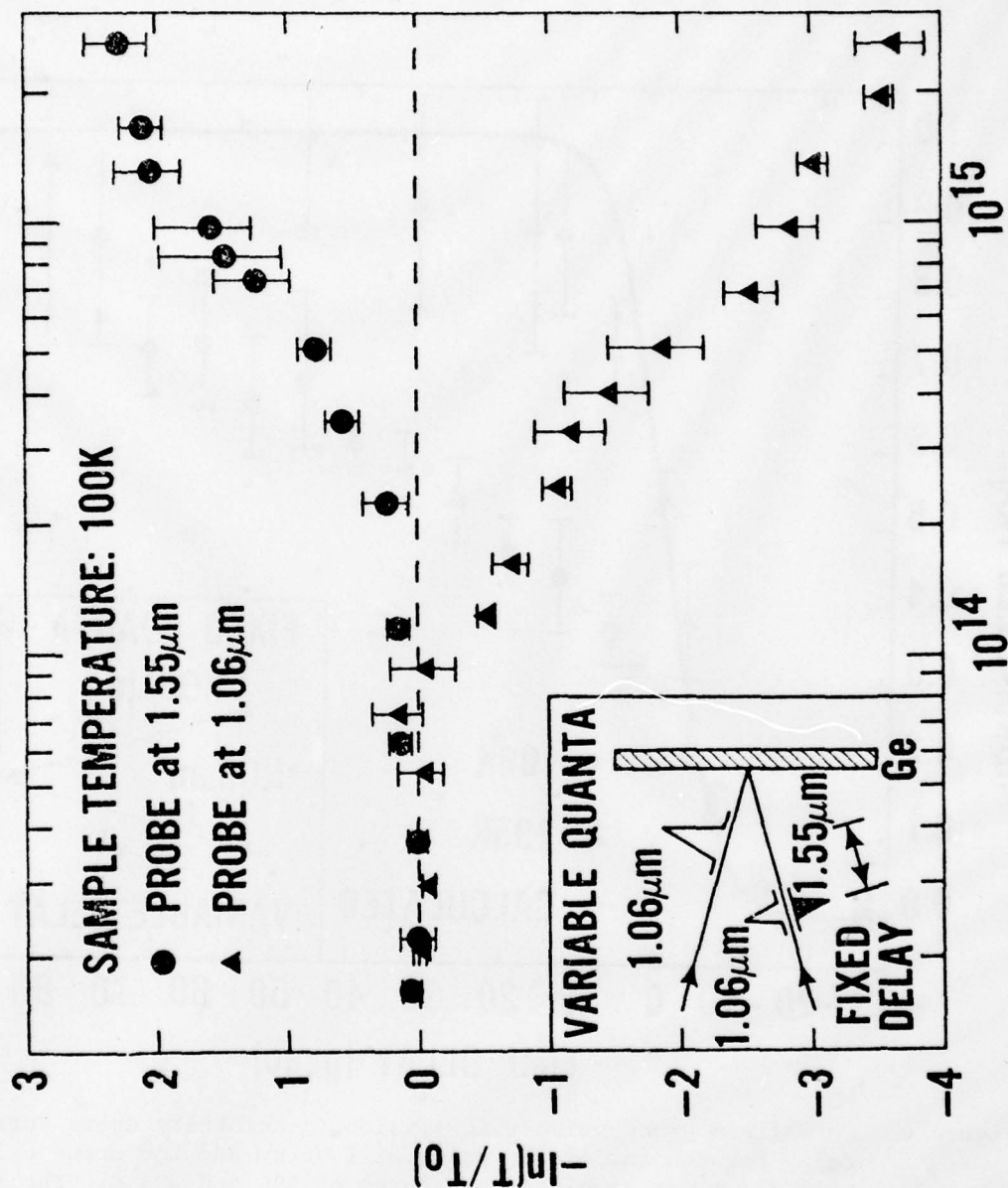


Figure 6. Normalized probe pulse transmission in arbitrary units versus delay between the excite pulse at $1.06\mu\text{m}$ and the probe pulse at $1.06\mu\text{m}$ for sample temperatures of 100 and 295 K. The solid line represents a theoretical integration curve assuming Gaussian-shaped optical pulses of 10 psec width (from Smirl *et al.*¹⁴).



INCIDENT QUANTA IN EXCITATION PULSE

Figure 7. Change in absorbance, $-\ln(I/I_0)$, of a 6- μm -thick germanium sample at 1.06 μm and 1.55 μm as a function of incident excite pulse energy at 1.06 μm , where T_0 is the linear transmission of the sample at the wavelength under consideration. Note that an excite pulse energy of 2×10^{15} quanta corresponds to an incident energy density of approximately 10^{-2} J/cm² (from Smirl et al.¹⁴).

carrier density alone cannot be combined with this absorption versus density relationship to account for the rise in probe transmission at $1.06\text{ }\mu\text{m}$ exactly as we discussed in the previous section and suggested by Auston *et al.*¹². In addition, these measurements indicate that the combined free-carrier, intervalence-band, and indirect absorbance changes are opposite in sign and smaller in magnitude than changes caused by saturation of the direct absorption. As a result, the authors concluded that the decrease in absorbance at $1.06\text{ }\mu\text{m}$ with increasing carrier number is dominated by a saturation of the direct absorption coefficient; however, the rate of this decrease in absorbance is slowed by the contributions of these "other" processes that are opposite in sign. Note that, when comparing the data discussed here (Fig. 7) with the earlier data by Smirl *et al.*⁵ (Fig. 3), one must realize that the sample thickness and focused optical spot sizes are not identical.

Finally, we measured the temporal evolution of the absorbance of a $1.55\text{ }\mu\text{m}$ probe pulse as a function of time delay after an intense excite pulse at $1.06\text{ }\mu\text{m}$. In this experiment, the sample was irradiated by an optical pulse at $1.06\text{ }\mu\text{m}$ containing roughly 2×10^{15} quanta (corresponding to surface energy density of $\sim 10^{-2}\text{ J/cm}^2$) and was probed by a weak pulse having a wavelength of $1.55\text{ }\mu\text{m}$ (See Fig. 8). The results of these probe measurements are similar to those obtained by Auston *et al.*⁴. However, Auston *et al.*⁴ stated that they performed their measurements at excite intensities such that the absorption of the excite pulse was linear. These experiments were clearly performed in the nonlinear region. In addition, the measurements of Auston *et al.*⁴ were performed on a $300\text{ }\mu\text{m}$ -thick sample, our sample was $6\text{ }\mu\text{m}$ thick. The measurements presented in Fig. 8 indicate that free-carrier, intervalence-band, and

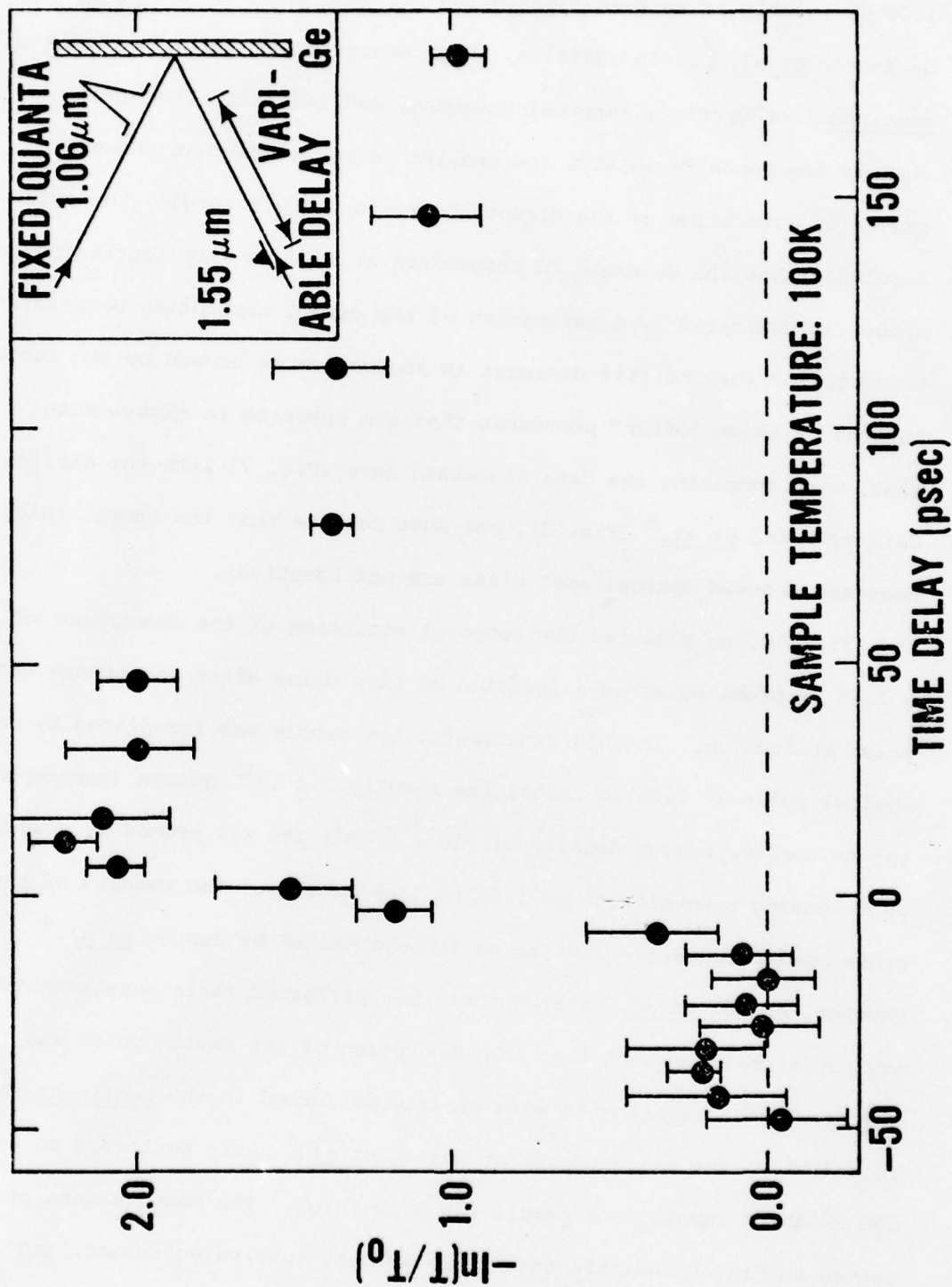


Figure 8. Change in probe pulse absorbance, $-\ln(I/I_0)$, versus delay between the excite pulse at 1.06 μm and the probe pulse at 1.55 μm , where T_0 is the linear transmission of the probe pulse at 1.55 μm (from Smirl et al. 14).

indirect absorption can be significant at the carrier densities encountered during excite and probe experiments described here. Recall that Auston et al.⁴ attributed the decrease in probe pulse absorbance at 1.55 μm to a decrease in free-carrier absorption caused by a temporal decay in carrier density due to Auger recombination. The experiments that we have just described only allow the measurement of the change in the combined free-carrier, intervalence-band and indirect absorbance, and they do not provide for a convenient separation of the individual contributions.

Summarizing the results of the measurements described in the previous three paragraphs, we conclude that the rise in probe transmission during the 1.06 μm excite and 1.06 μm probe experiments at 100 K is not an integration effect (i.e. not a simple band filling) and that it cannot be attributed to free-carrier, intervalence-band, and Coulomb-assisted transitions combined with Auger recombination. The contributions of these latter processes are significant, however, and they must be accounted for by any successful model. Unfortunately, the measurements described here yielded no direct information concerning carrier distribution temperatures or energy relaxation rates, and the question of attributing the rise in 1.06 μm probe transmission to a cooling of a hot carrier plasma created by the excite pulse remains unresolved. A detailed discussion of these experiments is contained in the reprint of Appendix A.

Having rejected two of the three possible explanations for the probe transmission listed earlier and with the other explanation all but rejected, to what do we attribute this rise in probe transmission? Recent suggestions are reviewed in the next chapter.

Parametric Scattering or State-Filling

Here, we present and discuss the results of measurements that separate the effects of parametric scattering from those of other processes such as state filling.

The particular experimental configuration that we employ to separate the effects of parametric scattering from those of other processes such as state filling is shown in Fig. 9. A single 1.06 μm pulse, approximately 11 psec in duration, is switched by an electro-optic shutter from a train of pulses produced by a mode-locked Nd-glass laser. The single pulse is split into two by a beam splitter, and a relative delay is introduced between the two pulses. The probe pulse intensity is attenuated to approximately 2% of the corresponding excitation pulse intensity. Both pulses are focused onto the germanium sample as shown in the figure. The angular separation between incident beams is 12° . This configuration is similar to the arrangement employed by Kennedy *et al.*¹ and Shank and Auston³ to measure the narrow spike in probe transmission. Our configuration, however, differs from theirs in two important respects. First, we have introduced a half wave plate into the probe path to provide for a continuous rotation of the probe pulse polarization with respect to the excite pulse. Second, we have positioned a detector to collect the first order diffracted light from the excitation pulse in the event that a grating should be produced by the interference of the two pulses. In previous studies of the probe spike, only the incident and transmitted probe and excite energies were measured.

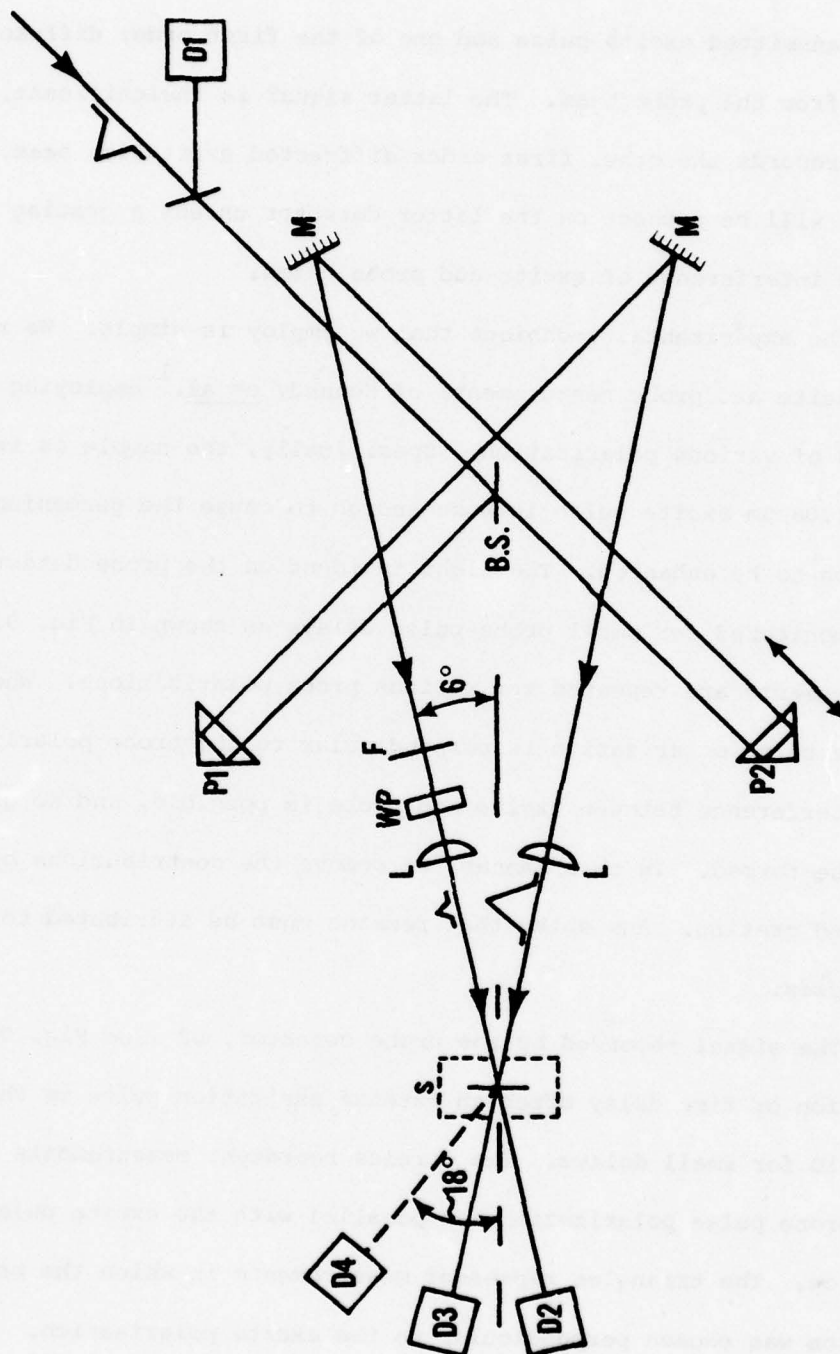


Figure 9. Schematic diagram for measuring the polarization dependence of the excite and probe response of Ge at 1.06 μm , where D denotes a detector, B.S. a beamsplitter, M a mirror, P a prism, F a filter, WP a halfwave plate, L a lens, and S the germanium sample. Note the P2 can be translated and W.P. can be rotated.

As shown in Fig. 9, Detector 1 monitors the incident pulse energy. Detector 2 measures the transmitted probe light and one of the first order scattered beams from the excitation pulse. Detector 3 collects the transmitted excite pulse and one of the first order diffracted beams from the probe beam. The latter signal is insignificant. Detector 4 records the other first order diffracted excitation beam. No signal will be present on the latter detector unless a grating is formed by the interference of excite and probe beams.

The experimental technique that we employ is simple. We repeat the excite and probe measurements of Kennedy et al.¹ employing probe pulses of various polarization. Specifically, the sample is irradiated by a 1.06 μm excite pulse intense enough to cause the germanium transmission to be enhanced. The light incident on the probe detector is then monitored for small probe pulse delays as shown in Fig. 9. These measurements are repeated for various probe polarizations. When the excite pulse polarization is perpendicular to the probe polarization, no interference between excite and probe is possible, and no grating will be formed. In this manner, we remove the contributions of the laser-induced grating. Any spike that remains must be attributed to other processes.

The signal recorded by the probe detector, D2 (See Fig. 9), as a function of time delay after an intense excitation pulse is shown in Fig. 10 for small delays. The circles represent measurements in which the probe pulse polarization was parallel with the excite pulse polarization. The triangles represent measurements in which the probe polarization was chosen perpendicular to the excite polarization. The most

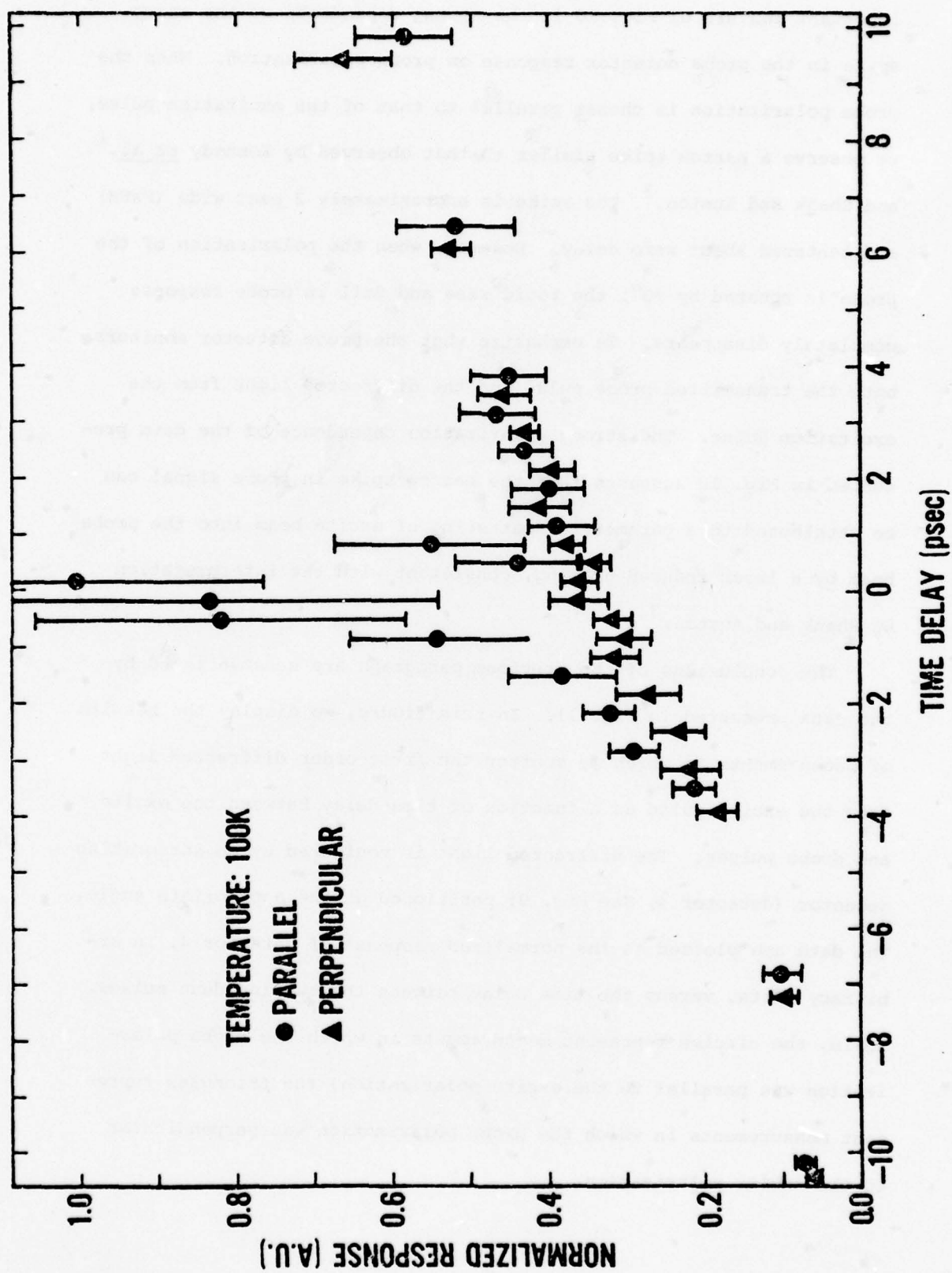


Figure 10. Normalized response of the probe detector, in arbitrary units, vs. time delay between excite and probe pulses.

important feature of Fig. 10 is the strong dependence of the sharp spike in the probe detector response on probe polarization. When the probe polarization is chosen parallel to that of the excitation pulse, we observe a narrow spike similar to that observed by Kennedy *et al.*¹ and Shank and Auston.³ The spike is approximately 2 psec wide (FWHM) and centered about zero delay. However, when the polarization of the probe is rotated by 90° , the rapid rise and fall in probe response completely disappears. We emphasize that the probe detector monitors both the transmitted probe pulse and the diffracted light from the excitation pulse. The strong polarization dependence of the data presented in Fig. 10 suggests that the narrow spike in probe signal can be attributed to a parametric scattering of excite beam into the probe beam by a laser induced grating, consistent with the interpretation by Shank and Auston.³

The conclusions of the previous paragraph are substantiated by the data presented in Fig. 11. In this figure, we display the results of measurements in which we monitor the first order diffracted light from the excite pulse as a function of time delay between the excite and probe pulses. The diffracted light is monitored by an integrating detector (detector 4, See Fig. 9) positioned at the appropriate angle. The data are plotted as the normalized response of detector 4, in arbitrary units, versus the time delay between the two incident pulses. Again, the circles represent measurements in which the probe polarization was parallel to the excite polarization; the triangles represent measurements in which the probe polarization was perpendicular to the excite polarization.

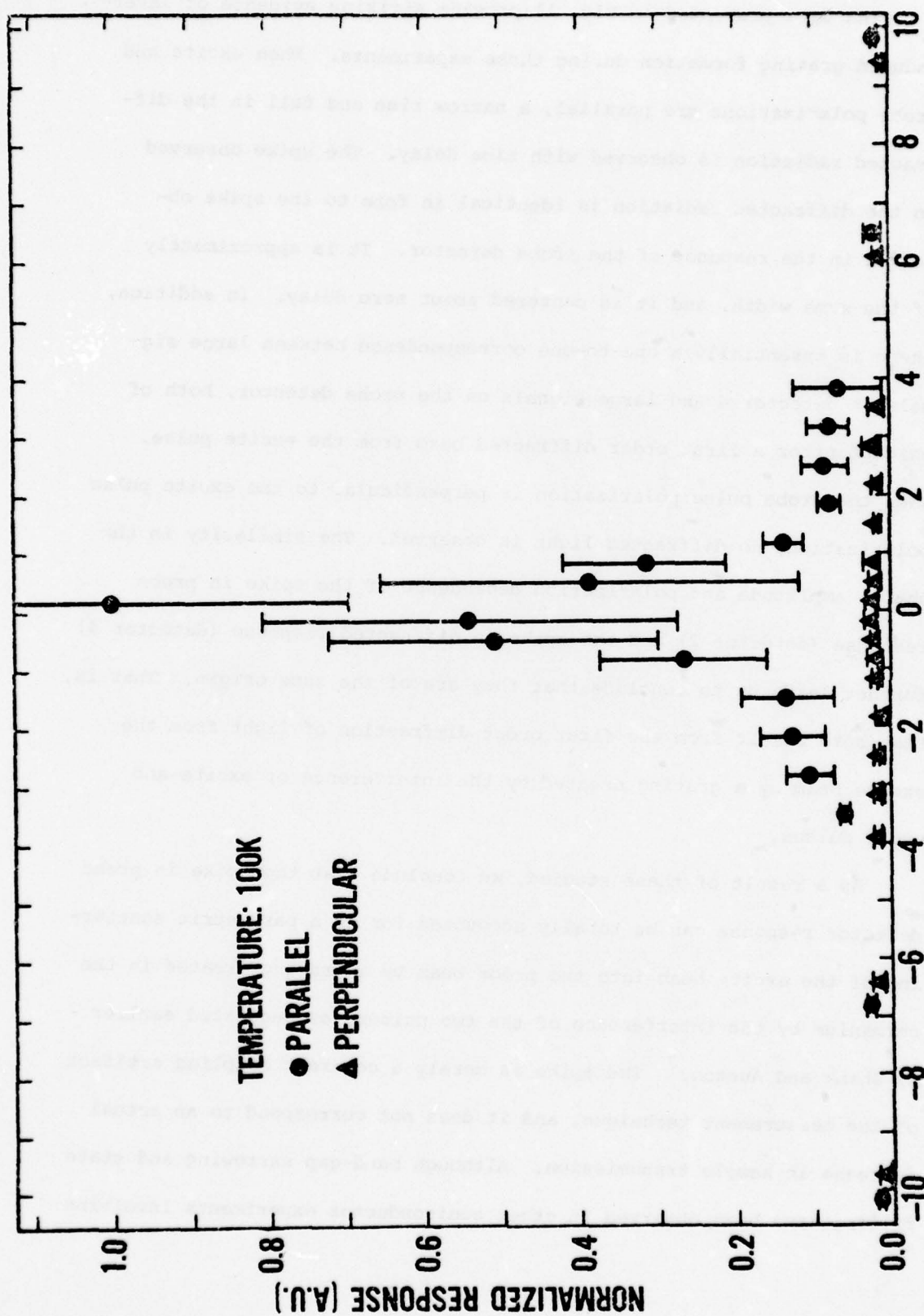


Figure 11. Normalized response of detector 4, in arbitrary units, vs. time delay between excite and probe pulses.

The data presented in Fig. 11 provide striking evidence of laser-induced grating formation during these experiments. When excite and probe polarizations are parallel, a narrow rise and fall in the diffracted radiation is observed with time delay. The spike observed in the diffracted radiation is identical in form to the spike observed in the response of the probe detector. It is approximately of the same width, and it is centered about zero delay. In addition, there is essentially a one-to-one correspondence between large signals on detector 4 and large signals on the probe detector, both of which monitor a first order diffracted beam from the excite pulse. When the probe pulse polarization is perpendicular to the excite pulse polarization, no diffracted light is observed. The similarity in the shape, amplitude and polarization dependence of the spike in probe response (detector 2) and the spike in diffracted response (detector 4) further leads us to conclude that they are of the same origin. That is, that both result from the first order diffraction of light from the excite beam by a grating created by the interference of excite and probe pulses.

As a result of these studies, we conclude that the spike in probe detector response can be totally accounted for by a parametric scattering of the excite beam into the probe beam by a grating created in the germanium by the interference of the two pulses, as suggested earlier by Shank and Auston.³ The spike is merely a coherent coupling artifact of the measurement technique, and it does not correspond to an actual increase in sample transmission. Although band-gap narrowing and state filling have been observed in other semiconductor experiments involving

optical excitation (and certainly they must be occurring here as well), they do not contribute to the spike in probe detector response, as recently suggested by Ferry.¹⁵ For further details, the reader should see Appendix B.

Measurement of Carrier Recombination Times and Diffusion at High Carrier Densities

The studies described above provide definite evidence of laser-induced grating formation during excite and probe studies at 1.06 μm . Such a grating is produced by a modulation of the optically-created carrier density near the sample surface. This modulation of the carrier density (or grating), once produced, can decay by two mechanisms: Carrier recombination or diffusion of carriers from regions of high concentrations to regions of lower concentration. A study of the grating lifetime as a function of the excite-probe geometry should allow a direct measurement of the two lifetimes. We are conducting such a study, although we presently have only rough preliminary results.

These measurements are conducted in the following manner. Two excite pulses and a single probe pulse are derived from a single ultra-short pulse by means of a beam splitter. The two excite pulses are both spatially and temporally overlapped on the sample surface as shown in Fig. 12. As a result, the interference of the two beams will produce a modulation of the optically-created carrier density to form a grating with spacing $d = \lambda / (2 \sin \theta)$, where θ is the angle between each excite beam and the sample surface. The grating lifetime is measured by monitoring the first order diffracted light from a third weak probe pulse as

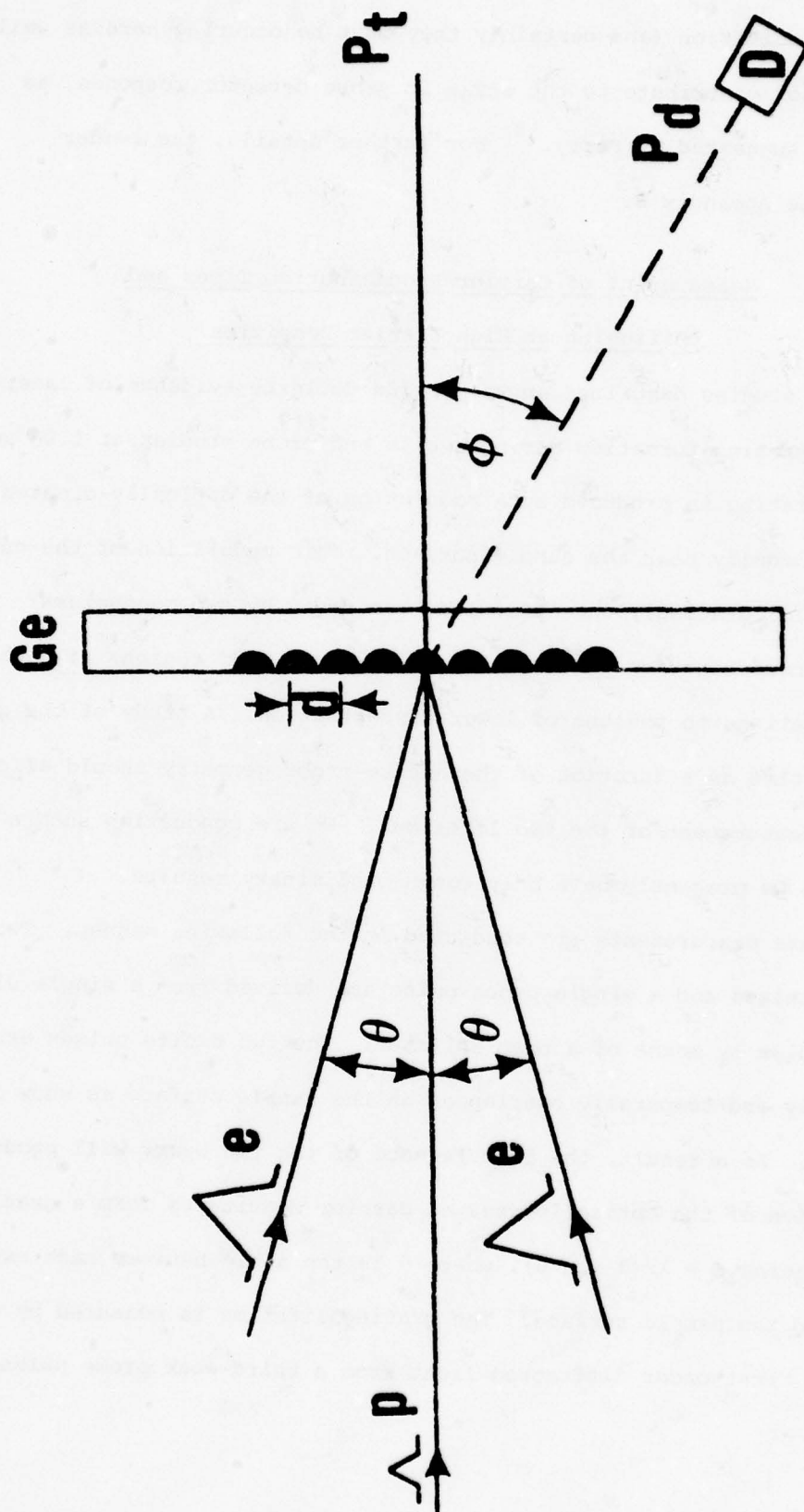


Figure 12. Configuration for measuring the laser-induced grating lifetime.

shown in Fig. 12. By controlling the geometry of the grating formation (θ), we can determine the grating spacing and control which process, carrier recombination or diffusion, dominates the grating lifetime. Thus, we can extract each rate separately. Preliminary results for grating spacings of 5 μm (diffusion dominated) and 11 μm (recombination dominated) are shown in Fig. 13. We expect to complete these studies in the next 6 months.

NATO Lecture and Seminar

As a result of the work conducted under ONR sponsorship over the past two years, I have been invited to lecture and present a seminar at the NATO Advanced Study Institute on the Physics of Nonlinear Transport in Semiconductors in Urbino, Italy, July 16-27, 1979. This lecture and seminar are to be published and are included as preprints in Appendix C and Appendix D.

Summary of Activity

The work described has resulted in two papers in the Physical Review, one APS talk, one talk at the International Conference on Picosecond Phenomena (published in the proceedings of the conference), and a lecture and a seminar at NATO Advanced Study Institute, as detailed above. The four published manuscripts resulting from work during this contract period are included as Appendices A, B, C and D.

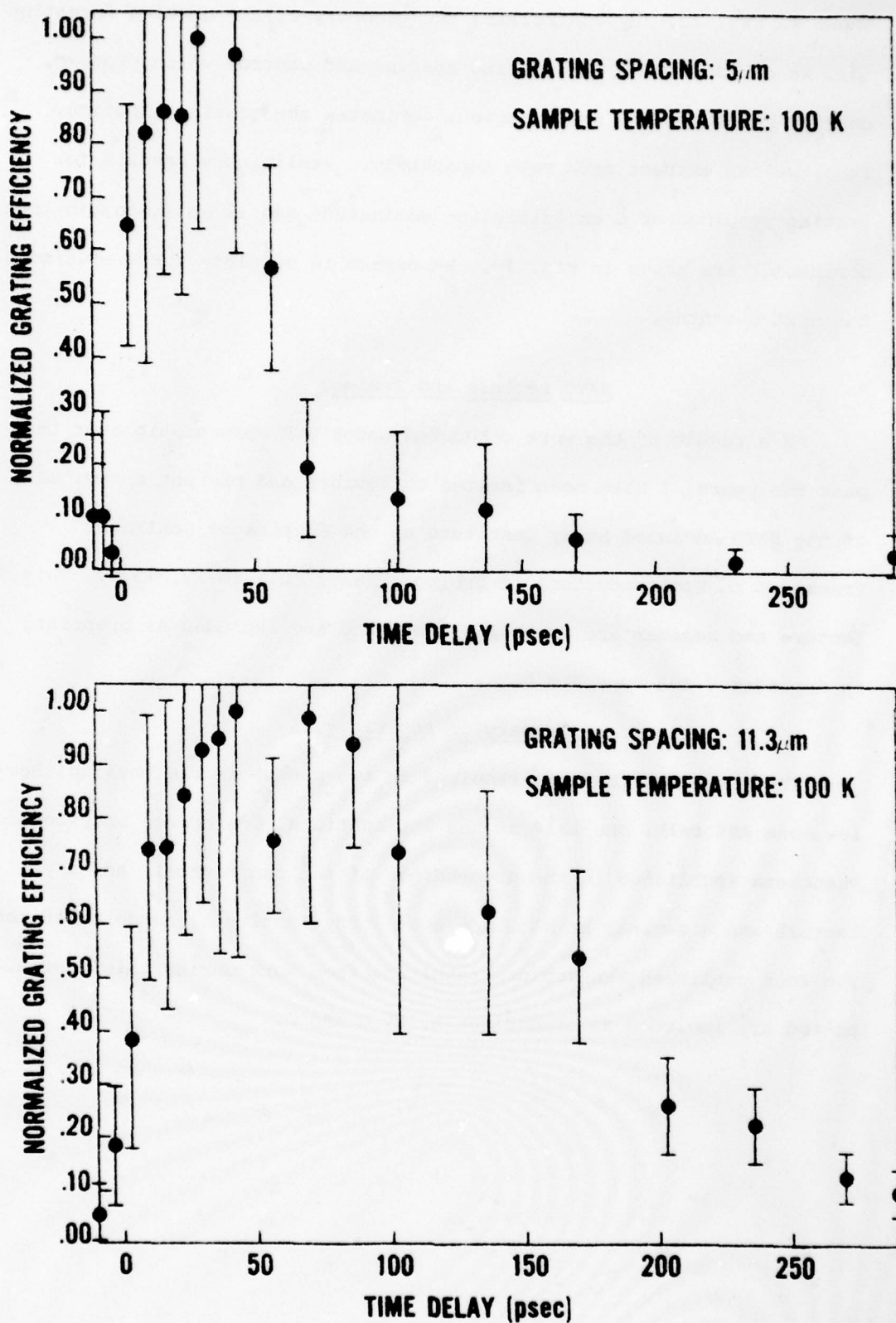


Figure 13. Preliminary measurements of laser-induced grating lifetimes. The top figure is diffusion dominated (grating spacing of 5 μm), and the lower figure is both diffusion and recombination dominated (grating spacing of 11.3 μm).

III. PROFESSIONAL PUBLICATIONS AND ACTIVITIES

FOR THE PERIOD

1 Sept. 1976 to 31 May 1979

Arthur L. Smirl - Principal Investigator

Publications

1. "Ultrafast Transient Response of Solid State Plasmas: I Germanium: Theory and Experiment," Ahmet Elci, M. O. Scully, A. L. Smirl, and J. C. Matter, Phys. Rev. B 16, 191 (1977).
2. "Pulsewidth Dependence of the Transmission of Ultrashort Optical Pulses in Germanium," John S. Bessey, Bruno Bosacchi, Henry M. van Driel, and Arthur L. Smirl, Phys. Rev. B 17, 159 (1978).
3. "The Role of Phonons and Plasmons in Describing the Pulsewidth Dependence of the Transmission of Ultrashort Optical Pulses through Germanium," W. P. Latham, Jr., A. L. Smirl, A. Elci, and J. S. Bessey, Solid-State Electron. 21, 159 (1978).
4. "Physics of Ultrafast Phenomena in Solid State Plasmas," A. Elci, A. L. Smirl, C. Y. Leung, and M. O. Scully, Solid State Electron. 21, 151 (1978).
5. "Gauge Invariant Perturbation Theory for the Interaction of Radiation and Matter," Donald H. Kobe and Arthur L. Smirl, Am. J. Phys. 46, 624 (1978).
6. "Simple Laser Pulse Energy Monitor," A. L. Smirl, R. L. Shoemaker, J. B. Hambenne, and J. C. Matter, Rev. Sci. Instrum. 49, 672 (1978).
7. "Picosecond Optical Measurement of Free-Electron, Free-Hole, and Indirect Absorption in Germanium at High Optically-Created Carrier Densities," Arthur L. Smirl, J. Ryan Lindle, and Steven C. Moss, Phys. Rev. B 18, 5489 (1978).
8. "Picosecond Optical Absorption at 1.06 μm and 1.55 μm in Thin Germanium Samples at High Optically-Created Carrier Densities," Arthur L. Smirl, J. Ryan Lindle, and Steven C. Moss, Proceedings of the Conference on Picosecond Phenomena, 174, Springer-Verlag (1978)
9. "The Effects of Parametric Scattering, Energy-Gap Narrowing, and State Filling on the Picosecond Optical Response of Germanium," J. Ryan Lindle, Steven C. Moss, and Arthur L. Smirl, Accepted for publication by Phys. Rev. B 1979.

10. "The Physics of Nonlinear Absorption and Ultrafast Carrier Relaxation in Semiconductors," Arthur L. Smirl, to be published in the Proceedings of the NATO Advanced Study Institute on "Nonlinear Electron Transport in Semiconductors."
11. "High Intensity Picosecond Photoexcitation of Semiconductors," Arthur L. Smirl, to be published in the Proceedings of the NATO Advanced Study Institute on "Nonlinear Electron Transport in Semiconductors."

Papers

1. "Ultrafast Transient Response of Optically Excited Plasmas in Germanium," Invited Paper presented at 1976 Annual Meeting of Optical Society of America, J. Opt. Soc. Am. 66, 1082 (1976).
2. "Gauge Invariant Formulation of the Interaction of Radiation and Matter," D. H. Kobe and A. L. Smirl, AAPT Summer Meeting, 1977, AAPT Announcer 7, 70 (1977).
3. The Role of Phonons and Plasmons in Describing the Pulsewidth Dependence of the Transmission of Ultrashort Optical Pulses through Germanium," A. L. Smirl, W. P. Latham, A. Elci, and J. S. Bessey, International Conference on Hot Electrons in Semiconductors, Bull. Am. Phys. Soc. 22, 706 (1977).
4. "Picosecond Optical Absorption at 1.06 μm and 1.55 μm in Thin Germanium Samples at High Optically-Created Carrier Densities," A. L. Smirl and J. R. Lindle, and S. C. Moss, Conference on Picosecond Phenomena, May 25, 1978, Hilton Head, S. C.
5. "The Effects of Parametric Scattering, Energy-Gap Narrowing, and State Filling on the Picosecond Optical Response of Germanium," Arthur L. Smirl, Steven C. Moss, and J. Ryan Lindle, Bull. Am. Phys. Soc. 24, 310 (1979).

Other Talks

1. "Ultrashort Optical Pulse Measurements at 10.6 Microns," Larry Tipton, A. L. Smirl, and D. G. Seiler, Texas Academy of Science Meeting at Baylor University, March 10, 1977.
2. "Ultrafast Transient Response of Hot Carriers in Germanium," S. C. Moss, J. R. Lindle, and A. L. Smirl, Texas Academy of Science Meeting at Baylor University, March 10, 1977.
3. "Gauge Transformations and Perturbation Theory," D. H. Kobe and A. L. Smirl, Texas Academy of Science Meeting at Baylor University, March 10, 1977.
4. "A Perturbing Question: How Do You Treat the Interaction of Electromagnetic Radiation and Matter?", D. H. Kobe and A. L. Smirl, Texas Section of AAPT Meeting at Southern Methodist University, November, 5, 1977.

5. "A Simple, Accurate, Inexpensive Energy Monitor for Short Laser Pulses," J. R. Lindle, S. C. Moss, and A. L. Smirl, Texas Academy of Science Meeting at Texas Tech, March 9, 1978.
6. "Measurement of the Ultrafast Relaxation of Saturation Phenomena in Semiconductors," S. C. Moss, J. R. Lindle, and A. L. Smirl, Texas Academy of Science Meeting at Texas Tech, March 9, 1978.
7. "Piezo-Transmission of p-type Germanium at CO₂ Laser Wavelengths," L. Tipton, D. G. Seiler, and A. L. Smirl, Texas Academy of Science Meeting at Texas Tech, March 9, 1978.
8. "Picosecond Optical Measurements of Diffusion Coefficients and Recombination Lifetimes in Semiconductors at High Optically-Created Carrier Densities," Steven C. Moss, J. Ryan Lindle, Paul G. Perrymand, and Arthur L. Smirl, Texas Academy of Science Meeting, University of Texas at Arlington, March 8, 1979.
9. "Picosecond Measurement of Exciplex Formation," James B. Clark, Benny R. Russel, Eric W. Van Stryland, and Arthur L. Smirl, Texas Academy of Science Meeting, University of Texas at Arlington, March 8, 1979.
10. "The Roles of Correlation Effects, Energy-Gap Narrowing, and State Filling in Ultrafast Optical Response of Semiconductors," J. Ryan Lindle, S. C. Moss, and Arthur L. Smirl, Texas Academy of Science Meeting, University of Texas at Arlington, March 8, 1979.
11. Invited Talk: "A 'Small' Inexpensive Dye Laser--Discussion and Demonstration," Arthur L. Smirl, Texas Academy of Science Meeting, University of Texas at Arlington, March 8, 1979.

IV. VITA

SMIRL, ARTHUR LEE

Assistant Professor Physics, North Texas State University

Personal

Born, November 8, 1944, Citizenship, USA;
Married, no children

Education

Ph.D.	Optical Sciences	University of Arizona	1975
M.S.E.	Electrical Engineering	University of Michigan	1969
B.S.	Electrical Engineering	Lamar University	1968
B.S.	Mathematics	Lamar University	1968

Experience

1975 - Assistant Professor, North Texas State University, Denton
Texas
1972-75 - Research Associate, University of Arizona, Tucson, Arizona
1968-71 - Staff member, Sandia Laboratories, Albuquerque, New Mexico

Research Specialization

Optical Interactions in Semiconductors
Picosecond Spectroscopy
Laser Physics

Vita: A. L. Smirl

Academic and Professional Society Affiliations, Honors:

Optical Society of America
 American Physical Society
 Institute of Electrical and Electronic Engineers
 Tau Beta Pi
 Eta Kappa Nu
 Sigma Pi Sigma
 Pi Mu Epsilon
 Blue Key
 Phillips Petroelum Company Scholarship (1963-67).

Refereed Publications:

1. "Holographic Recording with Limited Laser Light," C. D. Lenoard and A. L. Smirl, Appl. Opt. 10, 625 (1971).
2. "Nonlinear Absorption and Ultrashort Carrier Relaxation Times in Germanium Under Irradiation by Picosecond Pulses," Chandler J. Kennedy, John C. Matter, Arthur L. Smirl, Hugo Weichel, Frederic A. Hopf, and Sastry V. Pappu, Phys. Rev. Lett. 32, 419 (1974).
3. "Ultrafast Relaxation of Optically Excited Nonequilibrium Electron-Hole Distributions in Germanium," A. L. Smirl, J. C. Matter, A. Elci, and M. O. Scully, Opt. Commun. 16, 118 (1976).
4. "Saturable Transmission in Mercury Cadmium Telluride," J. C. Matter, A. L. Smirl, and M. O. Scully, App. Phys. Lett. 28, 507 (1976).
5. "Ultrafast Transient Response of Solid State Plasmas I: Germanium, Theory and Experiment," Ahmet Elci, M. O. Scully, A. L. Smirl, and J. C. Matter, Phys. Rev. B 16, 191 (1977).
6. "Pulsewidth Dependence of the Transmission of Ultrashort Optical Pulses in Germanium," John S. Bessey, Bruno Bosacchi, Henry M. Van Driel, and Arthur L. Smirl, Phys. Rev. B 17, 159 (1978).
7. "The Role of Phonons and Plasmons in Describing the Pulsewidth Dependence of the Transmission of Ultrashort Optical Pulses through Germanium," W. P. Latham, Jr., A. L. Smirl, A. Elci, and J. S. Bessey, Solid-State Electron. 21, 159 (1978).
8. "Physics of Ultrafast Phenomena in Solid State Plasmas," A. Elci, A. L. Smirl, C. Y. Leung, and M. O. Scully, Solid-State Electron. 21, 151 (1978).
9. "Gauge Invariant Perturbation Theory for the Interaction of Radiation and Matter," Donald H. Kobe and Arthur L. Smirl, Am. J. Phys. 46, 624 (1978).

Vita: A. L. Smirl

Refereed Publications (continued):

10. "Simple Laser Pulse Energy Monitor," A. L. Smirl, R. L. Shoemaker, J. B. Hambenne, and J. C. Matter, *Rev. Sci. Instrum.* 49, 672 (1978).
11. "Picosecond Optical Measurements of Free-electron, Free-Hole, and Indirect Absorption in Germanium at High Optically-Created Carrier Densities," Arthur L. Smirl, J. Ryan Lindle, and Steven C. Moss, *Phys. Rev. B* 18, 5489 (1978).
12. "Picosecond Optical Absorption at 1.06 μm and 1.55 μm in Thin Germanium Samples at High Optically-Created Carrier Densities," Arthur L. Smirl, J. Ryan Lindle, and Steven C. Moss, Proceedings of the Conference on Picosecond Phenomena, 174, Springer-Verlag (1978).
13. "The Effects of Parametric Scattering, Energy-Gap Narrowing, and State Filling on the Picosecond Optical Response of Germanium," J. Ryan Lindle, Steven C. Moss, and Arthur L. Smirl, Accepted for publication by *Phys. Rev. B* 1979.
14. "The Physics of Nonlinear Absorption and Ultrafast Carrier Relaxation in Semiconductors," Arthur L. Smirl, to be published in the Proceedings of the NATO Advanced Study Institute on "Nonlinear Electron Transport in Semiconductors."
15. "High Intensity Picosecond Photoexcitation of Semiconductors," Arthur L. Smirl, to be published in the Proceedings of the NATO Advanced Study Institute on "Nonlinear Electron Transport in Semiconductors."

Papers Presented at Conferences:

1. "Available Light Holography," A. L. Smirl and C. D. Leonard, 1969 Annual Meeting of the Optical Society of American, *J. Opt. Soc. Am.* 59, 1530 (1969).
2. Invited paper: "Ultrafast Transient Response of Optically Excited Plasmas in Germanium," presented at 1976 Annual Meeting of Optical Society of American, *J. Opt. Soc. Am.* 66, 1982 (1976).
3. "Gauge Invariant Formulation of the Interaction of Radiation and Matter," D. H. Kobe and A. L. Smirl, AAPT Summer Meeting, 1977, *AAPT Announcer* 7, 70 (1977).
4. "The Role of Phonons and Plasmons in Describing the Pulsewidth Dependence of the Transmission of Ultrashort Optical Pulses through Germanium," A. L. Smirl, W. P. Latham, A. Elci, and J. S. Bessey, International Conference on Hot Electrons in Semiconductors, *Bull. Am. Phys. Soc.* 22, 706 (1977).

Vita: A. L. Smirl

Papers Presented at Conferences (continued):

5. "Picosecond Optical Absorption at 1.06 μm and 1.55 μm in Thin Germanium Samples at High Optically-Created Carrier Densities," A. L. Smirl, J. R. Lindle, and S. C. Moss, Conference on Picosecond Phenomena, May 25, 1978, Hilton Head, S. C.
6. "The Effects of Parametric Scattering, Energy-Gap Narrowing, and State Filling on the Picosecond Optical Response of Germanium," Arthur L. Smirl, Steven C. Moss, and J. Ryan Lindle, Bull. Am. Phys. Soc. 24, 310 (1979).

Invited Lecturer:

1. NATO Summer School on "Nonlinear Electron Transport in Semiconductors," July 16-17, 1979, Urbino, Italy.

Other Presentations Given at Scientific Meetings:

1. "Ultrashort Optical Pulse Measurements at 10.6 Microns," Larry Tipton, A. L. Smirl, and D. G. Seiler, Texas Academy of Science Meeting at Baylor University, March 10, 1977.
2. "Ultrafast Transient Response of Hot Carriers in Germanium," S. C. Moss, J. R. Lindle, and A. L. Smirl, Texas Academy of Science Meeting at Baylor University, March, 10, 1977.
3. "Gauge Transformations and Perturbation Theory," D. H. Kobe and A. L. Smirl, Texas Academy of Science Meeting at Baylor University, March 10, 1977.
4. "A Perturbing Question: How Do You Treat the Interaction of Electromagnetic Radiation and Matter?", D. H. Kobe and A. L. Smirl, Texas Section of AAPT Meeting at Southern Methodist University, November 5, 1977.
5. "A Simple Accurate, Inexpensive Energy Monitor for Short Laser Pulses," J. R. Lindle, S. C. Moss, and A. L. Smirl, Texas Academy of Science Meeting at Texas Tech, March 9, 1978.
6. "Measurement of the Ultrafast Relaxation of Saturation Phenomena in Semiconductors," S. C. Moss, J. R. Lindle, and A. L. Smirl, Texas Academy of Science Meeting at Texas Tech, March 9, 1978.
7. "Piezo-Transmission of p-type Germanium at CO_2 Laser Wavelengths," L. Tipton, D. G. Seiler, and A. L. Smirl, Texas Academy of Science Meeting at Texas Tech, March 9, 1978.

Vita: A. L. Smirl

Other Presentations (continued):

8. "Picosecond Optical Measurement of Diffusion Coefficients and Recombination Lifetimes in Semiconductors at High Optically-Created Carrier Densities," Steven C. Moss, J. Ryan Lindle, Paul G. Perryman, and Arthur L. Smirl, Texas Academy of Science Meeting, University of Texas at Arlington, March 8, 1979.
9. "Picosecond Measurements of Exciplex Formation," James B. Clark, Benny R. Russel, Eric W. Van Stryland, and Arthur L. Smirl, Texas Academy of Science Meeting, University of Texas at Arlington, March 8, 1979.
10. "The Roles of Correlation Effects, Energy-Gap Narrowing, and State Filling in Ultrafast Optical Response of Semiconductors," J. Ryan Lindle, S. C. Moss, and Arthur L. Smirl, Texas Academy of Science Meeting, University of Texas at Arlington, March 8, 1979.
11. Invited Talk: "A 'small' Inexpensive Dye Laser--Discussion and Demonstration," Arthur L. Smirl, Texas Academy of Science Meeting, University of Texas at Arlington, March 8, 1979.

Research Colloquia:

- "The Roles of Free-Carrier, Free-Hole, and Indirect Absorption in Determining the Picosecond Optical Response of Germanium," Colorado State University, 1978.
- "Ultrashort Relaxation Processes in Germanium," University of Arkansas, 1978.
- "Optics Research at NTSU," Lamar University, 1978, Southwest Texas State University, 1978.
- "Picosecond Clocks and Ultrafast Processes," Lamar University, 1979.
- "The Physics of the Ultrafast Relaxation of Photoexcited Carriers in Semiconductors," University of Texas at Dallas, 1979.

Courses Taught:

- Physics 131, Physics for Liberal Arts Majors, an introductory course based on Hewitts; text "Conceptual Physics".
- Physics 620, Semiclassical Laser Theory, an advanced, semiclassical formulation of the interaction of radiation with matter based on the text by Sargent, Scully, and Lamb entitled "Laser Physics".
- Physics 625, Nonlinear Optics, a classical treatment of nonlinear scattering based on my own personal notes taken from current literature.

Vita: A. L. Smirl

Courses Taught (continued):

Physics 680, Selected Topics in Solid State Physics, Advanced topics selected from the area of optical interactions in Semiconductors with emphasis on ultrashort and nonlinear processes.

Physics 590, Special problems in picosecond spectroscopy for the Individual
591, 690, Graduate Student. Problem chosen by the student under supervision
and 691 vision of professor.

Physics 694, Individual Research for doctoral students.

Supervision of Thesis:

Steve C. Moss, Ph.D. student, 1976-
J. Ryan Lindle, Ph.D. student, 1976-
Gary Paul Perryman, Ph.D. student, 1978-
Paul K. Kennedy, masters student, 1978-

V. REFERENCES

1. C. J. Kennedy, J. C. Matter, A. L. Smirl, H. Weichel, F. A. Hopf, and S. V. Pappu, Phys. Rev. Lett. 32, 419 (1974).
2. D. H. Auston and C. V. Shank, Phys. Rev. Lett. 32, 1120 (1974).
3. C. V. Shank and D. H. Auston, Phys. Rev. Lett. 34, 479 (1975).
4. D. H. Auston, C. V. Shank, and P. LeFur, Phys. Rev. Lett. 35, 1022 (1975).
5. A. L. Smirl, J. C. Matter, A. Elci, and M. O. Scully, Opt. Commun. 16, 118 (1976).
6. H. M. van Driel, A. Elci, J. S. Bessey, and M. O. Scully, Opt. Commun. 20, 837 (1977).
7. A. Elci, M. O. Scully, A. L. Smirl, and J. C. Matter, Phys. Rev. B 16, 191 (1977).
8. H. M. van Driel, J. S. Bessey, and R. C. Hanson, Opt. Commun. 22, 346 (1977).
9. J. S. Bessey, B. Bosacchi, H. M. van Driel, and A. L. Smirl, Phys. Rev. B 17, 2782 (1978).
10. W. P. Latham, Jr., A. L. Smirl, and A. Elci, Solid State Electron. 21, 159 (1978).
11. A. Elci, A. L. Smirl, C. Y. Leung, and M. O. Scully, Solid State Electron. 21, 141 (1978).
12. D. H. Auston, S. McAfee, C. V. Shank, E. P. Ippen, and O. Teschke, Solid State Electron. 21, 147 (1978), and S. McAfee and D. H. Auston, private communication, 1977.
13. A. L. Smirl, J. R. Lindle, and S. C. Moss, Proceedings of the Conference on Picosecond Phenomena, 174, Springer-Verlag (1978).
14. A. L. Smirl, J. R. Lindle, and S. C. Moss, Phys. Rev. B 18, 5489 (1978).
15. D. K. Ferry, Phys. Rev. B 18, 7033 (1978).
16. H. M. van Driel, to be published.
17. T. C. Y. Leung, Ph.D. dissertation, University of Arizona, 1978.
18. J. R. Lindle, S. C. Moss, and A. L. Smirl, to be published.

APPENDIX A

PICOSECOND OPTICAL MEASUREMENTS OF
 FREE-CARRIER, INTERVALENCE-BAND, AND INDIRECT
 ABSORPTION IN GERMANIUM AT HIGH OPTICALLY CREATED CARRIER DENSITIES



Figure 1. Free-carrier absorption decay in Germanium at high carrier densities. The decay time is approximately 100 ps. The initial value is approximately 1.0, and the steady-state value is approximately 0.5.



Figure 2. Intervalence-band absorption decay in Germanium at high carrier densities. The decay time is approximately 100 ps. The initial value is approximately 1.0, and the steady-state value is approximately 0.5.

Picosecond optical measurement of free-carrier, intervalence-band, and indirect absorption in germanium at high optically created carrier densities

Arthur L. Smirl, J. Ryan Lindle, and Steven C. Moss

Department of Physics, North Texas State University, Denton, Texas 76203

(Received 6 March 1978; revised manuscript received 15 August 1978)

It has been suggested that enhanced intervalence-band and Coulomb-assisted indirect-absorption effects may be significant at the high optically created carrier densities encountered in the recent excite and probe experiments performed in germanium using intense picosecond optical pulses with a wavelength of $1.06\text{ }\mu\text{m}$, and that these processes may result in an absorption versus carrier-density curve containing a minimum. Such a curve could then be combined with a recombination process to explain the results of the excite and probe experiments. Here, we report measurement of the combined free-carrier, intervalence-band, and indirect absorbance in thin germanium samples during these excite and probe experiments by exciting at $1.06\text{ }\mu\text{m}$ and by probing both at $1.06\text{ }\mu\text{m}$ and with a Raman-generated probe at $1.55\text{ }\mu\text{m}$. The measurements suggest that these processes are significant at the high optically created carrier densities encountered in the present excite and probe experiments; however, they do not introduce a minimum in the absorption versus carrier-density curve as originally suggested.

1. INTRODUCTION

Recently, studies of the optical properties of high-density electron-hole plasmas generated in undoped germanium by intense ultrashort pulses have provided direct information concerning ultrafast electronic processes.¹⁻¹² Among these studies are the measurement of the enhanced transmission of single ultrashort optical pulses through germanium^{1,5} and the measurement of the temporal evolution of this enhanced transmission on a picosecond time scale using the excite and probe technique.^{3,5} In the first of these experiments, the nonlinear transmission of a single picosecond $1.06\text{-}\mu\text{m}$ pulse was investigated as a function of incident optical pulse energy for sample temperatures of

100 and 297 K. The resulting data, reproduced from Smirl *et al.*,⁵ are shown in Fig. 1 along with theoretical curves to be discussed later. In the second study, the sample was first irradiated by an excitation pulse of sufficient energy to cause the transmission of the germanium to be enhanced. This initial pulse was then followed at various time delays by a weak probe pulse, of the same wavelength, that measured the temporal evolution of the germanium transmission. Probable-pulse transmission data for various delay times and for sample temperatures of 100 and 297 K are presented in Fig. 2, again taken from Smirl *et al.*⁵ The latter mea-

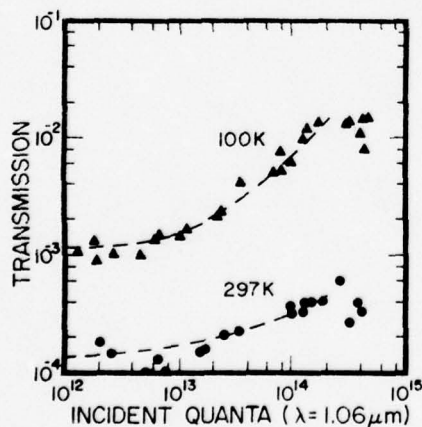


FIG. 1. Transmission of a $5.2\text{-}\mu\text{m}$ -thick germanium sample at $1.06\text{ }\mu\text{m}$ as a function of incident quanta at $1.06\text{ }\mu\text{m}$ for sample temperatures of 100 and 297 K. The dashed lines are theoretical curves from Elci *et al.* (Ref. 7). The data are from Smirl *et al.* (Ref. 5).

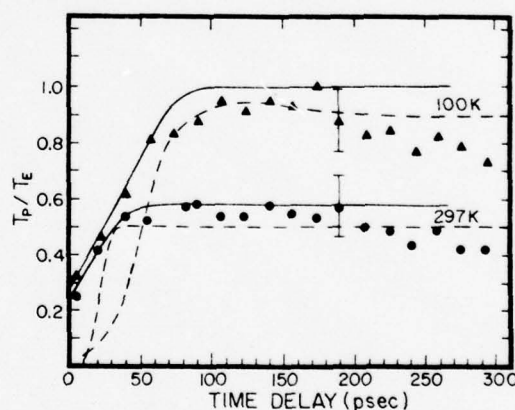


FIG. 2. Probe-pulse transmission vs delay between the excitation pulse at $1.06\text{ }\mu\text{m}$ and the probe pulse at $1.06\text{ }\mu\text{m}$ for sample temperatures of 100 and 297 K. The data are plotted as the normalized ratio of probe-pulse transmission to excitation-pulse transmission, T_p/T_e , arbitrary units. The dashed lines are theoretical curves from Elci *et al.* (Ref. 7). The solid lines are theoretical curves from van Driel (Ref. 15). The experimental data are from Smirl *et al.* (Ref. 5).

measurements reveal that the probe transmission increases for approximately 100 psec following excitation for a sample temperature of 100 K; however, the rise in probe transmission is less than 40 psec at 297 K. Originally, Shank and Auston³ attributed this rise in the probe transmission to a saturation of the absorption caused by a filling of the optically coupled conduction-band states and a depletion of the valence-band states by direct band-to-band transitions induced by the excitation pulse. Thus, the optically created carrier density, and consequently the increase in probe transmission, follows the integrated optical pulse energy. This interpretation was based on observations performed only at room temperature. As we shall later demonstrate, the rise in probe transmission at room temperature is indeed indistinguishable from other integration effects, in agreement with this interpretation. However, such a model cannot account for the slower rise observed at 100 K. Elci *et al.*,⁷ in a recently proposed model, have attributed this rise in the probe transmission to a cooling of a hot electron-hole plasma created by the excitation pulse. In sharp contrast to this interpretation, Auston *et al.*¹² have stated that they expect the energy relaxation time to be too short to account for the rise in probe transmission. Indeed, Auston and McAfee¹³ have suggested a plausible alternative explanation for the temporal evolution of the probe transmission in terms of enhanced Coulomb-assisted indirect absorption, intervalence-band absorption, and Auger recombination. This explanation does not require hot-electron effects.

Here, we report measurements of the combined free-carrier, intervalence-band, and indirect absorbance in thin germanium samples at a wavelength of 1.55 μm during excite and probe experiments at a wavelength of 1.06 μm . Our interests in these measurements are twofold. First, we want to ascertain whether or not free-carrier, intervalence-band, and indirect absorption effects are important in excite-probe experiments at 1.06 μm . Second, if these effects are important, can they, together with Auger effects, account for the rise in probe transmission.

In Sec. II, we briefly review the model presented by Elci *et al.*⁷ and emphasize the processes, or omission of processes, that are relevant to the present measurements. In addition, in Sec. III, we briefly describe a model suggested by Auston and McAfee¹³ that accounts for the rise in probe transmission without employing hot-electron effects. These reviews are then followed in Sec. IV by a description of the experimental apparatus and techniques for measuring the combined contributions of free-carrier, intervalence-band, and in-

direct absorption processes to the excite and probe response of germanium. Section V presents a discussion of our results, and the final section, Sec. VI, our conclusions.

II. COMMENTS ON THE HOT-ELECTRON MODEL

Briefly, according to the model proposed by Elci *et al.*,⁷ the transmission of a single optical pulse through a thin (5.2- μm -thick) germanium sample as a function of incident pulse energy (Fig. 1) and the transmission of a weak probe pulse as a function of time delay after an energetic pulse (Fig. 2) can be accounted for in terms of direct band-to-band absorption, free-carrier absorption, phonon-assisted intervalley scattering, phonon-assisted carrier relaxation, carrier-carrier collisions, and nonradiative recombination in the following manner. When an excitation pulse is incident on the germanium sample, the unreflected portion of the pulse enters the sample where most of it is absorbed by direct transitions, creating a large density of electrons (holes) in the central valley of the conduction (valence) band. The electrons are rapidly ($<10^{-14}$ sec) scattered to the conduction-band side valleys by long-wave-vector phonons. Carrier-carrier scattering events, which occur at a rate comparable to the direct absorption rate, ensure that the carrier distributions are Fermi-like and that both electron and hole distributions have the same temperature, which can be different from the lattice temperature. Since the photon energy $\hbar\omega_0$ is greater than either the direct energy gap E_0 or the indirect band gap E_G , such a direct absorption event followed by phonon-assisted scattering of an electron to the side valleys results in the photon giving an excess energy of $\hbar\omega_0 - E_G$ to thermal agitation. This excess energy results in an initial distribution temperature (approximately 1500 K for a lattice temperature of 300 K) due to direct absorption that is greater than the lattice temperature. Thus, the single-pulse transmission would begin at its Beer's-law value and increase as a function of incident optical pulse energy because of the partial filling (depletion) of the optically coupled states in the conduction (valence) band as a result of direct absorption. Other processes such as free-carrier absorption and nonradiative recombination events (i.e., Auger and plasmon-assisted recombination) can further raise the carrier temperature during the passage of the excitation pulse, while phonon-assisted intravalley relaxation processes can reduce the carrier temperature.

After the passage of the excitation pulse, the interaction region of the sample contains a large number of carriers (10^{19} – 10^{20} cm^{-3}) with a high

distribution temperature. The final temperature is determined by the number of quanta in the excitation pulse and the relative strengths of the non-radiative recombination and the phonon-assisted relaxation rates as discussed by Latham *et al.*¹⁰ As time progresses, the distribution will continue to cool by phonon-assisted intravalley relaxation. Experimentally, the probe pulse interrogates the evolution of the distribution after the passage of the excitation pulse and is a sensitive measure of whether the optically coupled states are available for absorption or are occupied. Immediately after the passage of the excitation pulse, the probe transmission is small since the electrons (holes) are located high (low) in the conduction (valence) bands because of the high distribution temperature, leaving the states that are optically coupled available for direct absorption. Later, as the distribution temperature cools and carriers fill the states needed for absorption, the transmission increases. The subsequent slow fall in probe transmission at longer delays, as seen in Fig. 2, is attributed to carrier recombination, which reduces the carrier density and once again frees the optically coupled states for absorption, and to diffusion.^{3,11}

The theoretical fits from Elci *et al.*⁷ to the single-pulse-transmission data and probe-pulse data are shown as dashed lines in Fig. 1 and Fig. 2. Given the complexity of the problem, the overall fit can be regarded as satisfactory. Nonlinear transmission measurements in which the energy band gap of the germanium sample was tuned by hydrostatic pressure⁸ have been accounted for by this model as well.

Despite the apparent successes of this model, some basic questions remain concerning the roles of the various physical processes in determining the saturation and temporal evolution of the optical transmission of thin germanium samples under intense optical excitations. Elci *et al.*⁷ noted that their calculations included only a limited number of the possible electronic interactions and contained serious assumptions that warranted further theoretical and experimental investigation. The major assumptions were the following: (i) The carrier-carrier collision rate was assumed to be high enough to justify taking the carrier distributions to be Fermi-Dirac. Ferry¹⁴ has recently re-examined this approximation by calculating the time and energy dependence of the distribution function at the high carrier photogeneration rates encountered here. He concludes that on a time scale of tens of picoseconds the distribution function does indeed approximate a Fermi distribution; however, on shorter time scales it contains a δ -function-like spike located at the optically coupled

states. Thus, for purposes of calculating the probe-pulse transmission, one may reasonably assume the distribution is Fermi-like. (ii) Carrier Fermi energies and temperatures were taken to depend only on time, rather than on both space and time, thus ignoring the pulse-propagation and carrier-diffusion problems within the optical interaction region of the sample. Therefore, parameters describing the electron-hole plasma, such as the electron number, must be viewed as spatial averages throughout the sample volume. Elci *et al.*¹¹ have recently extended their previous model, through a simple calculation, to indicate the possible effects of carrier diffusion on these optical measurements.

Elci *et al.*⁷ noted at the outset that their work contained only a few of the many possible electronic interactions. Recent studies^{4,12-14} indicate that processes other than those named above may be important. Most of these effects, such as band-gap narrowing,¹⁴ intervalence-band absorption,¹³ Auger recombination⁴ and Coulomb-assisted indirect absorption,¹² are only observed at large carrier densities. The possible importance of including these processes in any interpretation of the rise in probe transmission is demonstrated in the following sections. One of the main objectives of the present study is to investigate the effects of the combined intervalence-band, Coulomb-assisted indirect, and free-carrier absorption and Auger recombination on the excite and probe measurements at 1.06 μm .

In the previous two paragraphs, we have outlined the assumptions and omissions of the initial hot-electron model; however, there is another problem associated with the original calculations that is of importance to the present work. The physical constants for germanium, specifically the electron-phonon coupling constants, are not well-known enough to allow a precise calculation of the energy relaxation rate. Latham *et al.*¹⁰ have previously discussed this point in detail. For the theoretical fits shown in Fig. 2, the electron-phonon coupling constants are chosen as 6×10^{-4} erg cm^{-1} for a lattice temperature of 297 K and 2×10^{-4} erg cm^{-1} at 100 K. These values are within the range of the accepted theoretically and experimentally determined values listed by Latham *et al.*¹⁰; however, they are much lower than the mean value of 1×10^{-3} erg cm^{-1} as obtained from an average of the eight values listed. Since the carrier cooling rate is proportional to the square of the electron-phonon coupling constant, the fitted values result in carrier cooling rates that are 3 and 25 times slower than that obtained by using the average value. In fact, a repetition of the original calculations substituting the average electron-phonon coupling

constant shows (see Latham *et al.*,¹⁰ (Fig. 8) that carrier cooling is too rapid to account for the rise in probe transmission, in complete agreement with the claims by Auston *et al.*¹² However, van Driel¹⁵ has recently calculated the influence of hot phonons on the carrier-energy relaxation rate in these problems. These calculations suggest that the long equilibration time for the hot carriers is due to a relaxation bottleneck produced by a buildup of the optical-phonon population on a picosecond time scale. The results of these calculations, taking into account optical-phonon heating and employing only a single average temperature-independent electron-phonon coupling constant, are shown as solid curves in Fig. 2. Note that the inclusion of hot phonons accounts for one of the major discrepancies between the original theory and experiment. Namely, in contrast to the original theory that predicted a delayed, steep rise, the present theory shows a steep rise with gradual leveling off in agreement with the data. The solid curves in Fig. 2 were taken directly from van Driel.¹⁵ The agreement between the modified theory and experiment is remarkable; however, this agreement should be regarded as somewhat fortuitous in view of the simplifications of the model, the limited number of processes included, and the uncertainty in many of the physical constants.

For emphasis, we now summarize the principal points of this section: (i) According to Elci *et al.*, the rise of the optical transmission of the germanium with time as monitored by a weak probe pulse is attributed to the cooling of a hot-electron-hole plasma, created by the absorption of the excitation pulse. (ii) In view of the above discussions and in the absence of any direct experimental evidence, the authors regard the question of the magnitude of the energy relaxation rate and the question of the origin of the rise of the probe transmission as open. It is in this spirit of suggesting plausible alternative models for evaluation that McAfee and Auston¹³ first suggested the possibility of describing the rise in probe transmission in terms of free-carrier, intervalence-band, and Coulomb-assisted indirect absorption together with Auger recombination. This model is reviewed in Sec. III.

III. INDIRECT, INTERVALENCE-BAND, AND FREE-CARRIER ABSORPTION AND AUGER RECOMBINATION

In direct contrast to the above model, Auston and McAfee¹³ have recently suggested an alternative explanation for the delayed probe-pulse transmission in germanium without requiring the introduction of hot-electron effects. In fact, their suggested explanation is based on three of the processes neglected by the original calculations of

Elci *et al.*: Auger recombination, Coulomb-assisted indirect absorption, and intervalence-band absorption. Specifically, this model is based on experiments by Auston *et al.*,⁴ on 300- μm -thick samples, that are interpreted as demonstrating that Auger-recombination effects are important on picosecond time scales; on the observation of enhanced indirect Coulomb-assisted absorption in heavily doped *n*-type germanium by Haas¹⁶; and on the observation of strong intervalence-band absorption between the light- and heavy-hole and split-off valence bands in *p*-type germanium by Newman and Tyler.¹⁷ Since the present work is an attempt to experimentally investigate the role of these processes in determining the evolution of the optical properties of germanium at high carrier densities, we shall briefly state the conclusions of these last two works. We then review the manner in which enhanced indirect absorption and intervalence-band absorption together with Auger recombination could account for the probe transmission versus time delay after an intense excitation pulse in thin germanium samples.

Haas¹⁶ reports that the indirect absorption rises more rapidly with photon energy in *n*-type germanium than in pure germanium. The effects considered as sources for this extra absorption are (i) modification of the band structure by impurities, (ii) impurity-assisted indirect transitions, and (iii) Coulomb-assisted indirect transitions, where the virtual scattering of the electrons from the central to the side valley is by electron-electron scattering. Haas concludes that at high concentrations electron-electron scattering dominates the indirect transitions. If we extrapolate his results, they suggest that, at an optical wavelength of 1.06 μm and electron densities as large as $2 \times 10^{20} \text{ cm}^{-3}$, the indirect-absorption coefficient might be as large as 10^4 cm^{-1} .

Newman and Tyler¹⁷ report measurement of the free-hole absorption in *p*-type germanium as a function of impurity and carrier concentration. The effects to be considered in explaining the strong observed free-hole absorption at high carrier concentrations are (i) modification of the band structure by impurities, (ii) band-to-band transitions between light- and heavy-hole valence bands and the split-off valence band as the position of the Fermi level changes within the valence band with doping, and (iii) indirect transitions induced by charged-impurity centers. They conclude that their observations suggest that both intervalence band transitions and impurity-assisted indirect transitions contribute. In experiments employing undoped samples, where the carriers are generated by optical absorption, only the *intervalence-band* process will be significant. If their results

are extrapolated to a photon energy of 1.17 eV and a concentration of $2 \times 10^{20} \text{ cm}^{-3}$, the free-hole absorption coefficient could again be as large as 10^4 cm^{-1} .

The suggestion of an alternative explanation for the delayed probe transmission of optically excited germanium without requiring phonon-assisted relaxation of hot electrons is based on the two mechanisms discussed above. In particular, it is based on the details of the way germanium absorption might vary with increasing optically created carrier density. Consider the behavior of the total absorption coefficient as the carrier density increases because of band-to-band transitions during the passage of an intense excitation pulse. (The carrier temperature is taken to be that of the lattice, since all carrier energy relaxation processes are assumed to be too rapid for observation, in contrast to Elci *et al.*⁷) The direct absorption coefficient will decrease with increasing density as optically created electrons (holes) clog the states needed for optical absorption in the conduction (valence) band. Meanwhile, as the density increases, the additional mechanisms discussed previously, Coulomb-assisted indirect absorption, intervalence-band absorption, and free-carrier absorption, increase. Thus, the absorption coefficient could initially decrease with increasing density, as the direct absorption coefficient saturates, then increase with increasing density, as the free-carrier, intervalence-band, and indirect absorption coefficients dominate. In short, the fact that the direct absorption coefficient decreases with increasing carrier number and that the enhanced intervalence-band, free-carrier, and Coulomb-assisted indirect absorption coefficients increase can result in introducing a minimum in the absorption versus density relationship as suggested by Auston *et al.*¹² We denote the density at which the minimum absorption might occur as n_{\min} . The rise in the probe transmission with time can now be accounted for by combining the details of the way the absorption saturates with carrier density together with a monotonic decrease in carrier density with time due to Auger recombination in the following manner. The absorption of the excitation pulse creates an initial carrier density greater than n_{\min} . As the carrier density is decreased by Auger recombination, the absorption coefficient of the sample will decrease in time until the carrier density reaches n_{\min} , then increase. Thus, the probe transmission will increase then decrease if the initial, optically created carrier density is greater than n_{\min} . We shall henceforth refer to the model described in this section as the recombination model because of the role of the Auger recombination.

For emphasis, we summarize the features of the two models that are essential for comparison with present measurements. We note, once again, that Elci *et al.*⁷ attribute the rise in probe transmission with delay after an excitation pulse to phonon-assisted cooling of a hot carrier distribution and that free-carrier, intervalence-band, and Coulomb-assisted indirect transitions were either omitted from the model or judged to be insignificant. Auger-recombination processes were omitted from this model. The recombination model accounts for the rise in probe transmission by combining Auger recombination with an absorption versus density relationship containing a minimum. We stress that the success of the second model, as it now stands, depends on the absorption decreasing then increasing with carrier density: *there must be an absorption minimum.*

IV. EXPERIMENT

The particular experimental configuration used to measure the contributions of intervalence-band, free-carrier, and indirect absorption to the generation and evolution of dense, optically created electron-hole plasmas in thin germanium samples is depicted in Fig. 3. This arrangement is similar to the arrangement utilized by Auston *et al.*⁴ In this application of the excite and probe technique, a high-density plasma is created by direct absorption of an intense excitation pulse, and the evolution of the plasma is monitored by a second probe pulse. The excitation pulses were selected by a laser-triggered spark gap and a Pockel's cell from trains of pulses produced by a mode-locked Nd-glass laser. The pulses were 5 to 10 psec in duration and had peak powers of approximately 10^8 W at a wavelength of $1.06 \mu\text{m}$, and they produced a measured irradiance of approximately $1 \times 10^{-2} \text{ J/cm}^2$ when focused on the crystal surface. The

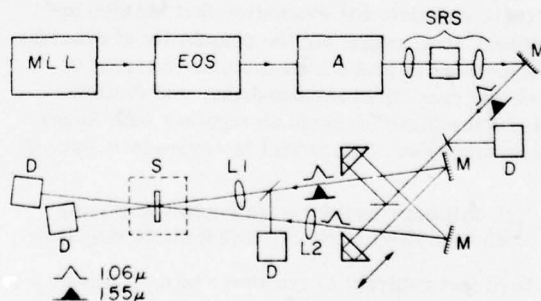


FIG. 3. Block diagram of the experimental configuration for excite and probe measurements at 1.06 and 1.55 μm , where MLL denotes the mode-locked laser, EOS the electro-optical switch, A the laser amplifier, SRS the stimulated-Raman-scattering cell, M a mirror, D a detector, L1 and L2 lens, and S the sample.

plasma produced by the absorption of the excitation pulse was probed using weak pulses of two types: one had an energy greater than the direct energy band gap for germanium, and the other had an energy less than the direct gap but greater than the indirect gap. The former was derived from the excitation pulse using a beam splitter as shown in Fig. 3. The latter, having a wavelength of 1.55 μm , was produced by stimulated Raman scattering in benzene. The desired probe wavelength was selected by employing either a thick wafer of silicon to reject the 1.06- μm radiation or narrow band-pass optical filters to reject the 1.55- μm radiation. Other wavelengths generated by the stimulated scattering in benzene, such as 1.18 μm , were rejected by carefully selected interference filters. We emphasize that the energy of a quanta at 1.06 μm (1.17 eV) is sufficient to excite direct band-to-band transitions in germanium as well as free-carrier, intervalence-band, and indirect transitions; whereas, the energy of a quanta at 1.55 μm (0.80 eV) falls below the direct band gap but above the indirect gap and is, thus, only a measure of the combined free-carrier, intervalence-band, and indirect processes. The incident excitation pulse irradiance was measured and the overlap of excitation and probe pulses was ensured employing techniques described in Ref. 4. The excitation pulse irradiance was determined by measuring the energy transmitted through a pinhole located at the focus of the excitation beam and coplanar with the germanium wafer using a calibrated detector. The probe beam was more tightly focused than the excitation beam to ensure complete spatial overlap with the excitation beam. The size of the pinhole was such that it transmitted 50% of the excitation pulse and 90% of the probe. Despite these precautions, we observed indications of day-to-day variations in excitation-beam and probe-beam overlap. We attribute these variations to "hot" spots in the focused multimode laser pulses.

The germanium sample was a high purity ($\rho_{\text{min}} = 40 \Omega \text{ cm}$) single crystal cut with the (111) plane as face. The sample was polished and etched with Syton to a thickness of 6 μm as determined by interferometric techniques.

V. RESULTS AND DISCUSSION

Here, we present and discuss the results of three separate measurements. (i) In the first of these, the sample is illuminated by an intense excitation pulse at a wavelength of 1.06 μm . The transmission of a weak probe pulse at 1.06 μm that arrives at a variable, delayed time after the excitation pulse is then monitored. We perform these measurements, which repeat those by Smirl *et al.*,⁵ to

ensure that the rise in probe transmission can be separated from any artifacts of the measurement technique. (ii) Next, the sample is irradiated by 1.06- μm -excitation pulses of various intensity that create electron-hole plasmas of varying density by direct band-to-band transitions. The change in absorbance at 0.80 and 1.17 eV, as a function of plasma density, is then measured by monitoring the transmission of weak probe pulses at 1.55 and 1.06 μm that arrive a short fixed delay after excitation. These 1.06- μm -probe transmission measurements will provide the absorbance versus density curve needed for investigation of the recombination model described in Sec. III. The 1.55- μm -probe measurements will give a measure of the importance of free-carrier, intervalence-band, and indirect absorbance as a function of carrier density. (iii) Finally, the transmission of a weak 1.55- μm -probe pulse is measured at various delays following an intense 1.06- μm -excitation pulse. The 1.55- μm -probe pulse monitors the temporal evolution of the change in the combined free-carrier, intervalence-band, and indirect absorbance following the photogeneration of a dense electron-hole plasma.

The results of experiments that measure the temporal evolution of the transmission of a thin germanium sample at a wavelength of 1.06 μm following the creation of a dense electron-hole plasma are shown in Fig. 4. The measurements were performed in the following manner (see insert, Fig. 4). The sample was irradiated by 1.06- μm -excitation pulses containing approximately 2×10^{15} quanta, and the transmission of each pulse was measured. Each excitation pulse was then followed

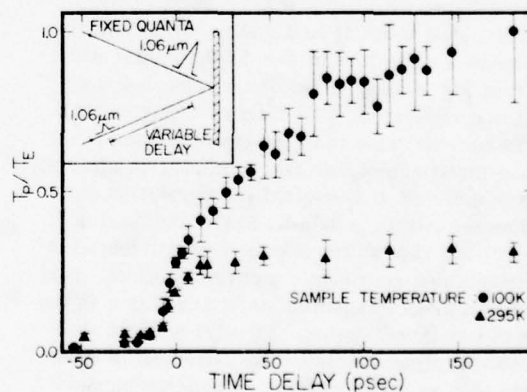


FIG. 4. Probe-pulse transmission vs delay between the excitation pulse at 1.06 μm and the probe pulse at 1.06 μm for sample temperatures of 100 and 295 K. The data are plotted as the normalized ratio of probe-pulse transmission to excitation-pulse transmission, T_P/T_E , in arbitrary units. The error bars represent one statistical standard deviation.

at various delays by a weak probe pulse at $1.06 \mu\text{m}$. These measurements were performed for sample temperatures of 100 and 295 K. The data are plotted as the ratio of probe-pulse transmission T_p to excitation-pulse transmission T_E , in arbitrary units, versus time delay in picoseconds. The arbitrary units are chosen so that the peak of the probe transmission at 100 K is unity. The actual value of the ratio T_p/T_E was observed to be as large as six; however, this value strongly depends on the quality of the spatial overlap of the focused excitation and probe pulse on the sample surface. These measurements are identical to those performed by Smirl *et al.*, as presented in Fig. 2. However, when comparing the two sets of data, one must realize that the sample thickness and focused optical spot sizes are not identical.

The measurements of Smirl *et al.*³ are repeated so that we can more carefully investigate the possibility that the rise in probe transmission follows the integrated optical energy. Specifically, we want to be assured that the rise in probe transmission is a real effect and that it is not an artifact of the excite-probe technique that can be attributed to the finite width of the optical pulses. For comparison, we have calculated the probe-pulse transmission by assuming a Drude model for the electron-hole plasma, calculating the optical polarization, and substituting into the wave equation. The details of such a procedure are published elsewhere,^{3,18} and they are not repeated here. The calculated rise in the probe-pulse transmission, neglecting all decay processes, is simply proportional to the integral of the pulse autocorrelation function. The resulting theoretical integration curve assuming Gaussian-shaped optical pulses of 10-psec width [full width at half maximum (FWHM)] is shown as a solid line in Fig. 5. Experimental data from Fig. 4 are plotted on an expanded time scale for comparison. The authors conclude that the experimental rise in probe transmission at 295 K is indistinguishable from integration effects, in agreement with the original interpretation of the room temperature data by Shank and Auston.³ However, the rise at 100 K cannot be attributed to such effects and represents a physical effect. It is this rise in probe transmission at 100 K that is the object of our investigation. Finally, we note that coherent coupling effects^{3,18} are observed in these experiments as well; however, the delay increments of Fig. 5 are too coarse to resolve them.

The results of the measurement of the change in absorbance of the thin germanium crystal as a function of increasing carrier number (incident excitation pulse energy at $1.06 \mu\text{m}$) are shown in Fig. 6 for photon energies of 1.17 and 0.8 eV. These data were obtained in the following manner.

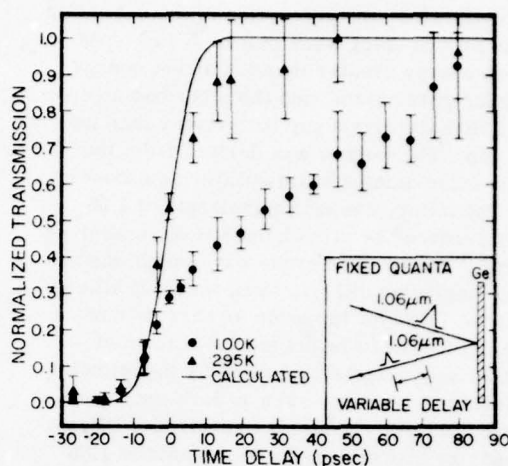


FIG. 5. Normalized probe-pulse transmission in arbitrary units vs delay between the excitation pulse at $1.06 \mu\text{m}$ and the probe pulse at $1.06 \mu\text{m}$ for sample temperatures of 100 and 295 K. The solid line represents a theoretical integration curve assuming Gaussian-shaped optical pulses of 10 psec width (FWHM).

The crystal was illuminated by variable energy pulses with a wavelength of $1.06 \mu\text{m}$, and the transmission of each pulse was measured. Each pulse at $1.06 \mu\text{m}$ was followed immediately (at fixed delays of 17 and 26 psec) by pulses that monitored the absorbance of the crystal at wavelengths of 1.55 and $1.06 \mu\text{m}$. The optical absorbance at 1.17 eV is seen to decrease by approximately 3.5 as the carrier number increases. This corresponds to a transmission increase by a factor of 30. By contrast, the absorbance at 0.8 eV increases

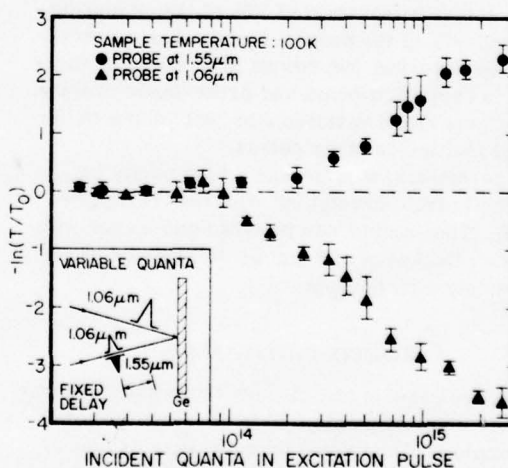


FIG. 6. Change in absorbance, $-\ln(T/T_0)$, of the germanium sample at 1.06 and $1.55 \mu\text{m}$ as a function of incident excitation-pulse energy at $1.06 \mu\text{m}$ where T_0 is the linear transmission of the sample at the wavelength under consideration.

roughly by 2.3, corresponding to a *decrease* in transmission by approximately an order of magnitude. Each datum point shown is the average of at least eight separate observations. The data were very reproducible within the error bars.

A striking feature of the data presented in Fig. 6 is that the absorbance of the crystal at 1.06 μm *does not decrease then increase* as required by the recombination model of Sec. III. In fact, as can be seen from Fig. 6, any *decrease* in carrier density with time caused by carrier recombination will be accompanied by an *increase* in the total absorbance at 1.06 μm . Thus, a temporal decay of carrier density alone cannot be combined with the absorption versus density relationship to account for the rise in probe transmission at 1.06 μm . The *total* change in absorbance of the crystal at 1.06 μm as the carrier density is increased is given by

$$-\ln\left(\frac{T}{T_0}\right) = \int_0^l \Delta\alpha_{\text{DA}}(x) dx + \int_0^l [\Delta\alpha_{\text{FC}}(x) + \Delta\alpha_{\text{IB}}(x) + \Delta\alpha_{\text{ID}}(x)] dx, \quad (1)$$

where T_0 is the linear transmission of the sample; $\Delta\alpha_{\text{DA}}(x)$ is the change in the direct-absorption coefficient caused by the increased carrier number at the position x into the crystal; $\Delta\alpha_{\text{FC}}(x)$, $\Delta\alpha_{\text{IB}}(x)$, and $\Delta\alpha_{\text{ID}}(x)$ are the changes in the absorption coefficient caused by free-carrier, intervalence-band, and indirect absorption, respectively; and l is the crystal thickness. The electron density and, consequently, the absorption coefficients are allowed to depend upon position. The last term on the right-hand side of Eq. (1) will be positive since free-carrier, intervalence-band, and Coulomb-assisted indirect absorption coefficients all increase with carrier density, and the first will be negative because of the partial saturation of the available optically coupled electronic states as the density increases. Since the overall absorbance at 1.17 eV is observed to monotonically decrease, we conclude that the saturation of the absorption is dominated by changes in the direct absorption coefficient. Although the free-carrier, intervalence-band, and indirect absorbance changes are smaller in magnitude and opposite in sign to those caused by saturation of the direct absorption, it is possible for them to significantly affect the overall magnitude of the total absorbance change. Inspection of Eq. (1) reveals that omission of these processes would result in a more rapid decrease in total absorbance with increasing carrier number than when they are included.

The measurement of the change in absorbance at 0.8 eV as the carrier number is increased by direct absorption of excitation pulses at 1.17 eV, as

displayed in Fig. 6, tends to substantiate the arguments of the previous paragraph. That is, the change in absorbance at 0.8 eV, which is sensitive to free-carrier, intervalence-band, and indirect absorption effects, is slightly smaller in magnitude and opposite in sign to that measured at 1.17 eV, which is sensitive to direct absorption effects as well. Thus, if the results of the measurement of free-carrier, intervalence-band, and indirect absorbance at 0.8 eV could be extrapolated to 1.17 eV, we would conclude that the change in absorbance due to these processes is smaller in magnitude and opposite in sign to that caused by the saturation of direct absorption coefficient. However, we would also conclude that the change in the *combined* free-carrier, intervalence-band, and indirect absorbance is of sufficient magnitude to substantially slow the saturation of the total absorbance at 1.06 μm with the increasing carrier number. However, care must be taken when extrapolating absorbance measurements at 0.8 to 1.17 eV. Free-carrier and intervalence-band absorption coefficients are expected to decrease with increasing photon energy for a given (large) carrier density¹⁷ while, according to Ref. 16, the Coulomb-assisted indirect absorption coefficient should increase.

The experiments shown schematically in the inset of Fig. 6 were repeated for a sample temperature of 295 K. Similar results were obtained. For the maximum carrier densities achieved at room temperature, the decrease in absorbance at 1.06 μm was 2.2 and the increase in absorbance at 1.55 μm was 1.8.

The results of excite-probe experiments that measure the temporal evolution of the change in absorbance at 1.55 μm are presented in Fig. 7. In this experiment, the sample was irradiated by

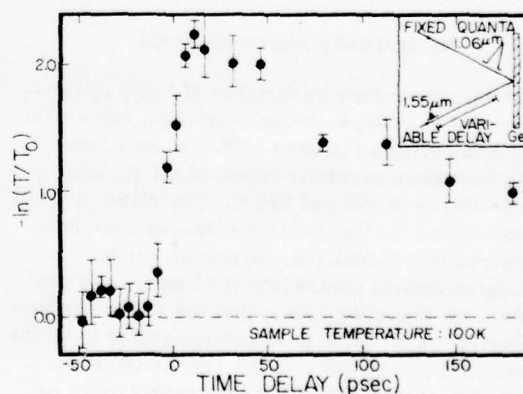


FIG. 7. Change in probe-pulse absorbance, $-\ln(T/T_0)$, vs delay between the excitation pulse at 1.06 μm and the probe pulse at 1.55 μm , where T_0 is the linear transmission of the probe pulse at 1.55 μm .

an optical pulse at 1.06 μm containing roughly 2×10^{15} quanta and was probed at various delays by a weak pulse having a wavelength of 1.55 μm . The results of the probe measurements at 1.55 μm are similar to those obtained by Auston *et al.*⁴ However, these authors stated that they performed their measurements at excitation intensities such that the absorption of the excitation pulse was *linear*. Our experiments are clearly performed in the *nonlinear* region. In addition, the measurements of Auston *et al.*⁴ were performed on a 300- μm -thick sample, our sample was 6- μm thick.

The measurements presented in Fig. 7 indicate that free-carrier, intervalence-band, and indirect absorption can be significant at the carrier densities encountered during the excite and probe experiments at 1.06 μm presented here. Auston *et al.*⁴ attribute this decrease of the probe pulse absorbance at 1.55 μm with delay to a decrease in free-carrier absorption caused by a temporal decay in carrier density due to Auger recombination. The present experiments only allow the measurement of the change in the combined free-carrier, intervalence-band, and indirect absorbance, and they do not provide for a convenient separation of their individual contributions. These measurements were performed for a sample temperature of 295 K, as well. The results are similar to those of Fig. 7. It is important to note that we observe a strong temperature dependence in the rise in probe transmission at 1.06 μm (see Fig. 4 or 5); however, we do not observe a similar *strong* temperature dependence at 1.55 μm . We believe this is a further indication that indirect, free-carrier, and intervalence-band processes do not dominate the rise in probe transmission at 1.06 μm .

VI. SUMMARY AND CONCLUSIONS

The measurements by Smirl *et al.*³ of the transmission of a 1.06- μm -probe pulse as a function of time delay after an intense 1.06- μm -excitation pulse have been carefully repeated for sample temperatures of 100 and 295 K. The rises in probe transmission for the two temperatures have been compared to a calculated integration curve, assuming an optical pulsewidth of 10 psec. We conclude from this comparison that the rise in probe transmission at 295 K is indistinguishable from the integration curve, but that the rise at 100 K is much slower than either the integration curve or the rise at 295 K and is not an artifact of the measurement technique.

The transmission of a thin germanium sample at 1.55 and 1.06 μm has been measured as a function

of optically created carrier densities. Over the range of densities encountered in these experiments, the absorption versus density relationship at 1.17 eV *does not* exhibit a minimum. Thus, a temporal decay of carrier density alone cannot be combined with this absorption versus density relationship to account for the rise in probe transmission at 1.06 μm exactly as suggested in Sec. III. In addition, these measurements indicate that the combined free-carrier, intervalence-band, and indirect absorbance changes are opposite in sign and smaller in magnitude than the changes caused by saturation of the direct absorption. As a result, we believe that the decrease in absorbance at 1.06 μm with increasing carrier number is dominated by a saturation of the direct absorption coefficient; however, the rate of this decrease in absorbance is slowed by the contributions of these "other" processes that are opposite in sign.

In addition, the absorbance of a 1.55- μm -probe pulse has been measured as a function of time delay after an intense 1.06- μm -excitation pulse. The 1.55- μm -probe absorbance decays by approximately 0.8 in the first 100 psec following excitation, corresponding to a transmission increase of a factor of approximately 2. This represents a significant decay in the combined free-carrier, intervalence-band, and indirect absorbance during this period. Contrary, however, to measurements of the probe rise at 1.06 μm , the decay of probe absorbance at 1.55 μm exhibited no strong dependence on sample temperature.

As a result of the present measurements, the authors feel that free-carrier, intervalence-band, and Coulomb-assisted transitions combined with Auger recombination are not the mechanisms dominating the rise in 1.06- μm -probe transmission at 100 K. The contributions of these processes are significant, however, and they must be accounted for by any successful model. Unfortunately, the present measurements yield no *direct* information concerning carrier distribution temperatures or energy relaxation rates, and the question of attributing the rise in 1.06- μm -probe transmission to a cooling of a hot carrier plasma created by the excitation pulse remains unresolved.

Finally, we emphasize that we are aware that our measurements at 1.55 μm (0.8 eV) monitor the free-carrier, free-hole, and indirect absorption at an energy different from that of the experiments we are attempting to interpret (rise in probe transmission at 1.17 eV); however, we believe these experiments give the best available indication of the possible importance of these processes at the high optically created carrier densities encountered in excite and probe studies at 1.06 μm .

ACKNOWLEDGMENTS

The authors wish to acknowledge their debt to Dave Auston and Sigrid McAfee of Bell Laboratories for suggesting and sharing the recombination

model presented in this paper and for their helpful discussions. This work was supported by the Office of Naval Research and the North Texas State University Faculty Research Fund.

- ¹C. J. Kennedy, J. C. Matter, A. L. Smirl, H. Weichel, F. A. Hopf, and S. V. Pappu, *Phys. Rev. Lett.* **32**, 419 (1974).
- ²D. H. Auston and C. V. Shank, *Phys. Rev. Lett.* **32**, 1120 (1974).
- ³C. V. Shank and D. H. Auston, *Phys. Rev. Lett.* **34**, 479 (1975).
- ⁴D. H. Auston, C. V. Shank, and P. LeFur, *Phys. Rev. Lett.* **35**, 1022 (1975).
- ⁵A. L. Smirl, J. C. Matter, A. Elci, and M. O. Scully, *Opt. Commun.* **16**, 118 (1976).
- ⁶H. M. van Driel, A. Elci, J. S. Bessey, and M. O. Scully, *Opt. Commun.* **20**, 837 (1977).
- ⁷A. Elci, M. O. Scully, A. L. Smirl, and J. C. Matter, *Phys. Rev. B* **16**, 191 (1977).
- ⁸H. M. van Driel, J. S. Bessey, and R. C. Hanson, *Opt. Commun.* **22**, 346 (1977).
- ⁹J. S. Bessey, B. Bosacchi, H. M. van Driel, and A. L. Smirl, *Phys. Rev. B* **17**, 2782 (1978).
- ¹⁰W. P. Latham, Jr., A. L. Smirl, and A. Elci, *Solid State Electron.* **21**, 159 (1978).
- ¹¹A. Elci, A. L. Smirl, C. Y. Leung, and M. O. Scully, *Solid State Electron.* **21**, 141 (1978).
- ¹²D. H. Auston, S. McAfee, C. V. Shank, E. P. Ippen, and O. Teschke, *Solid State Electron.* **21**, 147 (1978).
- ¹³This model was first discussed by D. H. Auston and

S. McAfee at the International Conference on Hot Electrons in Semiconductors, July 6-8, 1977, Denton, Texas (unpublished). The possible importance of enhanced Coulomb-assisted indirect transitions to the interpretation of experiments at high optical excitations and the possibility of these indirect transitions introducing a minimum in the absorption versus density relationship was first discussed in Ref. 12 by D. H. Auston, S. McAfee, C. V. Shank, E. P. Ippen, and O. Teschke. The details of the model as presented here are courtesy of S. McAfee and D. H. Auston (private communication). This model was presented by Auston and McAfee in the spirit of illustrating that processes other than those considered by Elci *et al.* (Ref. 7) could be important in interpreting the rise in probe transmission. We thought the model so attractive as to deserve investigation. As a result of their informal remarks, the authors undertook the present studies.

¹⁴D. K. Ferry (unpublished).

¹⁵H. M. van Driel (unpublished).

¹⁶C. Haas, *Phys. Rev.* **125**, 1965 (1962).

¹⁷R. Newman and W. W. Tyler, *Phys. Rev.* **105**, 885 (1957).

¹⁸E. P. Ippen and C. V. Shank, in *Ultrashort Light Pulses*, edited by S. L. Shapiro, (Springer-Verlag, New York, 1977), p. 110.

APPENDIX B

THE EFFECTS OF PARAMETRIC SCATTERING, ENERGY-GAP NARROWING, AND STATE FILLING ON THE OPTICAL RESPONSE OF GERMANIUM

The Effects of Parametric Scattering, Energy-Gap Narrowing,
and State Filling on the Picosecond Optical
Response of Germanium

J. Ryan Lindle, Steven C. Moss, and Arthur L. Smirl

Department of Physics
North Texas State University
Denton, Texas 76203

ABSTRACT

Recently the nonlinear, nonequilibrium optical properties of germanium at a wavelength of $1.06\text{ }\mu\text{m}$ have been studied on a picosecond time scale by employing the excite and probe technique. In addition to structure in the probe transmission vs. delay lasting many tens of picoseconds, investigators have observed a narrow spike in the probe transmission occurring near zero delay and having a width less than the optical pulse width of 11 psec. This spike has been attributed by some to a parametric scattering of the intense excitation pulse into the probe beam path by a grating created on the sample surface by the interference of the two beams and by others to the combined effects of state filling and band-gap narrowing. Although it is likely that both effects occur to some degree, we present the results of measurements that indicate that parametric scattering fully accounts for the observed spike. No contribution from state filling and band-gap narrowing is observed.

1. INTRODUCTION

Recently, picosecond excite and probe techniques have been utilized to measure the nonlinear, nonequilibrium optical properties of germanium in an effort to obtain information concerning ultrafast carrier relaxation processes at high optically-created carrier densities.¹⁻¹³ Specifically, in the studies of interest here,^{1,3,5} the sample is first irradiated by an 11 psec excitation pulse at 1.06 μm . The absorption of the excitation pulse creates a large, rapidly evolving, nonequilibrium carrier distribution that changes the transmission properties of the sample. This initial pulse is then followed at various time delays by a weak probe pulse of the same wavelength that monitors the evolution of the enhanced germanium transmission with time. A graph of the probe pulse transmission versus time exhibits two distinct features. The first is a rapid rise and fall in the probe transmission. This narrow spike in probe transmission is approximately two picoseconds wide and is centered about zero delay. This spike is followed by a gradual rise and fall of the probe transmission lasting hundreds of picoseconds. This slower feature in the probe transmission has been the subject of other studies.^{5,7,12} Here, we are concerned with the origin of the sharp spike in probe transmission.

The narrow spike in probe transmission was first observed by Kennedy *et al.*¹ and was attributed by them to a saturation and relaxation of the direct absorption. Subsequently, Shank and Auston³ observed, in addition to the narrow spike near zero delay, the slower structure at longer delays.

In light of this additional structure, they reinterpreted the narrow spike in probe transmission near zero delay as a parametric coupling between excite and probe beams caused by an index grating produced by the interference of the two beams in the germanium sample. While admitting that some parametric scattering is bound to occur during such measurements, Ferry¹⁴ has recently presented numerical studies that account for the spike in germanium transmission in terms of state filling and band gap narrowing. If, indeed, these processes are responsible for the narrow rise and fall in probe transmission, a careful study of this structure should yield information concerning carrier scattering rates from the optically coupled states.

Here, we present the results of experiments that attempt to separate the roles of parametric scattering and state filling in determining the picosecond optical response of germanium.

The remainder of this paper is organized as follows. In the next section, we briefly review the manner in which parametric scattering can account for the spike in probe transmission. In Sec. 3, we do the same for state filling and band-gap narrowing. Section 4 contains a description of the experimental apparatus and techniques for measuring the contribution of parametric scattering to the spike in probe transmission. In Section 5, we present a discussion of our results, and finally in Sec. 6, our conclusions.

2. PARAMETRIC SCATTERING

In the picosecond excite and probe studies described above the excite and probe pulses are derived from a single pulse by means of a beam

splitter. Consequently, the probe pulse is simply an attenuated version of the excite pulse. Near zero delay, the excite and probe pulses are both spatially and temporally overlapped. As a result, the interference of the two beams will produce a modulation of the optically-created carrier density to form a grating with spacing $d = \lambda / (2 \sin \theta)$, where θ is the angle between each beam and the sample normal as shown in Fig. 1. The grating is formed rapidly and will diffract both excitation and probe pulses as shown in Fig. 1. The first order diffracted beams for both excite and probe are shown. Notice that one of the first order diffracted beams from the excitation pulse will be scattered into the direction of the probe pulse detector. Also, one of the first order diffracted beams from the probe pulse will be scattered into the direction of the excitation pulse detector. Since the probe pulse energy is only a small fraction of the excitation pulse energy, the amount of light diffracted from the probe pulse into the excitation pulse detector is insignificant. On the other hand, a small fraction of the excitation beam scattered in the direction of the probe detector can produce a signal on the probe detector larger than that produced by the transmitted probe pulse.

The sharp increase (spike) in the signal observed on the probe detector as the two pulses are delayed with respect to one another can then be understood in terms of this parametric scattering in the following manner. An increase in probe detector signal will be observed so long as a grating is produced. Such a grating will be formed only if the delay between excite and probe pulses does not exceed the coherence length of the two pulses. It is well known that pulses produced by

mode-locking glass lasers are usually correlated over a length less than their optical pulse width because of various nonlinear processes involved in pulse generation. Consequently, parametric scattering results in an increase in probe detector signal for time delays less than the optical pulse width. Thus, according to Shank and Auston,³ the narrow spike in probe transmission is not an increase in sample transmission at all but a scattering of the excite pulse into the probe pulse. Such transient gratings have been observed in semiconductors by other investigators,¹⁵ and we think it reasonable to expect their formation here.

Of course none of the arguments presented above in favor of the parametric scattering scheme preclude the possibility that other effects could also contribute to the spike. In fact, in the next section, we briefly review the model suggested by Ferry¹⁴ that accounts for the spike in terms of state filling and band gap narrowing.

3. STATE FILLING

Direct absorption of the excitation pulse deposits electrons high in the conduction band, leaving holes in the valence band. Since both excitation and probe pulses are approximately monochromatic, a very narrow set of states in the valence band is optically coupled to a narrow set of states in the conduction band. The optically-excited carriers are initially deposited in these states. They are rapidly scattered from them by carrier-carrier collisions, intervalley phonon-assisted scattering, and intravalley phonon-assisted scattering. The number of carriers occupying the optically coupled states at any given time is

determined by the relative strengths of the optical generation rate into the states and of the combined scattering rates out. This state filling results in a delta-function-like spike in the distribution function located at the optically coupled states. If the generation rate exceeds the scattering-out rates, then the optically coupled states are partially filled, and the instantaneous transmission of the germanium will increase for the period of time that the excitation pulse is present in the sample.

The evolution of the germanium transmission is not as simple as we have just indicated; it is complicated by energy band-gap narrowing at the high carrier densities created by the excitation pulse. As the excitation pulse is absorbed, the carrier density increases with time, typically reaching densities in excess of 10^{19} cm^{-3} . As the carrier density increases, the bands move closer together causing electrons (holes) to be excited into states higher (lower) in the conduction (valence) band. Consequently, the optical excitation dwells on a particular set of states for only a short time. Now, for filling of the optically coupled states to be significant, the rate of excitation into these states must exceed the combined scattering rates out during the dwell time.

Ferry accounts for the spike in probe transmission in the following manner.¹⁴ Assume that a Gaussian shaped excitation pulse is incident on the germanium sample, and remember that the pulse width is much larger than the sample thickness. As the front edge of the pulse passes through the sample, the generation rate is too low to produce a significant amount of state filling. As the pulse progresses through the sample, Ferry¹⁴ calculates that, for very energetic pulses, a point is

reached where the generation rate significantly exceeds the combined scattering out rates during the dwell time. As the remainder of the excite pulse passes through the sample, the instantaneous transmission of the germanium is enhanced until, somewhere on the trailing edge of the pulse, the generation rate falls below the scattering out rates during the dwell time. Thus, the instantaneous transmission of the sample could be enhanced over a time interval shorter than the width of the laser pulse. The width of this enhancement is dependent upon the energy (or peak intensity) of the laser pulse. Ferry¹⁴ performs numerical calculations of the instantaneous transmission to fit the excite and probe data of Kennedy et al.¹

4. EXPERIMENT

The particular experimental configuration that we employ to separate the effects of parametric scattering from those of other processes such as state filling is shown in Fig. 2. A single 1.06 μm pulse, approximately 11 psec in duration, is switched by an electro-optic shutter from a train of pulses produced by a mode-locked Nd-glass laser. The single pulse is split into two by a beam splitter, and a relative delay is introduced between the two pulses. The probe pulse intensity is attenuated to approximately 2% of the corresponding excitation pulse intensity. Both pulses are focused onto the germanium sample as shown in the figure. The angular separation between incident beams is 12° . This configuration is similar to the arrangement employed by Kennedy et al.¹ and Shank and Auston³ to measure the narrow spike in probe transmission. Our configuration, however, differs from

theirs in two important respects. First, we have introduced a half wave plate into the probe path to provide for a continuous rotation of the probe pulse polarization with respect to the excite pulse. Second, we have positioned a detector to collect the first order diffracted light from the excitation pulse in the event that a grating should be produced by the interference of the two pulses. In previous studies of the probe spike, only the incident and transmitted probe and excite energies were measured.

As shown in Fig. 2, Detector 1 monitors the incident pulse energy. Detector 2 measures the transmitted probe light and one of the first order scattered beams from the excitation pulse. Detector 3 collects the transmitted excite pulse and one of the first order diffracted beams from the probe beam. The latter signal is insignificant, as we explained in Sec. 2. Detector 4 records the other first order diffracted excitation beam. No signal will be present on the latter detector unless a grating is formed by the interference of excite and probe beams.

The excitation pulse irradiance in these experiments was $1 \times 10^{-2} \text{ J/cm}^2$, as determined by measuring the energy transmitted through a pinhole located at the focus of the excitation beam and coplanar with the germanium wafer using a calibrated detector. The size of the pinhole was such that it transmitted 50% of both the excitation and probe pulses. We observed indications of day-to-day variations in excitation and probe beam overlap. We attribute these variations to "hot" spots in the focused multimode laser pulses.

The germanium sample is a high purity ($\rho_{\min} = 40\Omega\text{-cm}$) single crystal cut with the (111) plane as face. The sample was polished and etched with Syton to a thickness of $6\text{ }\mu\text{m}$ as determined by interferometric techniques.

5. RESULTS AND DISCUSSION

Here, we present and discuss the results of measurements that separate the effects of parametric scattering from those of other processes such as state filling. The experimental technique that we employ is simple. We repeat the excite and probe measurements of Kennedy *et al.*¹ employing probe pulses of various polarization. Specifically, the sample is irradiated by a $1.06\text{ }\mu\text{m}$ excite pulse intense enough to cause the germanium transmission to be enhanced. The light incident on the probe detector is then monitored for small probe pulse delays, as described in the previous section. These measurements are repeated for various probe polarizations. When the excite pulse polarization is perpendicular to the probe polarization, no interference between excite and probe is possible, and no grating will be formed. In this manner, we remove the contributions of the laser-induced grating. Any spike that remains must be attributed to other processes.

The signal recorded by the probe detector, D2 (See Fig. 2), as a function of time delay after an intense excitation pulse is shown in Fig. 3 for small delays. The circles represent measurements in which the probe pulse polarization was parallel with the excite pulse polarization. The triangles represent measurements in which the probe polarization was chosen perpendicular to the excite polarization. The data

are plotted as the normalized response of the probe detector versus the time delay between the two pulses. The normalized probe detector response is determined in the following manner. The total energy collected by the probe detector is divided by the probe energy incident on the germanium sample to give an apparent probe transmission. We use the word apparent because the probe detector receives diffracted light from the excitation beam as well as the transmitted light from the probe. This apparent probe pulse transmission is normalized by the excite pulse transmission and plotted in arbitrary units. We observed ratios of apparent probe transmission to excite transmission as large as 4. However, the magnitude of this ratio depends strongly on the quality of the spatial overlap of the focused multimode laser pulses and varies with the transverse mode structure of the laser. Each data point shown represents the average of at least 8 measurements. The error bars represent twice the statistical standard deviation. The data were reproducible.

The most important feature of Fig. 3 is the strong dependence of the sharp spike in the probe detector response on probe polarization. When the probe polarization is chosen parallel to that of the excitation pulse, we observe a narrow spike similar to that observed by Kennedy *et al.*¹ and Shank and Auston.³ The spike is approximately 2 psec wide (FWHM) and centered about zero delay. However, when the polarization of the probe is rotated by 90°, the rapid rise and fall in probe response completely disappears. We emphasize that the probe detector monitors both the transmitted probe pulse and the diffracted light from the excitation pulse. The strong polarization dependence of the data presented in

Fig. 3 suggests that the narrow spike in probe signal can be attributed to a parametric scattering of excite beam into the probe beam by a laser induced grating, consistent with the interpretation by Shank and Auston.³

Furthermore, we comment that we observed apparent probe transmissions at zero delay that were several times larger than the corresponding excitation transmissions. At zero delay and in the absence of coherent coupling artifacts, the probe and excite pulses should be indistinguishable to the sample since they were derived from a single pulse. Consequently, probe and excite transmissions should be identical in the absence of any coherent coupling artifacts. The observation of apparent probe transmissions greater than the corresponding excite transmissions at zero delay can be accounted for by a coherent scattering of the energetic excite beam into the weak probe beam by a laser-induced grating.

The conclusions of the previous paragraph are substantiated by the data presented in Fig. 4. In this figure, we display the results of measurements in which we monitor the first order diffracted light from the excite pulse as a function of time delay between the excite and probe pulses. The diffracted light is monitored by an integrating detector (detector 4, See Fig. 2) positioned at the appropriate angle. The data are plotted as the normalized response of detector 4, in arbitrary units, versus the time delay between the two incident pulses. Again, the circles represent measurements in which the probe polarization was parallel to the excite polarization; the triangles represent measurements in which the probe polarization was perpendicular to

the excite polarization. The normalized response of detector 4 is determined in a manner analogous to that for the normalized probe detector response. That is, the total energy measured by detector 4 is divided by the excite energy incident on the germanium sample. This ratio of diffracted excite energy to incident excite energy is then normalized by the excite pulse transmission and is plotted in arbitrary units. Each data point shown is the average of at least 8 observations.

The data presented in Fig. 4 provide striking evidence of laser-induced grating formation during these experiments. When excite and probe polarizations are parallel, a narrow rise and fall in the diffracted radiation is observed with time delay. The spike observed in the diffracted radiation is identical in form to the spike observed in the response of the probe detector. It is approximately of the same width, and it is centered about zero delay. In addition, there is essentially a one-to-one correspondence between large signals on detector 4 and large signals on the probe detector, both of which monitor a first order diffracted beam from the excite pulse. When the probe pulse polarization is perpendicular to the excite pulse polarization, no diffracted light is observed. The similarity in the shape, amplitude, and polarization dependence of the spike in probe response (detector 2) and the spike in diffracted response (detector 4) further leads us to conclude that they are of the same origin. That is, that both result from the first order diffraction of light from the excite beam by a grating created by the interference of excite and probe pulses.

In Fig. 5, we further emphasize the polarization dependence of the narrow spike recorded by the probe detector as a function of time delay between excite and probe. In this figure, we graph the response of the probe detector as the polarization of the probe pulse is rotated through 180° with respect to the polarization of the excitation pulse. The delay between the two pulses is held fixed at the peak of the observed spike (zero delay). The normalized units are identical to those used in Fig. 3. The height of the spike falls then rises again as the probe polarization is rotated with respect to the excitation polarization. When the relative angle reaches 90° , the probe pulse transmission is found to be equal to that of the excite pulse, consistent with the disappearance of diffraction effects.

Finally, we emphasize that the width of the spike in the probe detector response is approximately 2 psec, much less than the width of the probe pulse. The probe pulse width was measured to be 11 psec. We do not believe that the narrow width of the spike in the integrated probe detector response can be accounted for by an instantaneous change in sample transmission no matter how rapid that change. It is well known that the probe transmission will be determined in such a case by convolving the probe pulse with the instantaneous sample transmission curve and that the resulting structure in the integrated probe transmission curve will be at least as wide as the probe pulse. We illustrate this for a specific example in Fig. 6. In this figure, we have assumed that the instantaneous transmission of the sample is determined by state filling caused by the absorption of the excitation pulse as calculated by Ferry.¹⁴ The instantaneous transmission

calculated by Ferry¹⁴ is shown by a broken line in Fig. 6. The transmission of a 10 psec Gaussian pulse through a sample exhibiting this instantaneous transmission is shown (solid line) as a function of time delay between excite and probe pulses. The width of the resulting probe transmission curve is in sharp contrast to the observed spike.

6. SUMMARY AND CONCLUSIONS

We have performed excite and probe measurements of germanium using intense optical pulses approximately 11 psec in duration at a wavelength of 1.06 μm . The experimental configuration that we have employed is similar to that used by Kennedy *et al.*¹ That is, we have monitored the incident and transmitted excite pulse and probe pulse energies. The geometry was such that the formation of a grating by the interference of excite pulse and probe pulse would result in a scattering of a fraction of the excite beam into the direction of the probe beam. Our studies, however, differed from those of Kennedy *et al.*¹ in two respects. First, we positioned a detector to monitor the scattered light from any laser-induced grating that might be created by the interference of excite and probe pulses when they were spatially and temporally overlapped. Second, we varied the polarization of the probe pulse with respect to the polarization of the excite pulse. When the probe pulse polarization was parallel to the excite pulse polarization, we observed a rapid rise and fall in probe detector response versus time delay. This spike in probe detector response was approximately 2 psec in width and centered

about zero delay. This spike is identical to that observed by Kennedy *et al.*¹ During the same measurements, we recorded a similar spike in the diffracted light. The spike in diffracted light was similar in shape, duration and amplitude to that of the spike in probe detector response. When the polarization of the probe pulse was perpendicular to that of the excite pulse, we observed no spike in the probe detector response, and we observed no diffracted light.

The above experiments provide clear evidence of laser-induced grating formation during these picosecond excite and probe experiments in germanium at $1.06\text{ }\mu\text{m}$. In addition, our data indicate that the narrow spike in probe detector response exhibits the following important characteristics: (1) The spike strongly depends on the relative polarization of excite and probe pulses. (2) The width of the spike is narrow with respect to the width of the probe pulse. (3) Apparent probe pulse transmissions measured at zero delay are larger than the corresponding excite pulse transmission. (4) There is a strong similarity between this spike and the measured diffracted spike. For these reasons, we conclude that the spike in probe detector response can be totally accounted for by a parametric scattering of the excite beam into the probe beam by a grating created in the germanium by the interference of the two pulses, as suggested earlier by Shank and Auston.³ The spike is merely a coherent coupling artifact of the measurement technique, and it does not correspond to an actual increase in sample transmission. Although band-gap narrowing and state filling have been observed in other semiconductor

experiments involving optical excitation (and certainly they must be occurring here as well), they do not contribute to the spike in probe detector response, as recently suggested by Ferry.¹⁴

The authors wish to express their appreciation to E. W. Van Stryland and G. Paul Perryman for helpful comments and discussions.

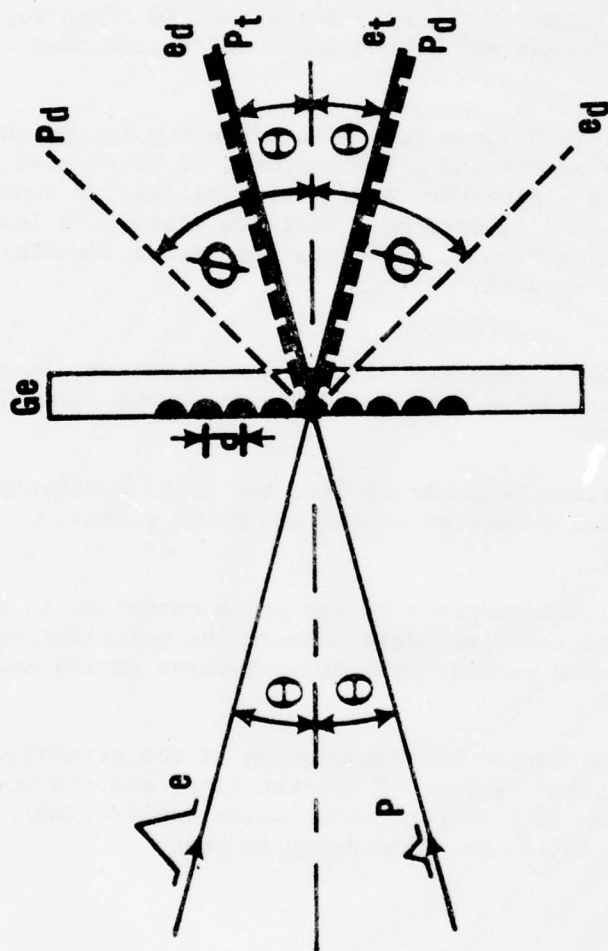
This work was supported by the Office of Naval Research and the North Texas State University Faculty Research Fund.

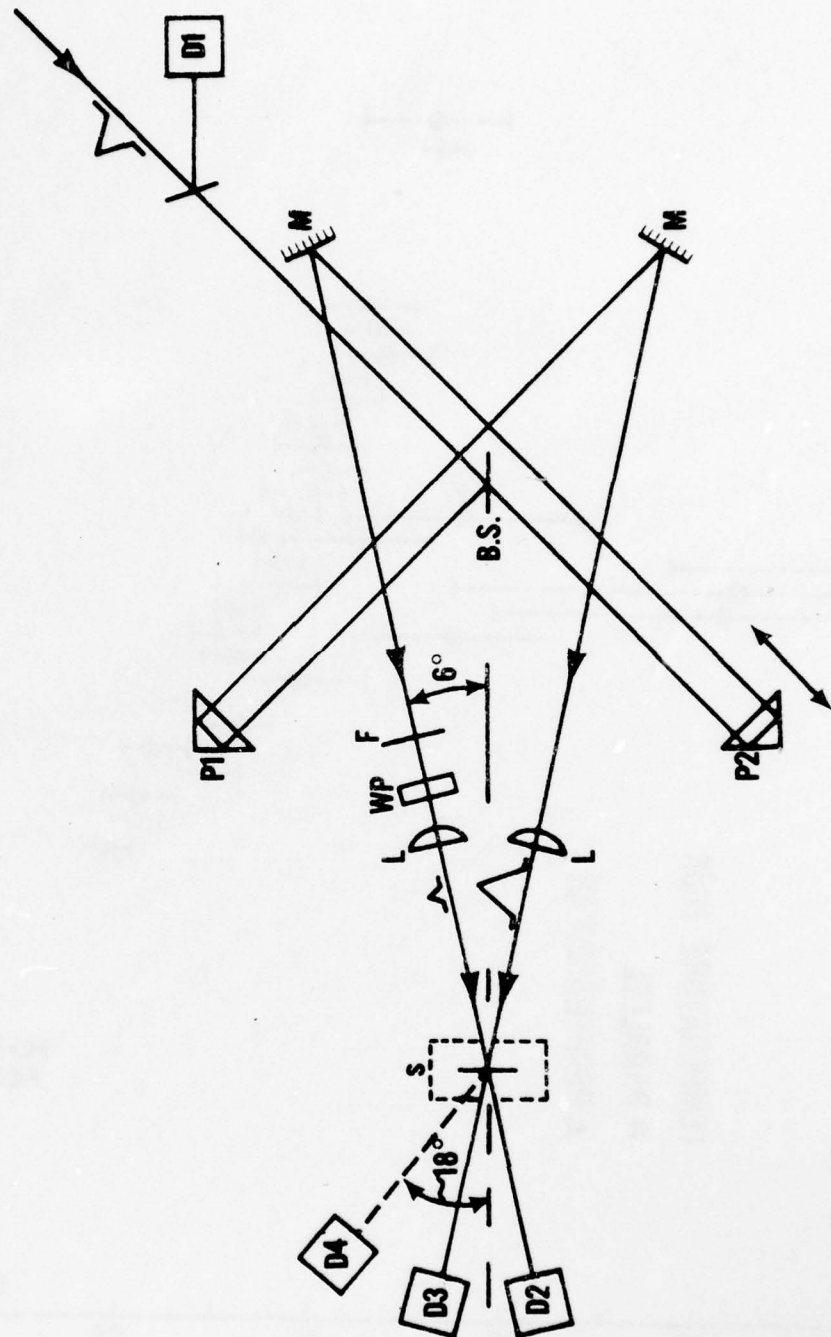
REFERENCES

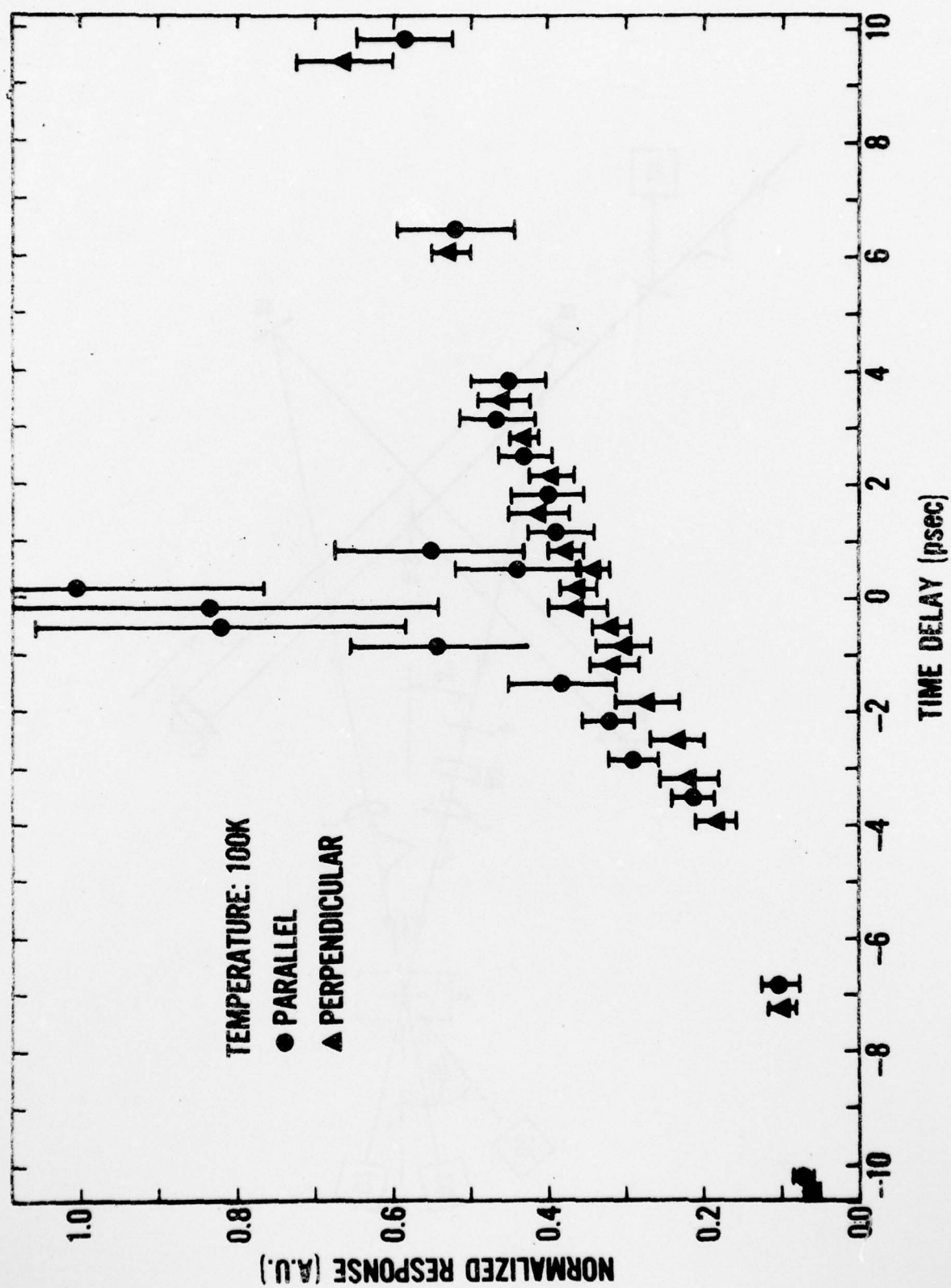
1. C. J. Kennedy, J. C. Matter, A. L. Smirl, H. Weichel, F. A. Hopf, S. V. Pappu, and M. O. Scully, Phys. Rev. Lett. 32 (1974) 419.
2. D. H. Auston and C. V. Shank, Phys. Rev. Lett. 32 (1974) 1120.
3. C. V. Shank and D. H. Auston, Phys. Rev. Lett. 34 (1975) 479.
4. D. H. Auston, C. V. Shank, and P. Lefur, Phys. Rev. Lett. 35 (1975) 1022.
5. A. L. Smirl, J. C. Matter, A. Elci, and M. O. Scully, Opt. Commun. 16 (1976) 118.
6. H. M. van Driel, A. Elci, J. S. Bessey, and M. O. Scully, Opt. Commun. 20 (1977) 837.
7. A. Elci, M. O. Scully, A. L. Smirl and J. C. Matter, Phys. Rev. B. 16 (1977) 191.
8. H. M. van Driel, J. S. Bessey, and R. C. Hanson, Opt. Commun. 22 (1977) 346.
9. J. S. Bessey, B. Bossachi, H. M. van Driel, and A. L. Smirl, Phys. Rev. B 17 (1978) 2782.
10. W. P. Latham, Jr., A. L. Smirl, and A. Elci, Solid-State Electron. 21 (1978) 159.
11. A. Elci, A. L. Smirl, C. Y. Leung, and M. O. Scully, Solid-State Electron. 21 (1978) 147.
12. A. L. Smirl, J. R. Lindle, and S. C. Moss, Phys. Rev. B 18 (1978) 5489.
13. B. Bossachi, C. Y. Leung, and M. O. Scully, Opt. Commun. 27 (1978) 475.
14. D. K. Ferry, Phys. Rev. B 18 (1978) 7033.
15. For a recent review of this area see H. J. Eichler, Opt. Acta 24 (1977) 631.

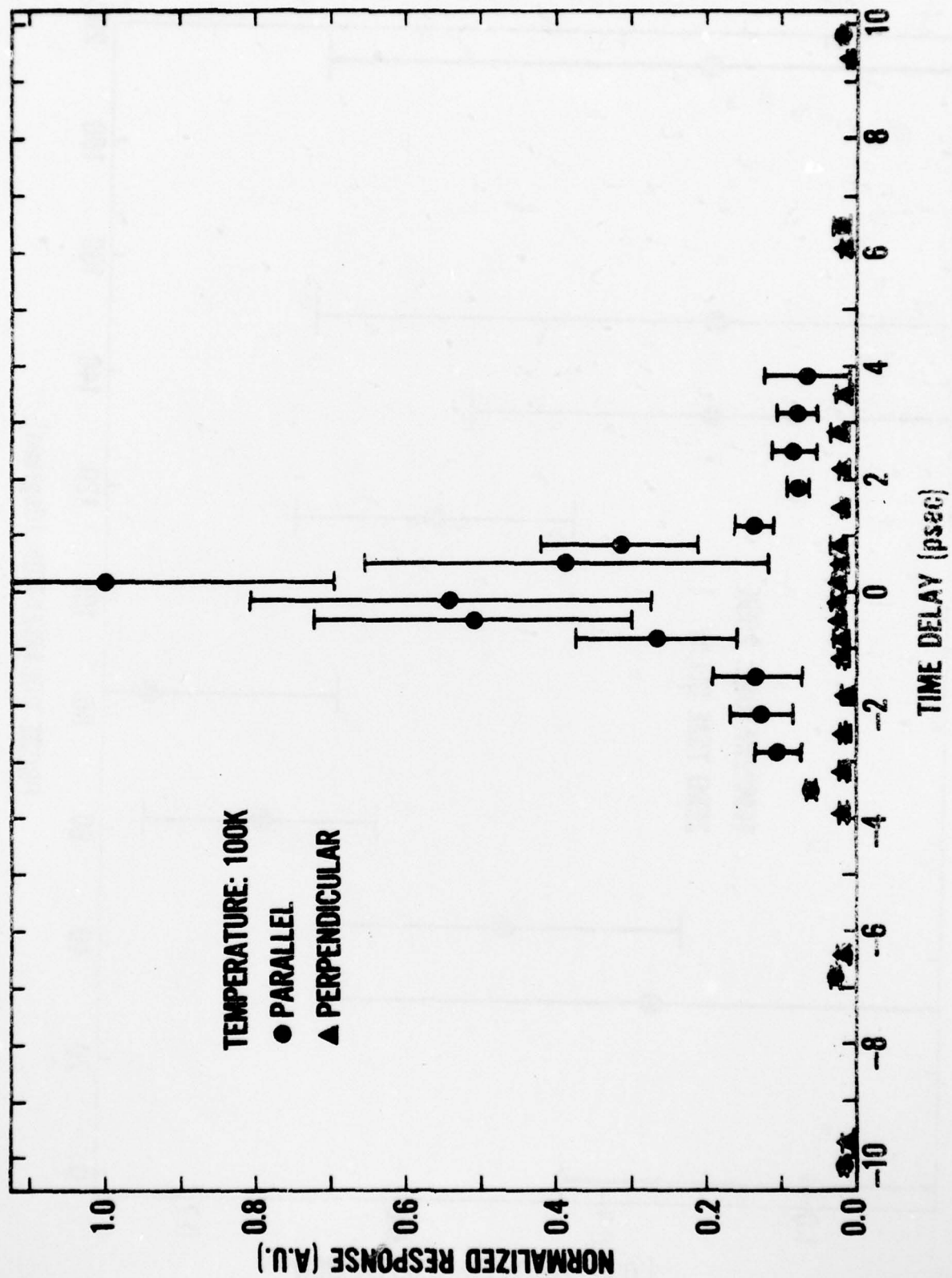
FIGURE CAPTIONS

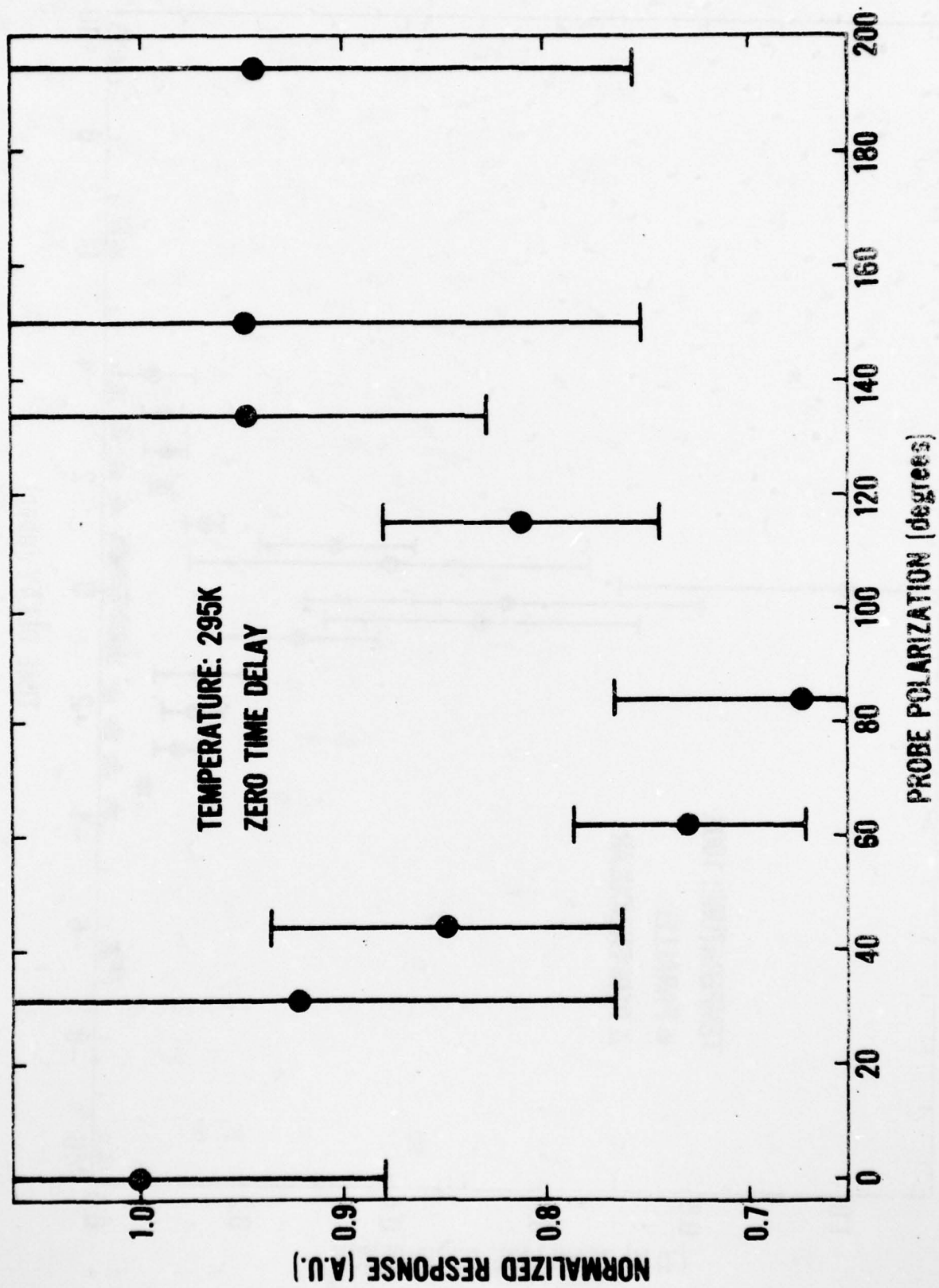
- Fig. 1. Geometry for the diffraction of excite and probe beams by a laser-induced grating, where e denotes the incident excite pulse, p the incident probe pulse, e_t the transmitted excite pulse, p_t the transmitted probe pulse, e_d the first order diffracted excite beams, p_d the first order diffracted probe beams, and $\sin\phi = 3\sin\theta$. Solid lines represent transmitted beams and broken lines diffracted beams.
- Fig. 2. Schematic diagram for measuring the polarization dependence of the excite and probe response of Ge at $1.06\text{ }\mu\text{m}$, where D denotes a detector, B.S. a beamsplitter, M a mirror, P a prism, F a filter, WP a halfwave plate, L a lens, and S the germanium sample. Note that P2 can be translated and W.P. can be rotated.
- Fig. 3. Normalized response of the probe detector, in arbitrary units, vs. time delay between excite and probe pulses.
- Fig. 4. Normalized response of detector 4, in arbitrary units, vs. time delay between excite and probe pulses.
- Fig. 5. Normalized response of the probe detector, in arbitrary units, vs. the relative angle between the polarizations of the excite and probe pulses. The delay between excite and probe was zero.
- Fig. 6. The instantaneous transmission of the germanium sample as calculated by Ferry¹⁴ (broken line) and the integrated transmission of a 10 psec probe pulse (solid line), both in arbitrary units, vs. time delay in psec.

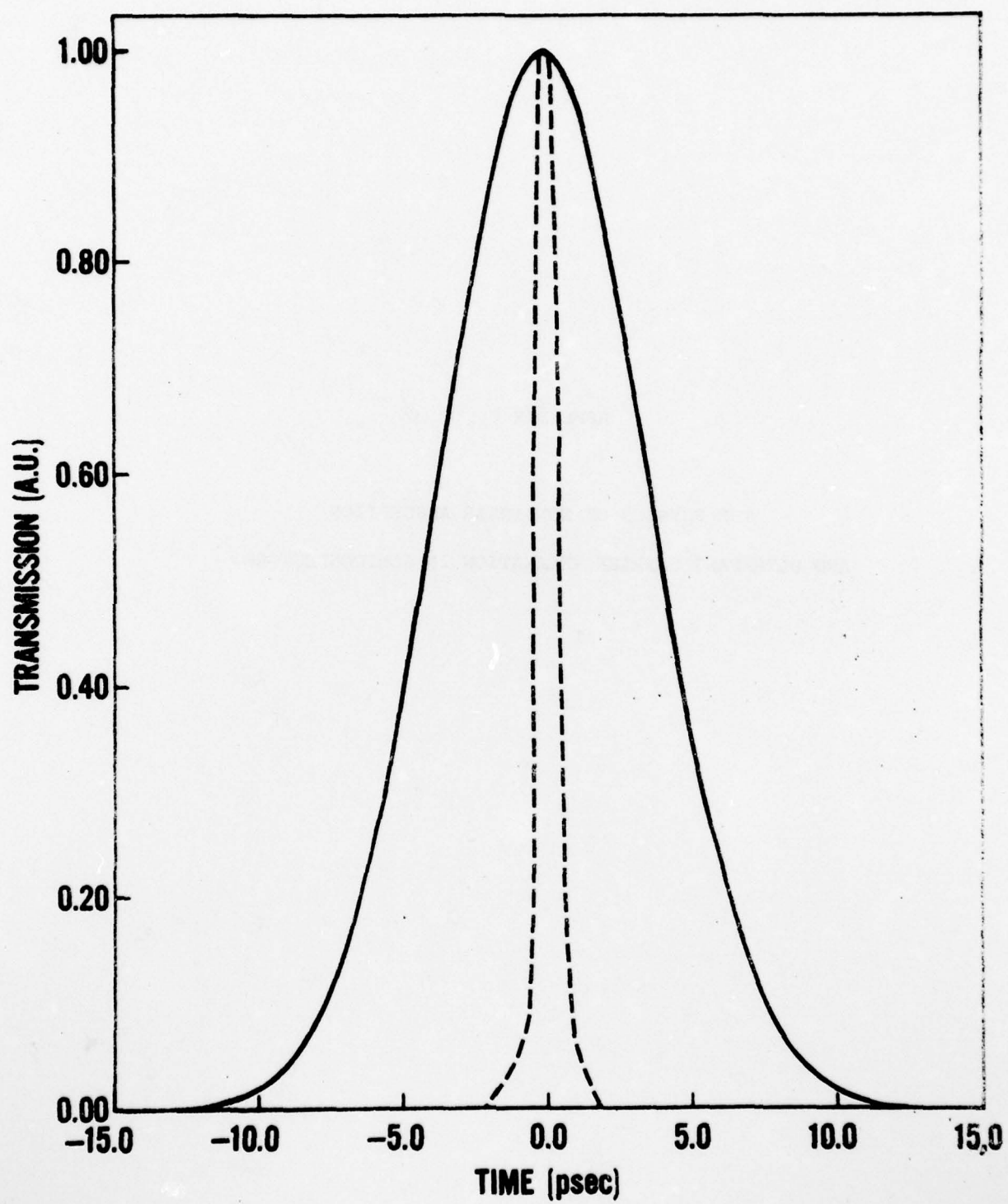












APPENDIX C

THE PHYSICS OF NONLINEAR ABSORPTION
AND ULTRAFAST CARRIER RELAXATION IN SEMICONDUCTORS

ABSTRACT

Recently, picosecond optical techniques have been used to measure the nonlinear, nonequilibrium optical properties of semiconductors in an effort to obtain information concerning ultrafast carrier dynamics at high optically-created carrier densities. A large number of processes or effects have been observed by experimentalists or invoked by theorists in these studies. Some of these are important only at high photogenerated carrier densities; others occur during optical excitation at any intensity. In addition, other apparent effects are simply coherent artifacts of the measurement technique. In this lecture, we shall review these processes and artifacts with an emphasis on the ultrashort time scales and high carrier densities involved in these studies. Our discussion centers on the results and interpretation of a single excite and probe experiment at $1.06\text{ }\mu\text{m}$ in the semiconductor germanium.

I. INTRODUCTION

The absorption of light quanta of energy greater than the band gap in a semiconductor induces an electron to make a transition from the valence band to a state high in the conduction band, leaving behind a hole in the valence band (Fig. 1). After such an absorption process, the photoexcited electron is left with an excess energy ΔE_e that is given by

$$\Delta E_e = (\hbar\nu - E_g)(1 + m_e/m_h)^{-1}, \quad (1)$$

where m_e is the electron effective mass and m_h is the hole effective mass.

The excess energy of the photogenerated hole is

$$\Delta E_h = (\hbar\nu - E_g) - \Delta E_e. \quad (2)$$

These energetic electrons (holes) will quickly relax through various collisional processes to the bottom (top) of the conduction (valence) band, where eventually they will recombine. It is well established that if the photoexcitation is sufficiently intense this relaxation process results in the generation of hot electron and phonon distributions.

The intraband relaxation kinetics of a photoexcited electron located energetically above the conduction band minimum are complex; moreover, as we shall see, the evolution of many of these processes occurs on a time scale too rapid for direct measurement by present electronic detection systems. In some cases, characteristic relaxation times for these ultrafast processes have been determined indirectly from transport measurements or from steady-state photoluminescence measurements.

In general, the measurement of a transport property such as the mobility or drift velocity always represents an integrated or average effect over the

distribution function. Consequently, it is usually necessary to assume the form of the distribution function. Once the distribution function has been assumed or determined, measurement of one of a number of transport properties such as the mobility, Hall effect, magnetoresistance, or the Shubnikov de Haas effect will yield the carrier temperature. Details of these studies have been provided by K. Hess and G. Bauer in earlier lectures. For additional discussion of the methods for determining hot electron temperatures from transport measurements the reader may find the reviews by E. M. Conwell¹ and G. Bauer² of interest.

By employing steady state optical techniques such as photoluminescence or optical absorption, information concerning the form of the distribution function as well as the carrier temperature can be obtained. This additional information concerning the distribution function is obtained primarily because a direct optical transition (absorption or emission) occurs between a well defined initial energy state E_i and a well defined final state E_f , where $E_f - E_i = \hbar\nu$. The transition rate between these two states depends on the occupancy of the initial state $f(E_i)$ and the availability of the final state $1 - f(E_f)$. As a result, we can measure the entire energy dependence of the distribution function by monitoring all possible optical transition energies. The methods for determining hot electron distribution functions and hot electron temperatures from radiative recombination, absorption, or inelastic light scattering have been reviewed by C. J. Hearn and R. G. Ulbrich in earlier lectures. Additional details are provided by the reviews of G. Bauer³, J. Shah⁴, R. G. Ulbrich⁵, R. C. C. Leite⁶, and C. Weisbuch⁷.

Generally, these detailed studies of hot electron and phonon distributions, both those employing transport techniques and those employing photoluminescence techniques, have been conducted under steady state conditions.

That is, the knowledge of the electron temperature and the form of the distribution function are determined by assuming that the rate at which the electron-hole gas receives energy from the electrical or optical field is equal to the rate at which the carriers lose that energy to the lattice or impurities. This detailed knowledge of the steady-state distribution functions then provides information concerning electron-electron and electron-phonon interactions; from this information, ultrafast relaxation rates are indirectly assigned. Direct time resolved studies have been performed⁸, but they have, previously, been limited in resolution to nanosecond time scales. With the advent of mode-locked lasers and the picosecond optical pulses that they produce, direct measurement of many of these relaxation times is now possible. The remainder of this lecture and my seminar to follow will describe the procedures, results, and interpretation of experiments that directly measure the nonlinear, nonequilibrium optical properties of semiconductors on a picosecond time scale in an effort to obtain information concerning ultrafast carrier relaxation processes.

As a rule, these direct experimental studies of ultrafast relaxation processes have employed a variation of the excite and probe technique. This method was first used on a picosecond time scale by Shelton and Armstrong⁹. In this technique, a single ultrashort (0.2 psec - 10 psec) optical pulse is switched by an electro-optic shutter from a train of such pulses produced by a mode-locked laser. This single pulse is split into two by a beam splitter, and a relative delay is introduced between the two pulses. The intensity of the second (probe) pulse is attenuated to a small fraction (e.g. 2%) of the corresponding intensity of the first (excite) pulse. Both pulses are focused onto the semiconductor sample as shown in Fig. 2. Intense ultrashort pulses (typically having peak powers on the order of 10^8 watts) whose photon energy

$h\nu$ is greater than the band gap E_g of the semiconductor, when tightly focused, can produce an enormous number ($10^{19} - 10^{20} \text{ cm}^{-3}$) of electron-hole pairs on a time scale that is short compared to many of the kinetic processes involved in the evolution of the carrier distribution. Thus, the absorption of the excite pulse creates a large, rapidly evolving, nonequilibrium carrier distribution that changes the transmission properties of the sample. This initial pulse is then followed at various time delays by the weak probe pulse that monitors the evolution of the enhanced sample transmission with time as it returns to its equilibrium condition. There are any number of variations of this technique. For example, the probe pulse can be monitored in reflection as well as transmission, the probe wavelength can be purposefully chosen to be different from the excite wavelength, and the probe polarization can be varied with respect to the polarization of the excite pulse. Another variation of the technique is to hold the time delay between excite and probe pulses constant while varying the energy of the excite pulse. Of course, in addition to varying the optical parameters, one can vary the environment of the optical sample as well (e.g. vary the sample temperature or subject the sample to hydrostatic pressure). We shall review the application of many of these techniques to the time-resolved measurement of the optically induced changes in the transmission and reflection spectrum of Ge and GaAs in our seminar to follow. In the remainder of this lecture, for pedagogical purposes, we shall restrict our discussion to a single application of the excite and probe technique to germanium.

Specifically, we intend to discuss an early excite and probe experiment performed in germanium using intense picosecond optical pulses with a wavelength of $1.06 \mu\text{m}$ as depicted in Fig. 3. In this particular application of

the excite and probe technique, the excite pulses were selected by a laser-triggered spark gap and a Pockel's cell from trains of pulses produced by a mode-locked Nd-glass laser. The pulses were approximately 10 psec in duration and had peak powers of approximately 10^8 watts at a wavelength of $1.06 \mu\text{m}$, and they produced a measured irradiance of approximately 10^{-2} J/cm^2 when focused on the crystal surface (to a spot size 2 mm in diameter). The electron-hole plasma produced by the absorption of the excitation pulse was probed using weak probe pulses at $1.06 \mu\text{m}$.

The germanium sample was a high purity ($\rho_{\text{min}} = 40 \Omega\text{cm}$) single crystal cut with the (111) plane as the face. The sample was polished and etched with Syton to a thickness of $6 \mu\text{m}$ as determined by interferometric techniques.

The results of a measurement of the change in transmission of the thin germanium crystal at $1.06 \mu\text{m}$ as a function of increasing carrier number (created by the direct absorption of the excitation pulse) are shown in Fig. 4. These data were obtained in the following manner (see inset of Fig. 4). The crystal was illuminated by variable energy excite pulses with a wavelength of $1.06 \mu\text{m}$ and the transmission of each pulse was measured. The crystal transmission at 1.17 eV ($1.06 \mu\text{m}$) is seen to increase by a factor of approximately 30 at high photoexcitation levels. These measurements were performed at 100 K. Thus, we see that our excite pulse can be made energetic enough to alter the optical properties of the germanium!

The results of measurements of the temporal evolution of the enhanced transmission of this thin germanium sample at a wavelength of $1.06 \mu\text{m}$ following the creation of a dense electron-hole plasma by the excitation pulse are shown in Fig. 5. The measurements were performed in the following manner (see inset Fig. 5). The sample was irradiated by $1.06 \mu\text{m}$ excite pulses containing

approximately 2×10^{15} quanta, and the transmission of each excite pulse was measured. Each excite pulse was then followed at various delays by a weak probe pulse at $1.06 \mu\text{m}$. These measurements were performed for a sample temperature of 100 K. The data are plotted as the ratio of the probe pulse transmission T_p to excite pulse transmission T_E , in arbitrary units, versus time delay in picoseconds. The arbitrary units are chosen so that the peak of the probe transmission at 100 K is unity. The actual value of the ratio T_p/T_E was observed to be as large as six; however, this value strongly depends on the quality of the spatial overlap of the focused excite and probe pulses on the sample surface. Notice that the graph of the probe transmission versus time exhibits two distinct features. The first is a rapid rise and fall in probe transmission. This narrow spike is approximately two picoseconds wide and is centered about zero delay. This spike is followed by a gradual rise and fall of the probe transmission lasting hundreds of picoseconds. These measurements are identical to those reported by Kennedy *et al.*¹⁰, Shank and Auston¹¹, and Smirl *et al.*¹². However, when comparing the different sets of data, one must realize that the sample thicknesses and focused optical spot sizes are not identical.

We are now in a position, for the first time, to clearly define our goals for the remainder of this lecture. We wish to enumerate and discuss the various effects and physical processes that can occur during and following the absorption of an intense, ultrashort optical pulse whose energy is greater than the bandgap. Our intent is to follow the temporal evolution of the nonequilibrium, optically-created electron distribution on a picosecond time scale in the hope of directly determining the characteristic scattering rates of these processes. In order to be specific, we shall use the excite and probe transmission studies at $1.06 \mu\text{m}$ presented in Fig. 4 and Fig. 5 as

the basis for our discussion. We choose this experiment and this semiconductor, for the following reasons. (1) To this point, more experimental studies have been performed on germanium than on any other semiconductor. This is because it is a well characterized material with a bandgap energy that is comparable to, but less than, the photon energy of the 1.06 μm Nd-glass laser. (2) More effort has been expended theoretically attempting to model the picosecond optical response of germanium than any other semiconductor. In particular, much of this theoretical work has been an attempt to interpret the data of Fig. 4 and Fig. 5. (3) Finally, we choose to emphasize this data because to this point in time there is no single accepted explanation for the slow rise in probe transmission displayed in Fig. 5. As a result, these particular early experiments graphically illustrate problems that can be encountered in the interpretation of the data obtained with such intense ultrashort pulses - unless care is taken in designing the experiment. During early experiments freedom in this regard was limited by the scarcity of picosecond sources at wavelengths other than 1.06 μm .

We emphasize, once again, that the picosecond optical studies described here, potentially, have all of the advantages of the studies described earlier by C. J. Hearn and R. G. Ulbrich. They differ from these studies, however, in two ways. First, picosecond clocks, such as the one pictured in Fig. 2, provide picosecond time resolution. Second, absorption of such intense optical pulses in a semiconductor create carrier densities much larger than those encountered in steady state optical experiments. This allows the study of processes that become significant only at high carrier densities. Traditionally, these phenomena have been studied in the presence of strong impurity effects caused by high concentrations of donors and acceptors in heavily-doped materials.

AD-A073 920

NORTH TEXAS STATE UNIV DENTON DEPT OF PHYSICS
OPTICALLY INDUCED HOT ELECTRON EFFECTS IN SEMICONDUCTORS.(U)
JUN 78 A L SMIRL

F/G 20/12

N00014-76-C-1077

UNCLASSIFIED

2 OF 3

AD
A073920

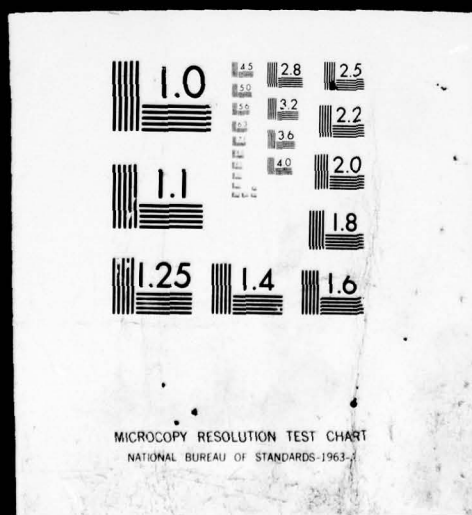


SIFIED

2 OF 3

AD

A073920



The remainder of this lecture is organized as follows. In the next section, we summarize the pertinent features of the germanium band structure. In Sec. III, we qualitatively discuss the physical processes that occur during and after the nonlinear absorption of the excite pulse by germanium. Finally, in Sec. IV, we discuss an initial attempt at modeling the picosecond optical response of germanium, as depicted in Fig. 4 and Fig. 5. In doing so, we shall have to invoke or consider a rather large number of physical processes. We shall review experimental attempts to separate the roles of these processes in determining the picosecond temporal evolution of the optically-created carrier distribution in germanium in a later seminar of this ASI.

Finally, the author notes that this is not a review article and no attempt has been made to provide a comprehensive survey of the area of picosecond spectroscopy or the application of picosecond techniques to semiconductors. Nor has any attempt been made to provide the reader with an exhaustive bibliography. For further information on the techniques and applications of picosecond optical pulses, the reader is referred to recent works edited by Shapiro¹³ and Shank, Ippen and Shapiro¹⁴. Our intent here is to provide the reader with an introduction to picosecond optical interactions in semiconductors. In this regard, we have relied heavily on our own work on germanium and work by others related to our own. Remarks that we make concerning areas of general agreement, controversy, and future study (the reader should be warned) reflect our own point of view and are by definition subjective. The reader should also be warned that our point of view has been known to change from time-to-time as these studies progress.

II. REVIEW OF THE GERMANIUM BAND STRUCTURE

The energy band structure of Ge is well known,¹⁵⁻¹⁹ and the relevant features are shown in Fig. 6. The significant features of the conduction band are the locations of the conduction band valleys. The minimum located at Γ is separated from the top of the valence band by 0.805 eV at 300 K. This separation increases to 0.889 eV at 77 K. This central conduction band valley is highly nonparabolic; however, an enormous simplification in calculations is obtained by replacing the actual central valley structure by a parabolic structure with effective mass $m_0 \approx 0.04 m$, where m is the electron rest mass. The consequences of such a simplification are discussed by Latham *et al.*²⁰ The indirect gap at L has a separation of 0.664 eV at 300 K and a separation of 0.734 at 77 K. There are four valleys like the one shown in the $[1\ 1\ 1]$ direction. The minima for these valleys are located exactly at the Brillouin-zone boundary. The band minimum at X is 0.18 eV higher than the minimum at L. There are six valleys like the one in the $[1\ 0\ 0]$ direction. The energy surfaces in the side valleys are elongated ellipsoids; the density of states effective mass for the side valleys is taken to be $m_c \approx 0.22 m$.

There are three valence bands that are separated by the spin-orbit interaction. The valence band maximum is at Γ . At the center of the Brillouin zone, the heavy hole band and the light hole band are degenerate, and the third band is separated from them by an energy $\Delta \approx 0.3$ eV. Near the center of the zone, the light hole band can be approximated by an effective mass of $m_1 \approx 0.04 m$. However, except for this small region near the center of the Brillouin zone, the structure introduced by the spin orbit coupling is

minor, and we can treat the heavy hole and light hole bands as having the same curvature, separated in energy by $\Delta' \approx 0.14$ eV. The effective mass of both heavy-hole and light-hole valence bands away from $k = 0$ is taken to be $m_h \approx 0.34 m$.

III. PHYSICAL PROCESSES

The transient properties of a dense electron-hole plasma created in a semiconductor by the interband absorption of an intense ultrashort optical pulse are determined by the simultaneous interaction of a large number of electronic processes. Thus, if we are to follow the dynamics of the carrier distribution on a picosecond time scale, we require a detailed knowledge of which processes occur, their rates, and their effects on the evolving plasma. In this section, we list the fundamental processes believed to be important, and we estimate their rates and effects on the carrier distribution. We use the word "estimate" because some of these processes occur on a time scale too rapid for direct measurement even by picosecond techniques, and others have yet to be measured in a clear and concise manner at these large carrier densities. We list only those processes or effects that have been observed by experimentalists or invoked by theorists in their interpretation of picosecond studies in germanium. As a result, we recognize from the outset that our list contains only a few of the myriad of possible electronic interactions. We discuss these processes in the context of understanding and interpreting the data of Fig. 4 and Fig. 5.

When an intense excite pulse is incident on a thin germanium sample, a fraction of the pulse is reflected; the unreflected portion enters the bulk of the crystal where most of it is absorbed. The light entering the bulk of the crystal is absorbed primarily by direct optical transitions. In this process (see process a of Fig. 7), a quanta of light from the excite pulse is absorbed inducing an electron to make a transition from near the top of the valence band to the conduction band valley near Γ , leaving behind a hole in the valence band. As shown in Fig. 7, such a transition is energetically

allowed between each of the three valence bands and the conduction band, since the energy of the light quanta $h\nu$ is substantially greater than the direct band gap energy E_0 . However, we shall ignore the contribution of the split-off band to the direct absorption coefficient because of its small contribution to the hole density of states (in fact, at temperatures below room temperature, e.g. 77 K, we are not energetically coupled to the split-off band at all). The linear direct absorption coefficient α_0 for germanium at 300 K and $1.06 \mu\text{m}^{21}$ is $1.4 \times 10^4 \text{ cm}^{-1}$, yielding an absorption length of approximately a micron. The direct absorption of an intense optical pulse generates carriers into a single optically-coupled state in the conduction band at a rate that is approximately given by

$$G(t) \approx \alpha_0 I(t) / [\eta(E) \Delta E h\nu] \quad , \quad (3)$$

where I is the incident optical intensity, $\eta(E)$ the density of states at the optically-coupled energy, and ΔE is the spread in optically-coupled energies caused by the finite bandwidth of the incident optical pulse. For typical 10 psec wide excite pulses at $1.06 \mu\text{m}$ with an energy density of 10^{-2} J/cm^2 and a bandwidth in the range of 10 Å to 100 Å, the generation rate into a single state is approximately 10^{13} to 10^{14} sec^{-1} . The absorption of such a pulse can create carrier densities between 10^{19} and 10^{21} cm^{-3} in a time period of 10 psec. In addition, each electron is deposited into the conduction band with an excess energy $\Delta E_e \approx 0.33 \text{ eV}$ with respect to the bottom of the central conduction band valley and an excess energy $\Delta E_e \approx 0.47 \text{ eV}$ with respect to the side valley at L. Consequently, the effect of direct absorption is the creation of a large number of carriers with excess energy ΔE_e .

Indirect phonon-assisted interband absorption processes, which involve the transition of an electron from the valence band near Γ to either the L

or X conduction-band valleys by the simultaneous absorption of a photon and the absorption or emission of a phonon, are also allowed (process b, Fig. 7). These processes are not important in our problems. As we shall see, the probability that an electron will reach the L valley by means of a real optical transition to the Γ valley followed by a phonon-assisted scattering to one of these side valleys is much greater than the probability that the electron will reach the same valley by means of a second-order phonon-assisted transition. The indirect absorption coefficient for germanium²¹ at 1.06 μm and room temperature is approximately $3.5 \times 10^2 \text{ cm}^{-1}$. For this reason, we ignore phonon-assisted indirect absorption effects in the remainder of our discussions.

As we have already stated, direct absorption of the excite pulse deposits electrons high in the conduction band, leaving behind holes in the valence band. Since the excite pulse is approximately monochromatic, a very narrow set of states in the valence band is optically coupled to a narrow set of states in the conduction band. The optically-excited electrons and holes are initially deposited in these states and initially occupy very localized regions within the conduction and valence bands, respectively. Because of the small number of optically-coupled electron (hole) states available in the conduction (valence) band, one might be tempted to conclude that the direct transitions are saturated at very low pulse energies. In fact, this need not be the case. The number of carriers occupying the optically-coupled states at any given time is determined by the relative strengths of the direct optical generation rate into the states (Eq. 3) and the combined scattering rates out. If the generation rate exceeds the scattering-out rates, then the optically-coupled states are partially filled, and the transmission of the germanium will be enhanced. This process is called state filling, and is distinct from band filling (to be discussed later). This state filling, if

significant, results in a delta-function-like spike in the distribution function located at the optically coupled states. We now consider the mechanisms by which the photoexcited electrons are scattered from the optically-coupled states and lose their excess energy ΔE_e .

One of the primary processes that removes the nonequilibrium electrons from their localized initial states is long wavevector phonon-assisted intervalley electron scattering (process c, Fig. 7). Such transitions are energetically allowed since $E_v > E_{L,X} + \hbar\Omega_{\mu\vec{q}}$, where $E_{L,X}$ refers to the indirect gaps at L and X and $\Omega_{\mu\vec{q}}$ to the phonon frequency of mode μ and momentum \vec{q} . Elci *et al.*²² have calculated the intrinsic state lifetime τ_0 of an electron initially in a state k in the central valley of the conduction band as it is scattered by long wavevector optical and acoustic phonons to available states k' in all side valleys. That is, they calculate

$$1/\tau_0 = \sum_{\vec{k}'} R(\vec{k}, \vec{k}') \quad , \quad (4)$$

where $R(\vec{k}, \vec{k}')$ is a scattering rate calculated from first order perturbation theory and Fermi's Golden Rule. They estimate the scattering rate $1/\tau_0$ to be greater than 10^{14} sec^{-1} . Consequently, electrons are emptied from the central to side conduction-band valleys at a rate that is comparable to, or larger than, the optical generation rate.

The electrons scattered to the side valleys by optical and acoustic phonons are deposited there with an excess energy $\Delta E_e \approx 0.47 \text{ eV}$. These nonequilibrium carriers might be thought to occupy very localized regions within the side valleys, and the holes expected to still occupy a localized set of states in the valence band. These energetic carriers can give up their excess energy to the distribution as a whole via carrier-carrier collisions (process d), or they can lose their excess energy by intravalley optical phonon

emission (process e), as shown in Fig. 7. Carrier-carrier scattering events (including electron-electron, electron-hole, and hole-hole collisions) occur because each carrier must move in the screened Coulomb field of the other carriers. The rate for such collisions is very large. Elci et al.²² have estimated this rate to be greater than 10^{14} sec^{-1} at carrier densities of 10^{20} cm^{-3} . These collisions ensure that the electron and hole distributions will be Fermi-like. They also ensure that the Fermi distribution for the holes and the Fermi distribution for the electrons will reach a common temperature, which is different from the lattice temperature. This initial temperature can be obtained by equating the total optical energy absorbed to the total energy of the electron-hole distribution,

$$\sum_c \sum_{\vec{k}} E_{ec}(\vec{k}) f_{ec}(\vec{k}) + \sum_v \sum_{\vec{k}} E_{hv}(\vec{k}) f_{hv}(\vec{k}) = nh\nu, \quad (5)$$

where $f_{ec}(\vec{k})$ represents the electron Fermi distribution function in the conduction band c , $f_{hv}(\vec{k})$ the hole distribution function in the valence band v , \sum_c denotes a summation over all conduction band valleys, and \sum_v a summation over all valence bands. Finally, n represents the number of photo-generated electron-hole pairs as determined by integrating the total optical generation rate over the optical pulse width. The approximate result of such a calculation is

$$T \approx \frac{1}{3k_B} (nh\nu - E_L), \quad (6)$$

where k_B is the Boltzmann constant. Consequently, we obtain an initial carrier temperature of approximately 1800 K!

Electrons located high in the tail of this hot Fermi distribution can relax by intravalley optical phonon emission. Similar comments also apply to the holes in the valence band. The effect of this relaxation mechanism (process

e, Fig. 7) is to reduce the carrier temperature and increase the lattice temperature. The rate at which the carrier distribution loses energy to the lattice is of fundamental importance in determining the temporal evolution of the germanium transmission. Unfortunately, the electron-optical phonon coupling constant Q_0 for germanium is uncertain by a factor of 3. Experimental measurements and theoretical estimates of this value range^{1, 23-32} from 6.4×10^{-4} erg/cm to 18.5×10^{-4} erg/cm. Since the carrier energy relaxation rate is proportional to Q_0^2 , the time required for the carrier distribution temperature to reach that of the lattice is uncertain by an order of magnitude. We shall return to this controversy later in this lecture and again in a later seminar. For the moment, it is sufficient to note that an individual nonequilibrium carrier in the side conduction band valley will emit optical phonons at a rate of approximately 10^{12} sec^{-1} . In other words, a carrier at 1800 K will initially lose its energy at a rate of roughly 0.03 eV/psec. We emphasize that these numbers represent only a rough order of magnitude, and they are uncertain by a factor of 10. In any event, it is clear that the phonon relaxation rate is much slower than the carrier-carrier thermalization rate discussed in the previous paragraph.

Also notice (Fig. 7) that a single electron will emit approximately 15 optical phonons while relaxing to the conduction band minimum. As 10^{20} carriers/cm³ cool to lattice temperature, an enormous number of such short wavevector optical phonons are created. These optical phonons eventually decay into two long wavevector acoustic phonons. If the rate at which the optical phonons decay into acoustic phonons is smaller than the rate at which optical phonons are created by hot carrier relaxation, the result will be a nonequilibrium phonon distribution with a temperature T_p greater than the lattice temperature. According to Safran and Lax³³, the optical phonons decay with a characteristic time of 10 psec at 77 K and 5 psec at 297 K.

Once there are electrons in the conduction band and holes in the valence band, as a result of direct absorption of the excite pulse, then free-carrier absorption is possible. Free-carrier absorption (process f, Fig. 8) denotes a process where an electron in any one of the conduction band valleys is induced to make a transition to a state higher in that same valley by the simultaneous absorption of a photon and the absorption or emission of a phonon (optical or acoustic). An identical process occurs for holes in the valence band. The rate for direct absorption is usually larger than that for free-carrier absorption; however, the rate at which direct absorption events occur decreases as the number of occupied states in the Γ valley increases. On the other hand, the rate for free-carrier absorption events increases as the number of electrons (holes) in the conduction (valence) band increases. The total number of free-carrier events occurring per unit time per unit volume in our experiments can be estimated from

$$R_{FCA}^{Total} = \alpha_{FCA} I / \hbar \nu \quad , \quad (7)$$

where α_{FCA} is the free carrier absorption coefficient and I the optical intensity. The rate per carrier can then be obtained by dividing Eq. 7 by the number of carriers/volume present in the sample:

$$R_{FCA} = \alpha_{FCA} I / \hbar \nu n \quad . \quad (8)$$

The free-carrier absorption coefficient α_{FCA} is directly proportional to carrier density and is estimated²² to reach values between 3×10^2 and $3 \times 10^3 \text{ cm}^{-1}$ at the optically-created carrier densities encountered in the experiments of Fig. 4 and Fig. 5. Since α_{FCA} is directly proportional to n , the rate/carrier R_{FCA} is independent of carrier concentration. For optical energy densities 10^{-2} J/cm^2 and optical pulsewidths of 10 psec, the rate/carrier is between

10^{10} and 10^{11} sec^{-1} . As a result of a free-carrier absorption event, a carrier will gain an excess energy $\hbar\nu$. This excess energy is quickly redistributed to the distribution as a whole through carrier-carrier collisions. As a result, free-carrier absorption serves to further elevate the carrier temperature.

It is important to notice that, of the processes discussed to this point, only direct and indirect absorption events will increase the carrier number. Free-carrier absorption and phonon-assisted relaxation serve only to elevate or reduce, respectively the carrier temperature. Various recombination processes can reduce the carrier number, as discusses below.

The recombination processes can be divided into two general categories: radiative and nonradiative. Radiative recombination can be of two types: direct and indirect. The recombination of an electron in the Γ -valley of the conduction band with a hole in the valence band by means of emission a photon is termed direct (process g, Fig. 8); the recombination of an electron in the L or X-valley with a hole in the valence band by means of the simultaneous emission of a photon and emission (or absorption) of a phonon is termed indirect (not shown). Direct gap recombination is the faster of the two processes. The transition probability is energy and distribution function dependent. At the high carrier densities under consideration here, the rate has been estimated^{22,34} to be approximately 10^9 sec^{-1} . Much shorter effective lifetimes have been predicted³⁵; however, we presently have no direct experimental evidence to substantiate these claims. Consequently, we assume that these processes occur on nanosecond time scales and ignore them for the remainder of our discussion.

At very high carrier densities, such as those produced here, third-order nonradiative Auger recombination can become important. Auger recombination is a Coulombic three-body interaction conserving energy and momentum. In this process (h, Fig. 8), an electron recombines with a hole, and the excess energy is transferred to another electron (or hole) in the form of kinetic energy. The Auger equation for electron-hole recombination has the form

$$dn/dt = -\gamma_A n^3, \quad (9)$$

where γ_A is defined as the Auger rate constant. This rate constant has been estimated³⁶ to be approximately $10^{-31} \text{ cm}^6 \text{ sec}^{-1}$. We can use Eq. (9) to determine an estimate of the initial decay rate immediately following carrier creation by direct absorption of the excitation pulse:

$$\left. \frac{dn}{dt} \right|_{0+} \approx -(\gamma_A n_0^2) n, \quad (10)$$

where n_0 is the initial photogenerated carrier density and $\gamma_A n_0^2$ the initial rate. For typical carrier densities generated here ($10^{20} - 10^{21} \text{ cm}^{-3}$), this yields an initial recombination rate of $10^9 - 10^{11} \text{ sec}^{-1}$. Obviously, this rate is strongly dependent on the carrier density; an uncertainty of an order of magnitude in carrier density results in two orders of magnitude error in the initial carrier loss rate. We shall report on picosecond optical measurement of these Auger rates in a later seminar. Because of the small magnitude of γ_A , Auger events are only observed at very high carrier densities. They serve to reduce the carrier number and heat the carrier distribution.

In passing, we note that the inverse of the Auger process, the so-called Kane process is also allowed. This process (not shown in Fig. 8) is also a three-body Coulombic interaction. Here, however, an electron located high in

the conduction band makes a transition to lower in the band, and the excess energy is used to create an electron-hole pair. For this process to be significant a substantial number of carriers must be located high enough in the conduction band to possess an excess kinetic energy larger than the direct band gap energy E_0 . As a result, this process depends strongly on carrier temperature. The rate for this process has been estimated³⁷ to be less than 10^8 sec^{-1} for typical distribution temperatures encountered here.

As the carrier density builds up (primarily as a result of direct absorption of the excite pulse), the plasma frequency of the carriers increases. At sufficiently large plasma frequencies, an electron in the Γ valley can recombine with a hole near the top of the valence bands via emisison of a plasmon. The plasma frequency, given by

$$\omega_p^2 = \frac{e^2 n}{\epsilon} \left(\frac{1}{m_c} + \frac{1}{m_h} \right) \quad , \quad (11)$$

where e is the elementary electron charge, ϵ the dielectric constant, n the carrier density, and m_c and m_h are the electron and hole effective masses, respectively. Since most of the electrons are located in the side valleys, the side-valley electron effective mass occurs in Eq. (11). Normally, an electron near the conduction-band edge (at Γ) can recombine with a hole by emission of a plasmon only if the plasma frequency ω_p is larger than the direct gap frequency E_0/\hbar . However, in our problem according to Elci et al.²², the plasmon resonance is substantially broadened during the period the excitation pulse is passing through the sample. This is because direct absorption populates only the Γ valley. As a result, the Fermi energy of the Γ -valley electrons is perturbed relative to the Fermi energy of the L-X valley electrons when the excitation pulse is present in the sample. This relative perturbation is rapidly damped as the two Fermi energies try to rapidly equalize

by means of phonon-assisted intervalley scattering. This rapid damping causes the broadening of the plasmon resonance. As a result of the broadening, the plasmon lifetime is short compared to a picosecond. The energy lost in the decay of the plasma oscillations is rapidly transferred to single electron and hole states, and ultimately increases the temperature of the carrier distribution. Consequently, the end result of plasmon assisted recombination is the same as that of Auger recombination; it reduces the carrier number and raises the distribution temperature. As a matter of interest, a carrier density of 10^{21} cm^{-3} would result in a plasma energy $\hbar\omega_p$ equal to the band gap energy E_0 . The effect of plasmons in early theoretical models may have been overestimated because of errors in early estimates of the carrier density.

Once a large population of holes has been created in the valence band (again by the direct absorption of the excite pulse), we must consider the importance of another process that occurs only at high carrier densities - direct intervalence-band absorption. These band-to-band transitions occur between light- and heavy-hole valence bands and the split-off valence band. While quantum selection rules forbid direct transitions between valence subbands at $\vec{k} = 0$, they are allowed at $\vec{k} \neq 0$. The energetically allowed direct intervalence-band transitions are indicated by arrows (process j) in Fig. 8. These transitions occur relatively far from the center of the Brillouin zone. As a result, unless the hole concentration is large, the intervalence-band transition rate will be small compared to that for direct interband absorption, since both initial and final states will be occupied. The availability of the final state for absorption depends on both the hole number and temperature. The direct intervalence-band absorption coefficient in germanium for a lattice temperature of 300 K, a carrier temperature of

approximately 1800 K, and a carrier number of 10^{20} cm^{-3} has been estimated³⁷ to be 10^3 cm^{-1} . Intervalence-band absorption does not change the carrier number but, like free-carrier absorption, serves only to elevate the distribution temperature.

At high carrier densities, Coulomb-assisted indirect transitions might enhance absorption as well. A Coulomb assisted indirect transition is one in which an electron makes an indirect transition from the valence band near Γ to a conduction band side valley by the absorption of a light quanta. In contrast to phonon-assisted indirect transitions, here the momentum required for the virtual scattering of the electrons from central to side valley is provided by electron-electron scattering. This process is shown as process k of Fig. 7. The expected importance of this process in our experiments is based on observations of enhanced indirect absorption in heavily doped n-type germanium by Haas.³⁸ By extrapolating his results on heavily-doped samples, we can obtain a rather crude estimate of the importance of this process at our photon energies and our carrier densities. His measurements suggest that at a wavelength of $1.06 \mu\text{m}$ and at carrier densities of 10^{20} cm^{-3} , the Coulomb-assisted indirect absorption coefficient might be in the range of $10^3 - 10^4 \text{ cm}^{-1}$. One of the problems associated with this extrapolation is the presence of the large hole densities in our experiments; these holes can partially fill the initial states required for the transition. The effect of this process is to increase the carrier number. Since the momentum required for the virtual transition is provided by carrier-carrier scattering, this process is sensitive to carrier density.

The diffusion of carriers from and within the interaction region (focused spot size times sample thickness) will reduce the carrier density seen by the probe pulse. Because of the size of the focused spot for the optical pulse (typically 1 - 2 mm

in diameter), diffusion transverse to the direction of light propagation is entirely negligible on picosecond time scales. However, diffusion of carriers from the region near the surface of the sample into the crystal bulk in the direction of light propagation can be significant. We term the diffusion in the direction of light propagation longitudinal. Under the assumption that the photogenerated carriers (10^{20} cm^{-3}) that are created by the excite pulse are initially deposited in an exponential absorption depth of approximately $1 \mu\text{m}$, the time required for the carrier plasma layer to double its thickness has been estimated^{37,39} to be 75-100 picoseconds. Consequently, longitudinal diffusion effects can be significant in our problems.

One final effect of the huge carrier densities deserves mention here: band-gap renormalization. At high carrier concentrations, exchange contributions and free-carrier induced shifts in phonon frequencies cause a narrowing of the energy gap. Ferry³⁵ has estimated this narrowing to be approximately 32 meV when the carrier density in the central Γ -valley is $2 \times 10^{19} \text{ cm}^{-3}$. Thus, we see that all of the processes and interactions discussed above are complicated by the presence of a dynamic energy-gap narrowing as the carrier densities evolve with time. Since this energy-gap narrowing is electronic in origin, we expect the gap to instantaneously (10^{-15} to 10^{-14} sec) reflect any change in carrier density.

This concludes our brief survey of the basic physical processes that could be important in describing the picosecond optical response of germanium. The key features of this review are summarized in Table I. This table illustrates, once again, the large number of processes that must be considered if we are to describe the evolution of a large photogenerated carrier distribution on a picosecond time scale. Although many of these processes are important in low intensity experiments as well, their rates are drastically altered at the high

photoexcitation levels and large carrier densities present here. Others (e.g. Auger recombination, Kane processes, plasmon recombination, direct intervalence band absorption, Coulomb-assisted indirect absorption, and band-gap narrowing) are only significant at high excitation levels and huge carrier densities. In the following section, we present an early model that attempts to account for the excite pulse transmission and probe pulse transmission as displayed in Fig. 4 and Fig. 5 in terms of some of these processes.

IV. INITIAL MODELS

In Fig. 5, we have presented a graph of the probe pulse transmission versus time delay between the excite pulse at $1.06\text{ }\mu\text{m}$ and the probe pulse at $1.06\text{ }\mu\text{m}$ for a sample temperature of 100 K. As we have already noted, this curve exhibits two distinct features. The first is a narrow spike in probe transmission approximately two picoseconds wide and centered about zero delay. The second is a gradual rise and fall in probe transmission lasting hundreds of picoseconds. In this section, we review early attempts to interpret this data.

Parametric Scattering

The narrow spike in probe transmission (shown on an expanded scale in Fig. 9) was first observed by Kennedy *et al.*¹⁰ and was attributed by them to a saturation and relaxation of the direct absorption. Subsequently, Shank and Auston¹¹ observed, in addition to the narrow spike near zero delay, the slower structure at longer delays. In light of this additional structure, they reinterpreted the narrow spike in probe transmission near zero delay as a parametric coupling between excite and probe beams caused by an index grating produced by the interference of the two beams in the germanium sample. In this section, we review the manner in which parametric scattering can account for the spike in the probe transmission.

In the picosecond excite and probe studies described previously, the excite and probe pulses are derived from a single pulse by means of a beam splitter. Consequently, the probe pulse is simply an attenuated version of the excite pulse. Near zero delay, the excite and probe pulses are both spatially and temporally overlapped. As a result, the interference of the two beams will produce

a modulation of the optically-created carrier density to form a grating with spacing $d = \lambda / (2 \sin \theta)$, where λ is the optical wavelength and θ is the angle between each beam and the sample normal as shown in Fig. 10. The grating is formed rapidly and will diffract both excitation and probe pulses as shown in Fig. 10. The first order diffracted beams for both excite and probe are shown. Notice that one of the first order diffracted beams from the excitation pulse will be scattered into the direction of the probe pulse detector. Also, one of the first order diffracted beams from the probe pulse will be scattered into the direction of the excite pulse detector. Since the probe pulse energy is only a small fraction of the excite pulse energy, the amount of light diffracted from the probe pulse into the excite pulse detector is insignificant. On the other hand, a small fraction of the excite beam scattered in the direction of the probe detector can produce a signal on the probe detector larger than that produced by the transmitted probe pulse.

The sharp increase (spike) in the signal observed on the probe detector as the two pulses are delayed with respect to one another can then be understood in terms of this parametric scattering in the following manner. An increase in probe detector signal will be observed so long as a grating is produced. Such a grating will be formed only if the delay between excite and probe pulses does not exceed the coherence length of the two pulses. It is well known that pulses produced by mode-locking glass lasers are usually correlated over a length less than their optical pulse width because of various nonlinear processes involved in pulse generation. Consequently, parametric scattering results in an increase in probe detector signal for time delays less than the optical pulse width. Thus, the narrow spike in probe transmission is not an increase in sample transmission at all but a scattering of the excite pulse into the probe pulse. As such, the spike is merely a coherent coupling artifact of the measurement technique.

While recognizing that some parametric scattering is bound to occur during such measurements, Ferry³⁵ has recently presented numerical studies that account for the spike in germanium transmission in terms of state filling and band gap narrowing. If, indeed, these processes were responsible for the narrow rise and fall in probe transmission, a careful study of this structure would yield information concerning carrier scattering rates from the optically coupled states. Subsequently, however, Lindle *et al.*⁴⁰ have presented the results of measurements that indicate that parametric scattering fully accounts for the observed spike. As a result, we ignore this spike in probe detector response in the remainder of our discussion. We caution the reader at this point, however, that band-gap narrowing and state filling have been observed in other semiconductor experiments involving optical excitation, and certainly, they must be occurring to some degree here as well. They simply do not contribute to the spike in a measureable way.

Hot Electron Relaxation Model

Recently, Elci *et al.*²² have presented an initial first principles theoretical treatment that attempts to account for both the generation and the subsequent transient behavior of the electron-hole plasmas, created in germanium by the absorption of intense picosecond optical pulses, in terms of direct band-to-band absorption, free-carrier absorption, phonon-assisted intervalley scattering, phonon-assisted carrier relaxation, carrier-carrier collisions, and nonradiative recombination. In these calculations, rate equations were obtained for the parameters (electron number, temperature, Fermi energies) characterizing the electron-hole distributions, and the rates for the individual processes were computed from perturbation theory and Fermi's Golden Rule to provide a quantitative description of the transient optical properties of germanium. (These calculations are presented in detail in Ref. 22). Briefly, this model

(hereafter referred to as the ESSM model) accounts for the transmission of a single optical pulse through a thin germanium sample as a function of incident pulse energy (Fig. 4) and the transmission of a weak probe pulse as a function of time delay after an energetic pulse (Fig. 5) in terms of these processes in the following manner. When an excite pulse is incident on the germanium sample, the unreflected portion of the pulse enters the sample where most of it is absorbed by direct transitions, creating a large density of electrons (holes) in the central valley of the conduction (valence) band. The electrons are rapidly ($\sim 10^{-14}$ sec) scattered to the conduction-band side valleys by long-wave-vector phonons. Carrier-carrier scattering events, which occur at a rate comparable to the direct absorption rate, ensure that the carrier distributions are Fermi-like and that both electron and hole distributions have the same temperature, which can be different from the lattice temperature. Since the photon energy $\hbar\nu$ is greater than either the direct energy gap E_0 or the indirect gap E_L , such a direct absorption event followed by phonon-assisted scattering of an electron to the side valleys results in the photon giving an excess energy of $\hbar\nu - E_L$ to thermal agitation. This excess energy results in an initial distribution temperature (approximately 1800 K for a lattice temperature of 300 K) due to direct absorption that is greater than the lattice temperature. Thus, the single-pulse transmission (Fig. 4) would begin at its Beer's-law value and increase as a function of incident optical pulse energy because of the partial filling (depletion) of the optically coupled states in the conduction (valence) band as a result of band filling caused by direct absorption. Other processes such as free-carrier absorption and nonradiative recombination events (i.e., Auger and plasmon-assisted recombination) can further raise the carrier temperature during the passage of the excite pulse, while phonon-assisted intravalley relaxation processes can reduce the carrier temperature.

After the passage of the excite pulse, the interaction region of the sample contains a large number of carriers ($10^{19} - 10^{20} \text{ cm}^{-3}$) with a high distribution temperature. The final temperature is determined by the number of quanta in the excite pulse and the relative strengths of the nonradiative recombination and the phonon-assisted relaxation rates as discussed by Latham *et al.*²⁰ As time progresses, the distribution will continue to cool by phonon-assisted intravalley relaxation. Experimentally, the probe pulse interrogates the evolution of the distribution after the passage of the excite pulse and is a sensitive measure of whether the optically coupled states are available for absorption or are occupied. The probe pulse transmission versus time delay (Fig. 5) can be understood in the following way. Immediately after the passage of the excite pulse, the probe transmission is small since the electrons (holes) are located high (low) in the conduction (valence) bands because of the high distribution temperature, leaving the states that are optically coupled available for direct absorption (Fig. 11). Later, as the distribution temperature cools and carriers fill the states needed for absorption, the transmission increases. In short, the ESSM model attributes the slow rise in probe transmission with delay to a cooling of the hot carrier distribution created by the absorption of the excite pulse. The subsequent slow fall in probe transmission at much longer delays is attributed to carrier recombination, which reduces the carrier density and once again frees the optically coupled states for absorption, and to diffusion.

The theoretical fits from Elci *et al.*²² to the single pulse transmission data and probe pulse data of Smirl *et al.*¹² are shown as solid lines in Fig. 12 and Fig. 13. Given the complexity of the problem, the overall fit can be regarded as satisfactory. Nonlinear transmission measurements in which the energy band gap of the germanium sample was tuned by hydrostatic pressure⁴¹ have been accounted for by this model as well.

Despite the apparent successes of this model, some basic questions remain concerning the roles of the various physical processes in determining the saturation and temporal evolution of the optical transmission of thin germanium samples under intense optical excitations. Elci *et al.*²² noted that their calculations contained serious assumptions that warranted further theoretical and experimental investigation. The major assumptions were the following: (i) The carrier-carrier collision rate was assumed to be high enough to justify taking the carrier distributions to be Fermi-Dirac. Ferry³⁵ has recently reexamined this approximation by calculating the time and energy dependence of the distribution function at the high carrier photogeneration rates encountered here. He concludes that on a time scale of tens of picoseconds the distribution function does indeed approximate a Fermi distribution; however, on shorter time scales it contains a δ -function-like spike located at the optically coupled states. Thus, for purposes of calculating the probe-pulse transmission, one may reasonably assume the distribution is Fermi-like (ii) Carrier Fermi energies and temperatures were taken to depend only on time, rather than on both space and time, thus ignoring the pulse-propagation and carrier-diffusion problems within the optical interaction region of the sample. Therefore, parameters describing the electron-hole plasma, such as the electron number, must be viewed as spatial averages throughout the sample volume. (iii) To simplify the calculations, the actual germanium energy band structure was replaced with a highly idealized parabolic band structure having two degenerate valence bands and a conduction band with a direct valley and 10 equivalent side valleys. The split-off band was totally ignored.

Elci *et al.*²² also noted at the outset that their work contained only a few of the many possible electronic processes. Recent studies^{35,37,42,43} indicate

that processes other than those named above may be important. Most of these effects, such as band-gap narrowing,³⁵ intervalence-band absorption,^{37,42} Auger recombination⁴³ and Coulomb-assisted indirect absorption,⁴² are only observed at large carrier densities. The possible importance of including these processes in any interpretation of the rise in probe transmission will be examined in Seminar S4 to follow.

In the previous two paragraphs, we have outlined the assumptions and omissions of the initial hot-electron model; however, there is another problem associated with the original calculations that is of importance to the present work. The physical constants for germanium, specifically the electron-phonon coupling constants, are not well-known enough to allow a precise calculation of the energy relaxation rate. Latham *et al.*²⁰ have previously discussed this point in detail. For the theoretical fits shown in Fig. 13, the electron-phonon coupling constants are chosen as $6 \times 10^{-4} \text{ erg cm}^{-1}$ for a lattice temperature of 297 K and $2 \times 10^{-4} \text{ erg cm}^{-1}$ at 100 K. These values are within the range of the accepted theoretically and experimentally determined values listed by Latham *et al.*²⁰; however, they are much lower than the mean value of $1 \times 10^{-3} \text{ erg cm}^{-1}$ as obtained from an average of the eight values listed. Since the carrier cooling rate is proportional to the square of the electron-phonon coupling constant, the fitted values result in carrier cooling rates that are 3 and 25 times slower than that obtained by using the average value.

The ESSM model was the first comprehensive theoretical model to attempt to account for the ultrafast response of optically-excited semiconductors. Because of the large number of processes that actually occur, the approximations taken to simplify the mathematics, and the uncertainties in the magnitudes of certain physical constants, the theory is, unavoidably, rather incomplete

as it was first presented and as we have reviewed it here. We have chosen to present the model in its early form primarily for tutorial purposes. In spite of its limitations, the theory does represent a first step toward an understanding of a very complicated problem. It provides both a historical perspective and a solid base for further developments. In addition, it is a model that is still evolving. In fact, in Seminar S4 of this ASI, we shall review experimental studies that provide evidence that processes other than those originally included in the model are important and that indicate that certain approximations of the original ESSM model must be removed. We shall then describe recent attempts to modify the model to accomodate these findings. We shall find that these refinements significantly alter our interpretation of the slow rise in probe transmission as shown in Fig. 5 and Fig. 13. In this seminar, we shall also discuss alternative models. The interpretation of the rise in probe transmission is still a matter of active debate.

V. CONCLUSION

In this lecture, in an attempt to provide the reader with an introduction to the physics of ultrafast carrier relaxation processes in semiconductors, we have discussed an early excite and probe experiment in germanium, enumerated the processes that could occur during such studies, and presented an early interpretation of these experiments. Throughout, we have tried to emphasize the ultrashort time scales and high carrier densities involved in these recent studies. It is evident from our discussions here that these picosecond excite and probe studies can yield direct measurements of ultrafast carrier relaxation processes that were heretofore inaccessible. It is equally clear, however, that as experimentors we must be more clever in designing our experimental configuration if we hope to unambiguously extract these rates. We must choose our experimental technique so as to isolate the effect of a single process. In the experiments that we described in this lecture, almost every imaginable process was active. The large number of active processes makes these experiments attractive for tutorial purposes, but it ensures that the interpretation of the data will be a nightmare. We will review some more recent attempts to isolate the rates of single processes in Seminar S4 of this ASI.

This work was supported by the Office of Naval Research and the North Texas State University Faculty Research Fund.

REFERENCES

1. E. M. Conwell, "High field transport in semiconductors," Solid State Physics, Supplement 9, (Edited by Seitz, Turnbull, and Ehrenreich), Academic Press, New York (1967).
2. G. Bauer, "Determination of electron temperatures and of hot electron distribution functions in Semiconductors," Springer Tracts in Modern Physics, Vol. 74, Springer-Verlag, Berlin (1974).
3. G. Bauer, "Optical determination of hot carrier distribution functions," NATO Advanced Study Institute on Linear and Nonlinear Electron Transport in Solids, (Edited by Devreese and van Doren), Plenum Press (1976).
4. J. Shah, "Hot electrons and phonons under high intensity photoexcitation of semiconductors," Solid-State Electron. 21, 43 (1978).
5. R. G. Ulbrich, "Low density photoexcitation phenomena in semiconductors: aspects of theory and experiment," Solid-State Electron. 21, 51 (1978).
6. R. C. C. Leite, "Radiative spectra from hot photocarriers," Solid-State Electron. 21, 177 (1978).
7. C. Weisbuch, "Photocarrier thermalization by laser excitation spectroscopy," Solid-State Electron. 21, 179 (1978).
8. R. G. Ulbrich, "Energy relaxation of photoexcited hot electrons in GaAs," Phys. Rev. B8, 5719 (1973).
9. J. W. Shelton and J. A. Armstrong, "Measurement of the relaxation time of the Eastman 9740 bleachable dye," IEEE JQE QE-3, 696 (1967).
10. C. J. Kennedy, J. C. Matter, A. L. Smirl, H. Weichel, F. A. Hopf, and S. V. Pappu, "Nonlinear absorption and ultrashort carrier relaxation times in germanium under irradiation by picosecond pulses," Phys. Rev. Lett. 32, 419 (1974).
11. C. V. Shank and D. H. Auston, "Parametric coupling in an optically excited plasma in Ge," Phys. Rev. Lett. 34, 479 (1975).
12. A. L. Smirl, J. C. Matter, A. Elci, and M. O. Scully, "Ultrafast relaxation of optically excited nonequilibrium electron-hole distributions in germanium," Opt. Commun. 16, 118 (1976).
13. S. L. Shapiro, "Ultrashort light pulses: picosecond techniques and applications," Topics in Applied Physics, Vol. 18, Springer-Verlag, Berlin (1977).
14. C. V. Shank, E. P. Ippen, and S. L. Shapiro, "Picosecond Phenomena," Springer Series in Chemical Physics, Vol. 4, Springer-Verlag, Berlin (1978).

15. M. Neuberger, "Group IV semiconductor materials," Handbook of Electronic Materials, Vol. 5, Plenum Press, New York (1971).
16. M. Cardona, "Band parameters of semiconductors with zincblende, wurtzite, and germanium structure," J. Phys. Chem. Solids 24, 1543 (1963).
17. W. Fawcett, "Valence band structure of germanium," Proc. Phys. Soc. 85, 931 (1965).
18. M. Cardona and F. H. Pollak, "Energy-band structure of germanium and silicon: the $\mathbf{k} \cdot \mathbf{p}$ method," Phys. Rev. 142, 530 (1966).
19. J. van Borzeszkowski, "Approximate analytical description of the $E(k)$ - dependence of the bands of heavy and light holes in Si and Ge," Phys. Stat. Sol. (b) 61, 607 (1974).
20. W. P. Latham, Jr., A. L. Smirl, A. Elci, and J. S. Bessey, "The role of phonons and plasmons in describing the pulsewidth dependence of the transmission of ultrashort optical pulses through germanium," Solid-State Electron. 21, 159 (1978).
21. W. C. Dash and R. Newman, "Intrinsic optical absorption in single-crystal germanium and silicon at 77K and 300K," Phys. Rev. 99, 1151 (1955).
22. A. Elci, M. O. Scully, A. L. Smirl, and J. C. Matter, "Ultrafast transient response of solid-state plasmas. I. Germanium: theory and experiment," Phys. Rev. B 16, 191 (1977).
23. H. J. G. Meyer, "Infrared absorption by conduction electrons in germanium," Phys. Rev. 112, 298 (1958).
24. S. M. de Veer and H. J. G. Meyer, in Proceedings of the 6th International Conference on Semiconductor Physics, Exeter, (1962).
25. H. S. Reik and H. Risken, "Drift velocity and anisotropy of hot electrons in n-germanium," Phys. Rev. 126, 1737 (1962).
26. M. H. Jorgensen, N. I. Meyer, and K. J. Schmidt - Teidemann, in Proceeding of the 7th International Conference on Semiconductor Physics (Paris), Academic Press, New York, (1964).
27. R. Ito, H. Kawamura, and M. Fukai, "Anisotropic phonon scattering of electrons in germanium and silicon," Phys. Lett. 13, 26 (1964).
28. M. H. Jorgensen, "Warm-electron effects in n-type silicon and germanium," Phys. Rev. 156, 834 (1967).
29. W. Fawcett and E. G. S. Paige, "Negative differential mobility of electrons in germanium: a Monte Carlo calculation of the distribution function, drift velocity and carrier population in the $\langle 111 \rangle$ and $\langle 100 \rangle$ minima," J. Phys. C: Solid St. Phys. 4, 1801 (1971).

30. D. C. Herbert, W. Fawcett, A. H. Lettington, and D. Jones, in Proceedings of the 11th International Conference on Semiconductor Physics, Warsaw (1972).
31. K. Seeger, Semiconductor Physics, Springer-Verlag, Berlin (1973).
32. M. Costato, S. Fontanesi, and L. Reggiani, "Electron energy relaxation times in Si and Ge," J. Phys. Chem. Solids 34, 547 (1973).
33. S. Safran and B. Lax, "Temperature dependence of the Raman linewidth and frequency shift in Ge and Si," J. Phys. Chem. Solids, 36, 753 (1975).
34. H. M. van Driel, A. Elci, J. S. Bessey, and M. O. Scully, "Photoluminescence spectra of germanium at high excitation intensities," Opt. Commun. 20, 837 (1976).
35. D. K. Ferry, "Energy-gap narrowing and state filling in semiconductors under intense laser radiation," Phys. Rev. B 18, 7033 (1978).
36. R. Conradt and J. Aengenheister, "Minority carrier lifetime in highly doped Ge", Solid State Commun. 10, 321 (1972).
37. T. C. Y. Leung, Ph.D. dissertation, University of Arizona, 1978.
38. C. Haas, "Infrared absorption in heavily doped n-type germanium," Phys. Rev. 125, 1965 (1962).
39. D. H. Auston and C. V. Shank, "Picosecond ellipsometry of transient electron-hole plasmas in germanium," D. H. Auston and C. V. Shank, Phys. Rev. Lett. 32, 1120 (1974).
40. J. R. Lindle, S. C. Moss, and A. L. Smirl, "The effects of parametric scattering, energy-gap narrowing, and state filling on the picosecond optical response of germanium," to be published.
41. H. M. van Driel, J. S. Bessey, and R. C. Hanson, "Pressure tuning of picosecond pulse transmission in germanium," Opt. Commun. 22, 346 (1977).
42. D. H. Auston, S. McAfee, C. V. Shank, E. P. Ippen, and O. Teschke, "Picosecond spectroscopy of semiconductors," Solid State Electron. 21, 147 (1978).
43. D. H. Auston, C. V. Shank, and P. LeFur, "Picosecond optical measurements of band-to-band Auger recombination of high-density plasmas in germanium," Phys. Rev. Lett. 35, 1022 (1975).

FIGURE CAPTIONS

- Figure 1. Direct optical transitions in a semiconductor.
- Figure 2. Experimental technique for measuring ultrafast relaxation times in semiconductors.
- Figure 3. Block diagram of the experimental configuration for excite and probe measurements at $1.06\text{ }\mu\text{m}$, where MLL denotes the mode-locked laser, EOS the electro-optical switch, A the laser amplifier, M a mirror, D a detector, L1 and L2 lens, and S the germanium sample.
- Figure 4. Change in transmission of a $6\text{ }\mu\text{m}$ -thick germanium sample as a function of incident excite pulse energy at $1.06\text{ }\mu\text{m}$. Note a pulse energy of 2×10^{15} quanta corresponds to a surface irradiance of approximately 10^{-2} J/cm^2 .
- Figure 5. Probe pulse transmission vs delay between the excite pulse at $1.06\text{ }\mu\text{m}$ and the probe pulse at $1.06\text{ }\mu\text{m}$ for a sample temperature of 100 K. The data are plotted as the normalized ratio of probe pulse transmission to excite pulse transmission, T_P/T_E , in arbitrary units. The error bar represents twice the typical statistical standard deviation.
- Figure 6. Approximate germanium band structure at 300 K.
- Figure 7. Schematic representation of (a) direct interband absorption, (b) phonon-assisted indirect absorption, (c) long-wavevector phonon-assisted intervalley electron scattering, (d) electron-electron scattering, (e) phonon-assisted intravalley electron relaxation, and (k) Coulomb-assisted indirect absorption processes in germanium.
- Figure 8. Schematic representation of (f) free carrier absorption, (g) radiative recombination, (h) Auger recombination, (i) plasmon-assisted recombination, and (j) direct intervalence-band absorption processes in germanium.
- Figure 9. Normalized response of the probe detector, in arbitrary units, vs. time delay between the excite pulse at $1.06\text{ }\mu\text{m}$ and the probe pulse at $1.06\text{ }\mu\text{m}$.
- Figure 10. Geometry for the diffraction of excite and probe beams by a laser-induced grating, where e denotes the incident excite pulse, p the incident probe pulse, e_t the transmitted excite pulse, p_t the transmitted probe pulse, e_d a first order diffracted excite beam, p_d a first order diffracted probe beam, and $\sin \phi = 3 \sin \theta$. Solid lines represent transmitted beams and broken lines diffracted beams.

Figure 11. Schematic diagram for the temporal evolution (cooling) of the carrier distribution created by the absorption of the excite pulse. The solid curve represents the density of states at an energy E , and the broken curve the distribution function. The height of the cross hatched region (density of states times distribution function) is proportional to the number of carriers between E and $E + \Delta E$. The area under the cross hatched curve is proportional to the carrier number (approximately constant here). T_1 and t_1 represent the distribution temperature and time immediately after excitation.

Figure 12. Transmission of a 5.2- μm -thick germanium sample as a function of incident excite pulse energy at 1.06 μm for sample temperatures of 100 and 297 K. The solid lines are theoretical curves from Elci *et al.* (Ref. 22) and the data are from Smirl *et al.* (Ref. 12). Note that the focused spot size for the optical beam was roughly a factor of 10 smaller than for measurements depicted in Fig. 4.

Figure 13. Probe pulse transmission vs. delay between the excite pulse at 1.06 μm and the probe pulse at 1.06 μm for sample temperatures of 100 and 297 K. The data are plotted as the normalized ratio of probe pulse transmission to excite pulse transmission, T_p/T_E , in arbitrary units. The solid lines are theoretical curves from Elci *et al.* (Ref. 22) and the data are from Smirl *et al.* (Ref. 12).

TABLE I. Fundamental Processes

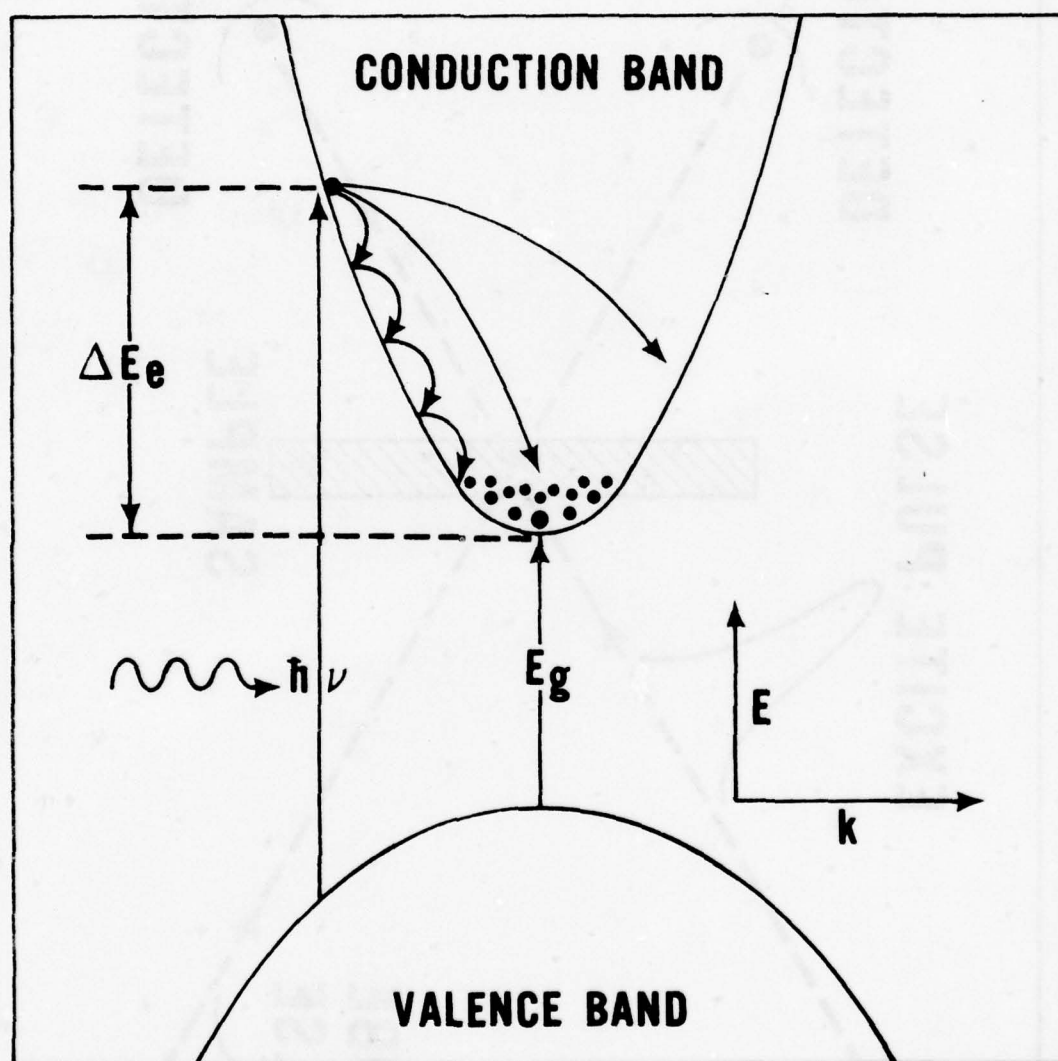
Process	Function	Characteristic Constants
a. Direct Interband absorption	generates carriers with excess energy $\Delta E \approx 0.5$ eV	$\alpha_0 = 1.4 \times 10^4 \text{ cm}^{-1}$
b. Phonon-assisted indirect absorption	increases carrier density	$\alpha_{ID} = 3.5 \times 10^2 \text{ cm}^{-1}$
c. Phonon-assisted intervalley scattering	populates side valleys	scattering rate/state $\sim 10^{14} \text{ sec}^{-1}$
d. Carrier-carrier scattering	thermalizes carriers	scattering rate [†] $> 10^{14} \text{ sec}^{-1}$
e. Phonon-assisted intra-valley relaxation	cools carriers, creates "hot" phonon distribution	phonon emission rate/carrier $\sim 10^{12} \text{ sec}^{-1}$
f. Free-carrier absorption	heats carriers	$\alpha_{FCA}^+ = 3 \times 10^2 - 3 \times 10^3 \text{ cm}^{-1}$
g. Radiative recombination	reduces carrier density	recombination rate $\sim 10^9 \text{ sec}^{-1}$
h. Auger recombination*	reduces carrier density, heats carriers	recombination rate [†] $< 10^{11} \text{ sec}^{-1}$
Kane process	increases carrier density	pair creation rate [#] $< 10^8 \text{ sec}^{-1}$
i. Plasmon-assisted recombination*	reduces carrier number, heats carriers	recombination rate [†] $< 10^{13} \text{ sec}^{-1}$
j. Direct intervalence band absorption*	heats carriers	$\alpha_{IB}^{+\#} \sim 10^3 \text{ cm}^{-1}$
k. Coulomb-assisted indirect absorption*	increases carrier number	$\alpha_{CID}^+ \sim 10^3 - 10^4 \text{ cm}^{-1}$
Diffusion	decreases carrier density	diffusion rate $\sim 1 \mu\text{m}/100\text{psec}$
Band-gap narrowing	decreases band gap	$< 32 \text{ meV}^{\dagger}$

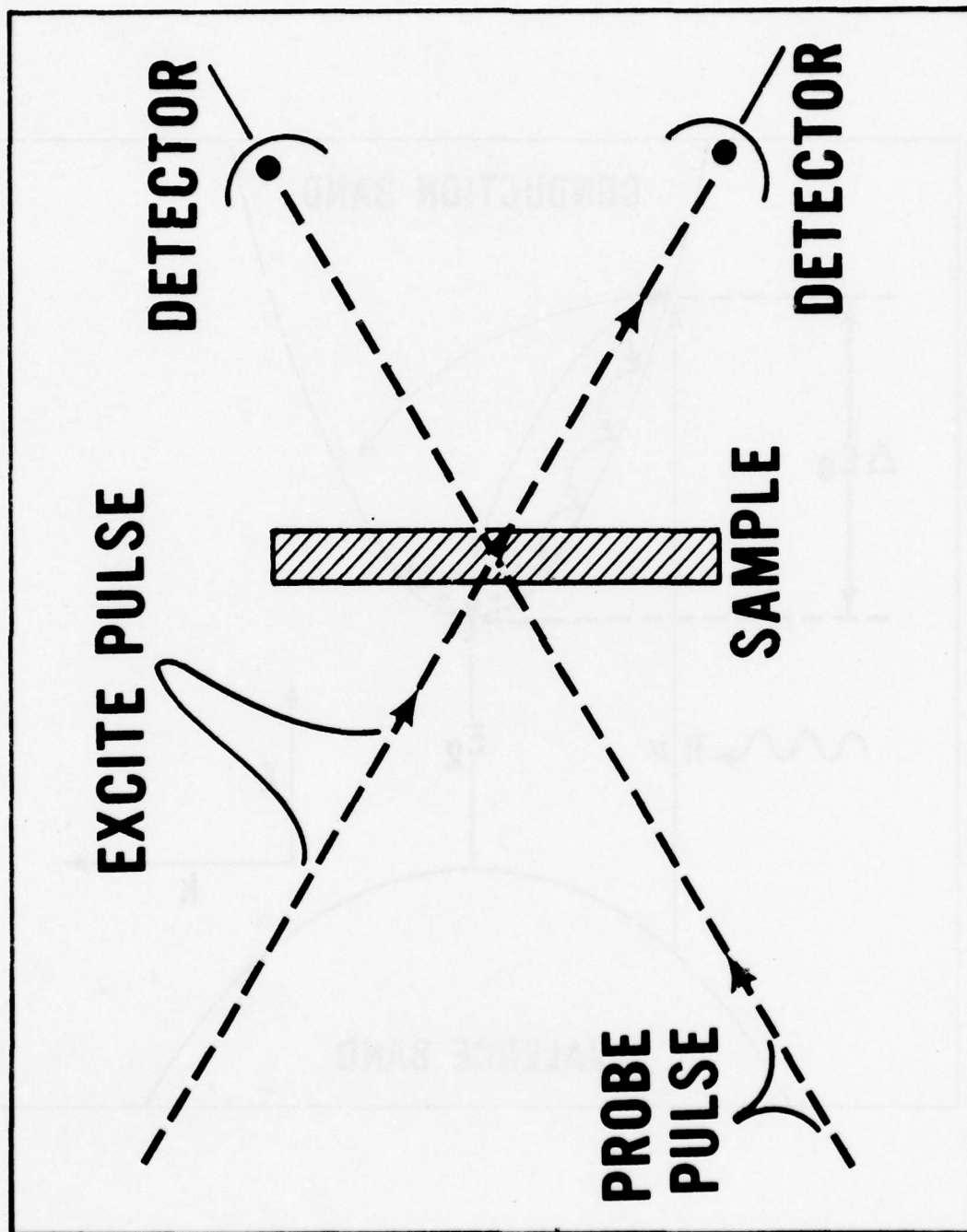
All values are estimated for carrier densities of $\sim 10^{20} \text{ cm}^{-3}$ and carrier temperatures of $\sim 1800 \text{ K}$

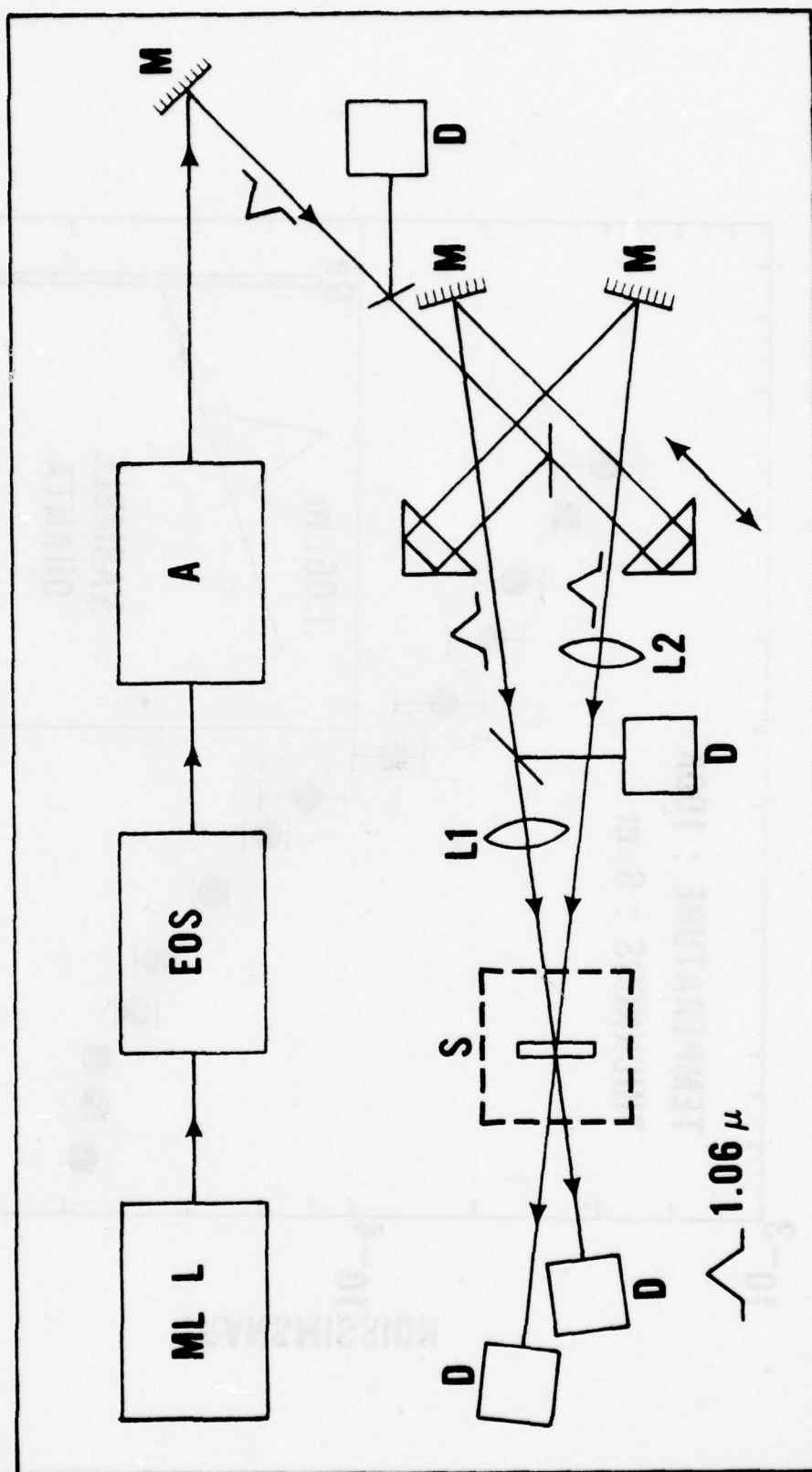
*Important only at high carrier densities

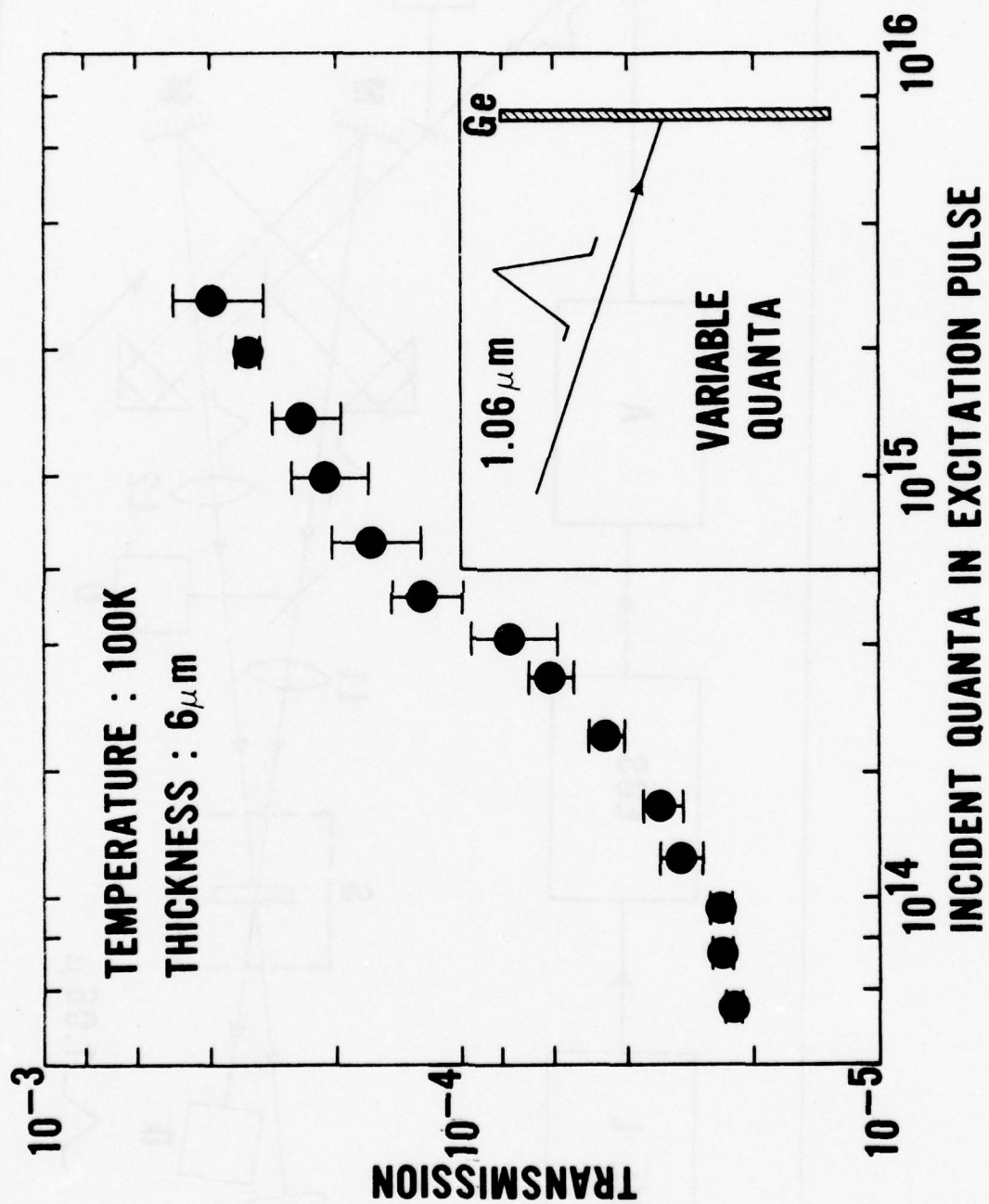
[†]Strongly dependent on carrier concentration

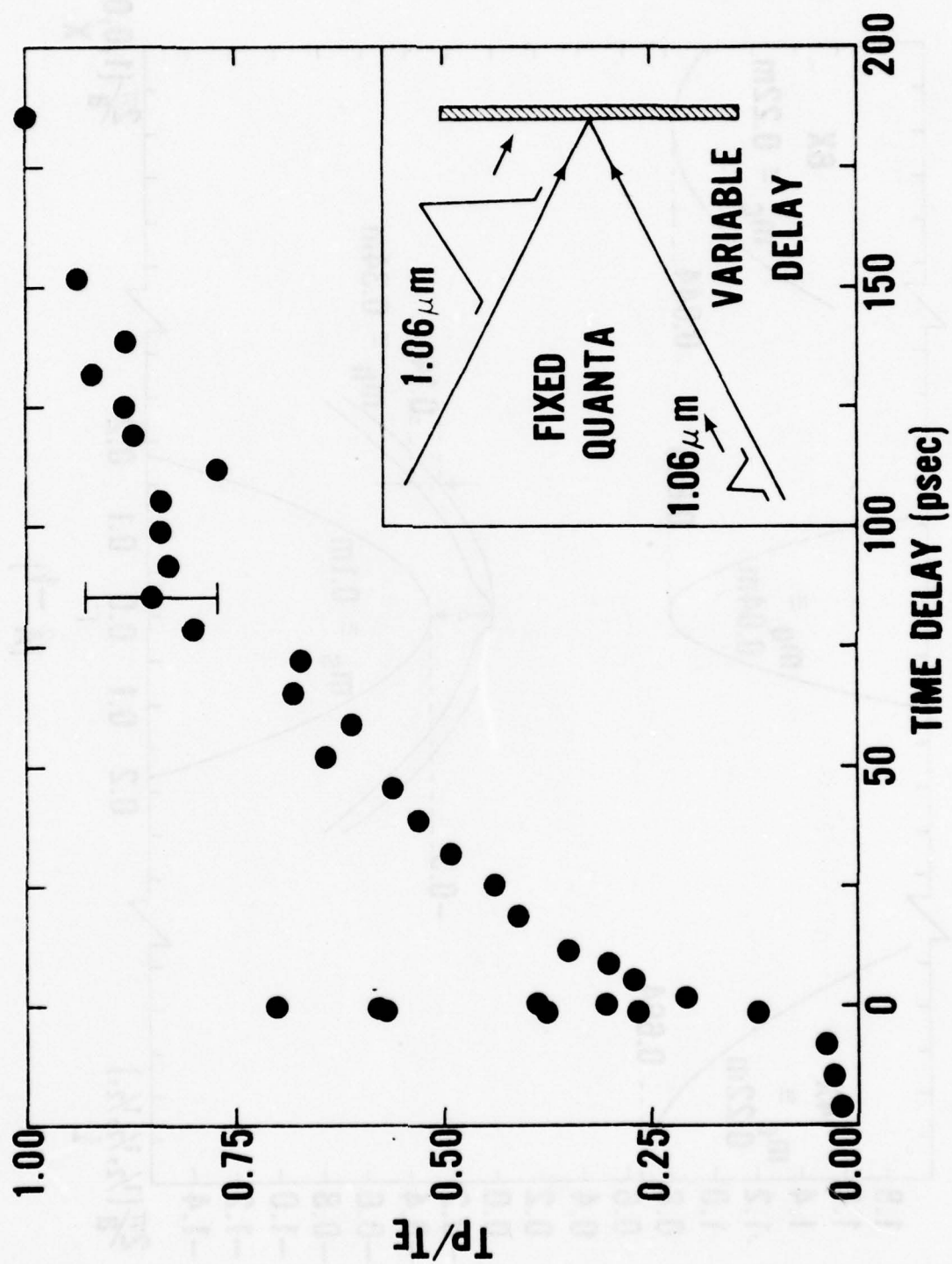
[#]Strongly dependent on carrier temperature

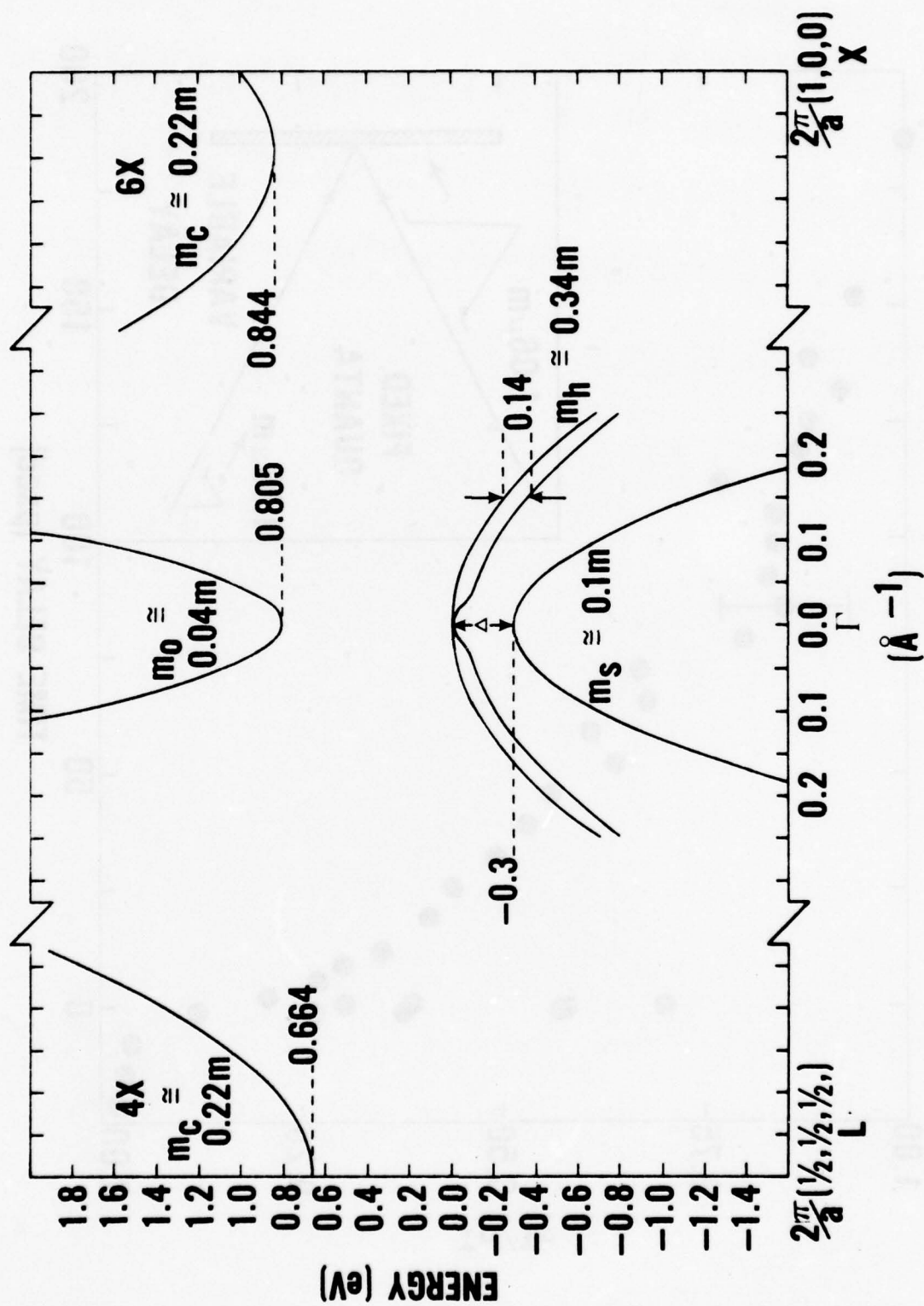


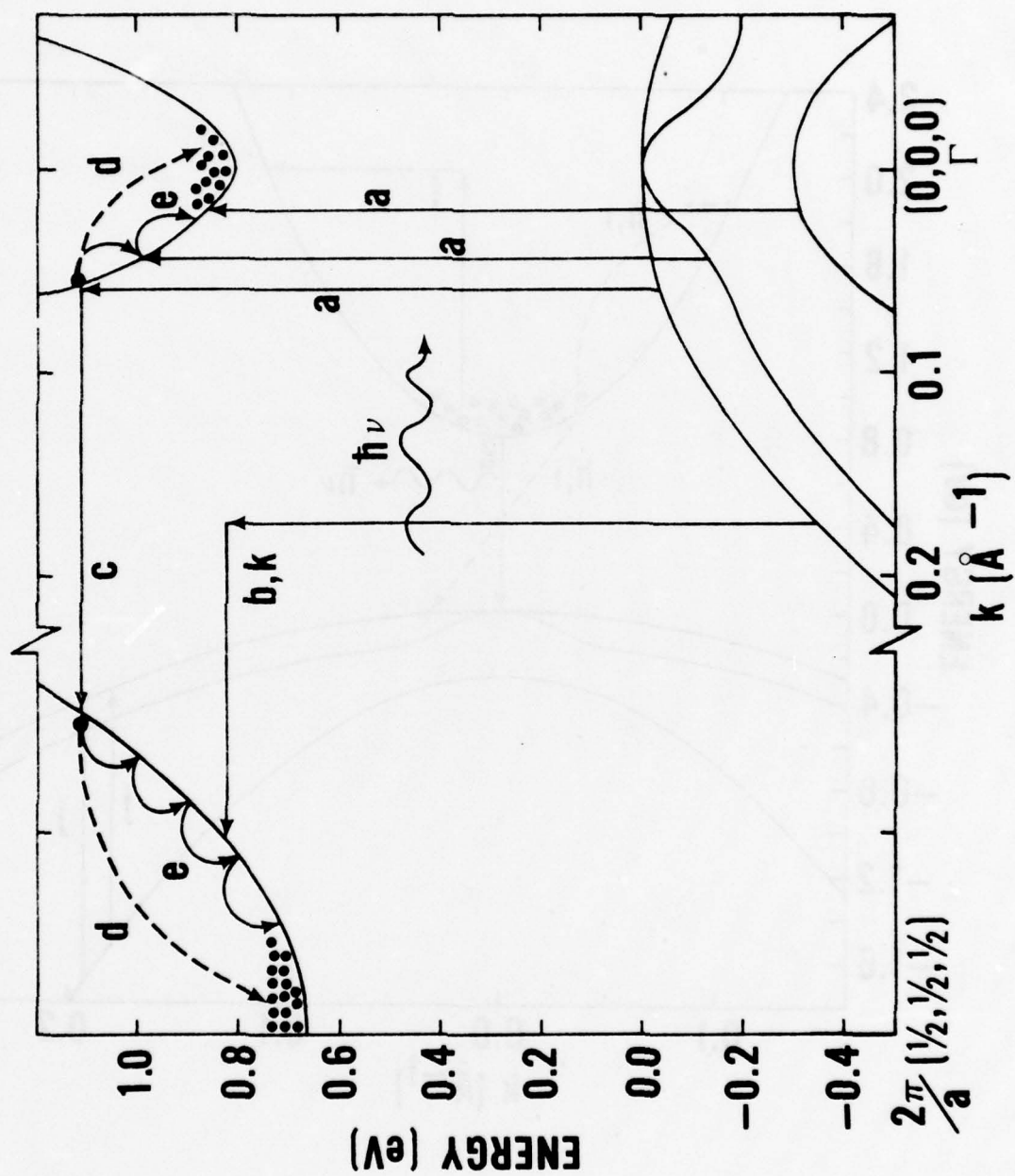


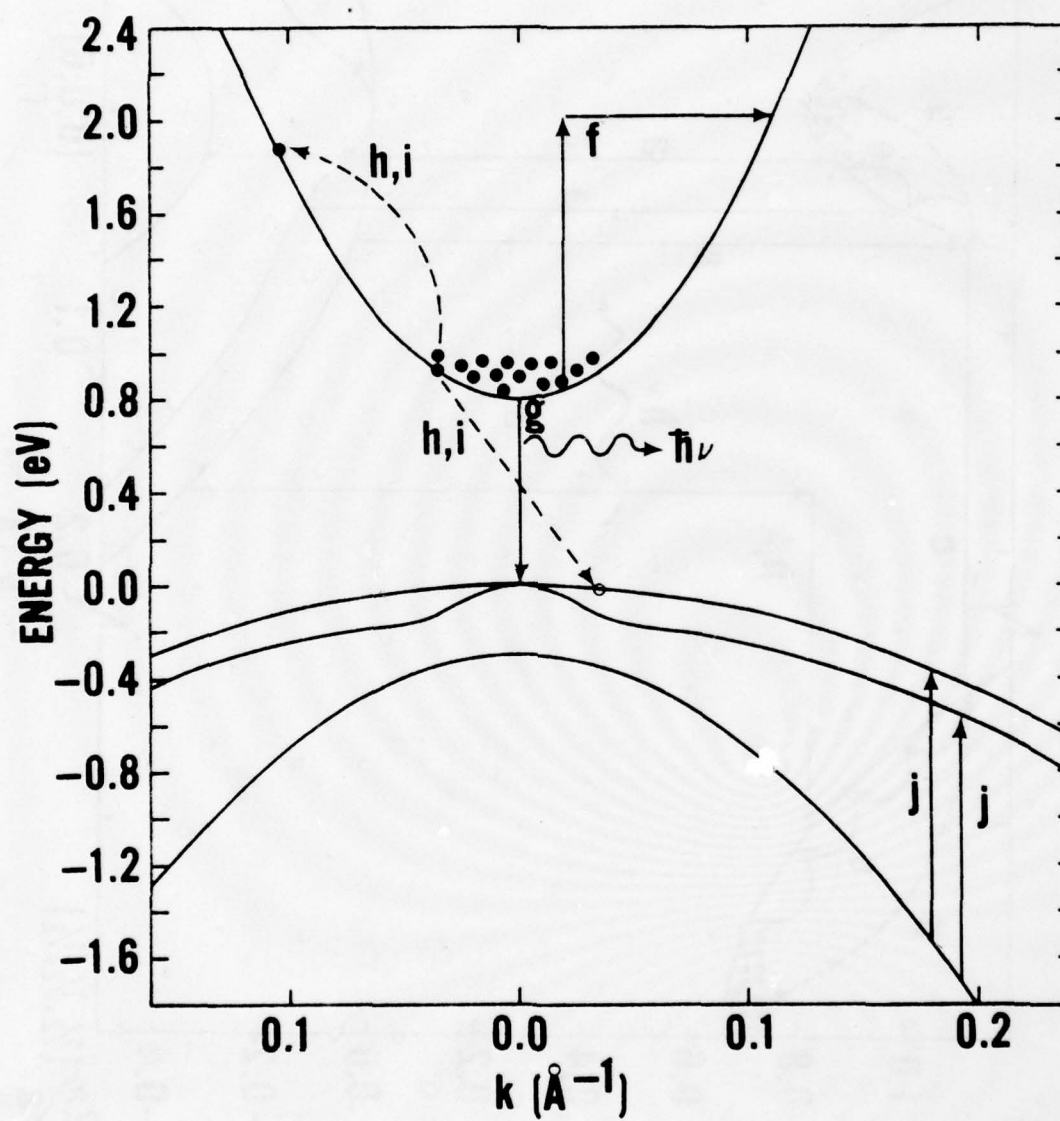


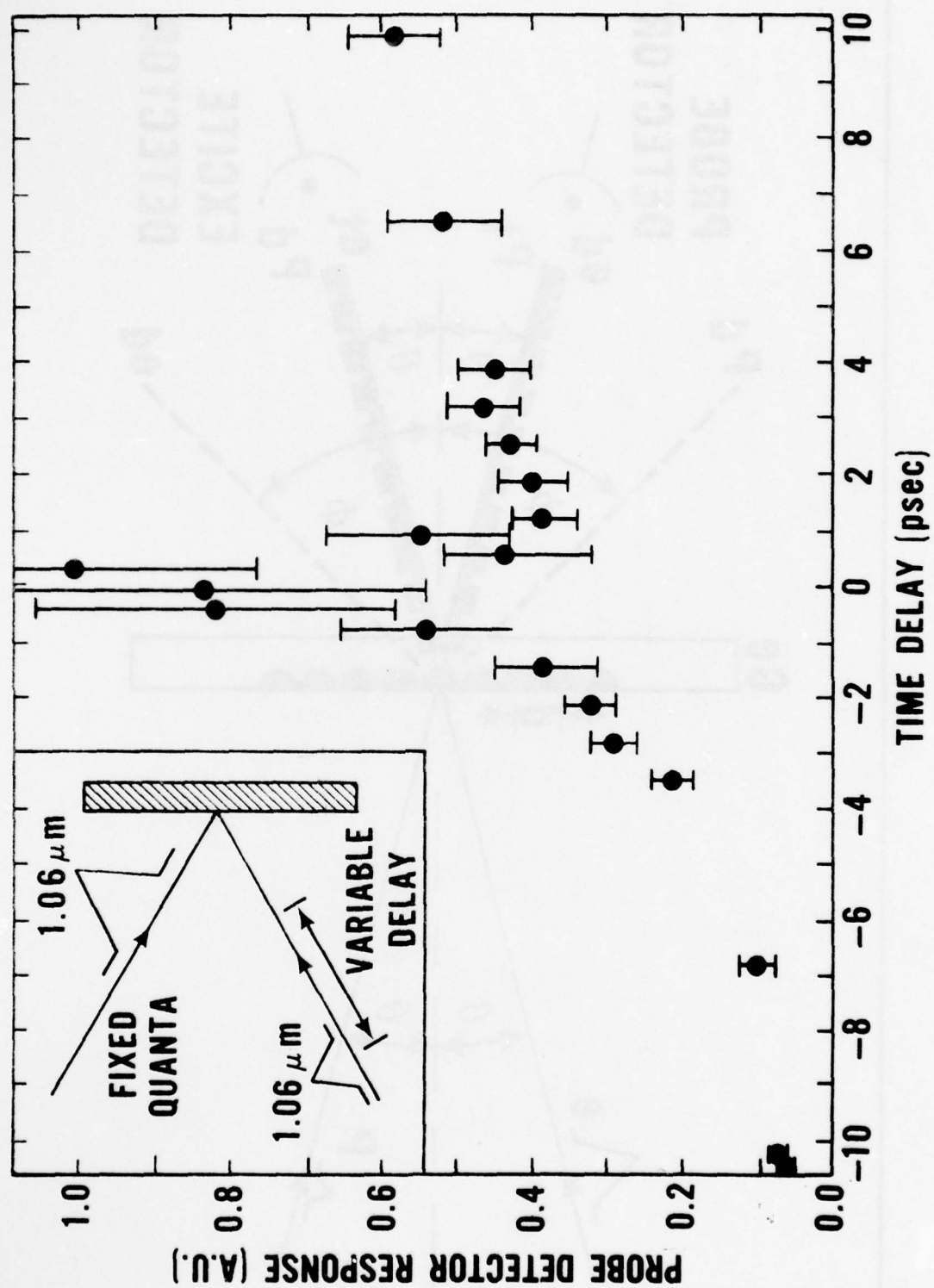


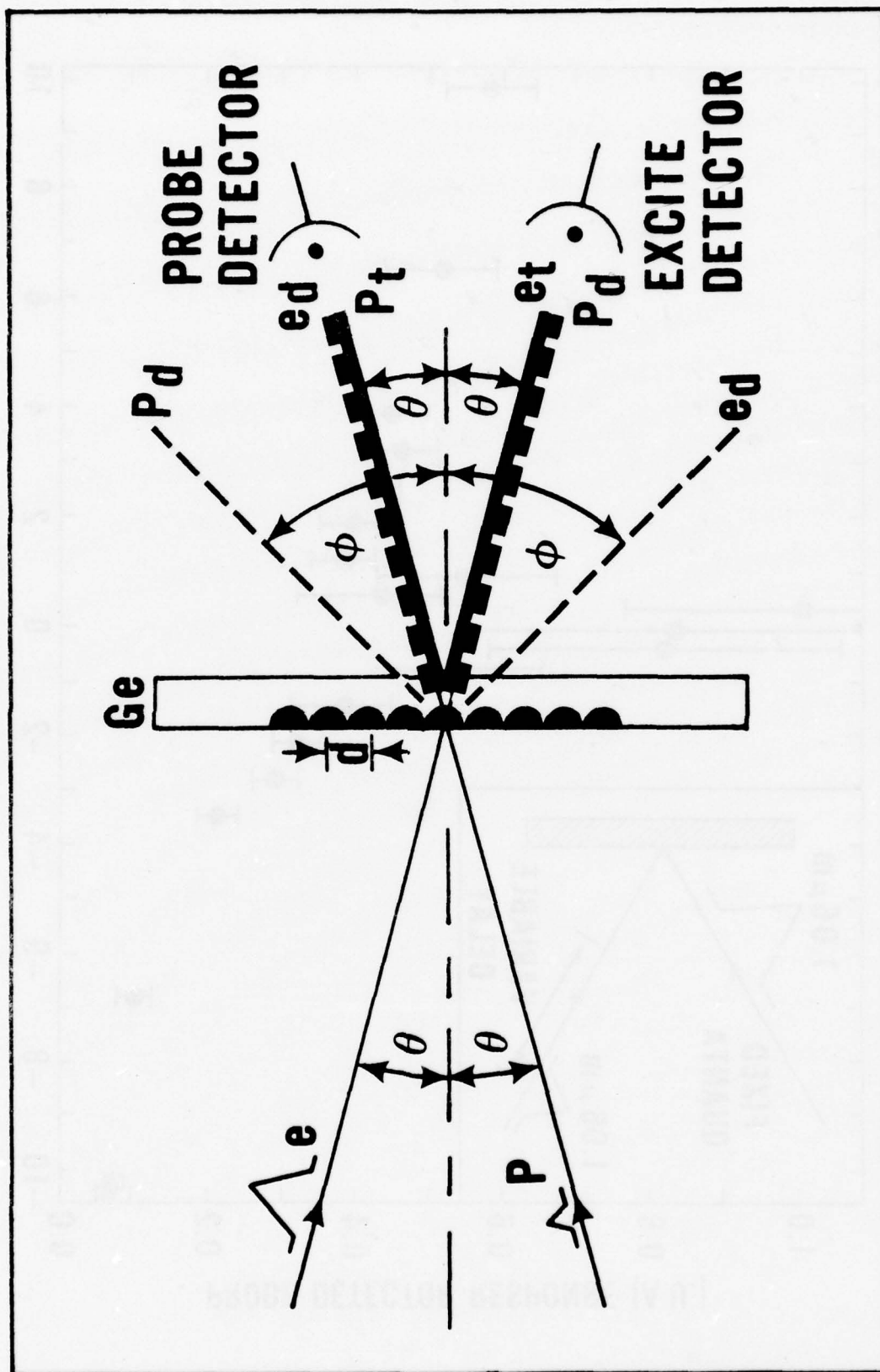




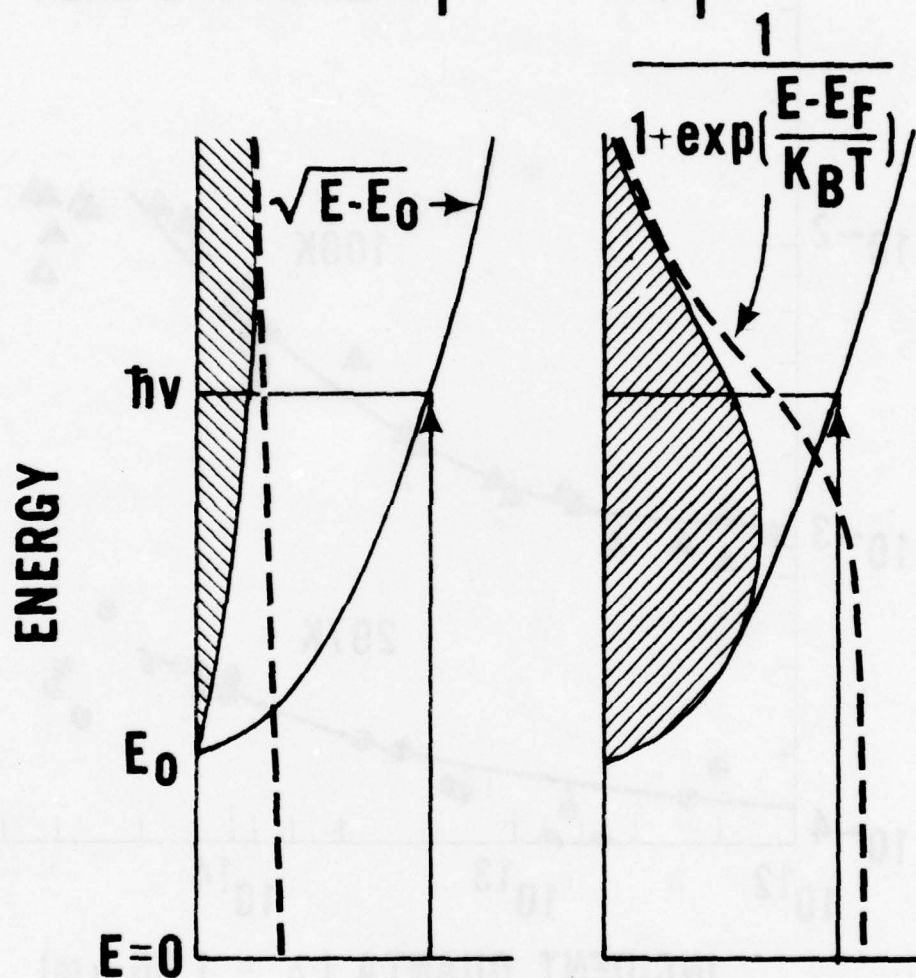


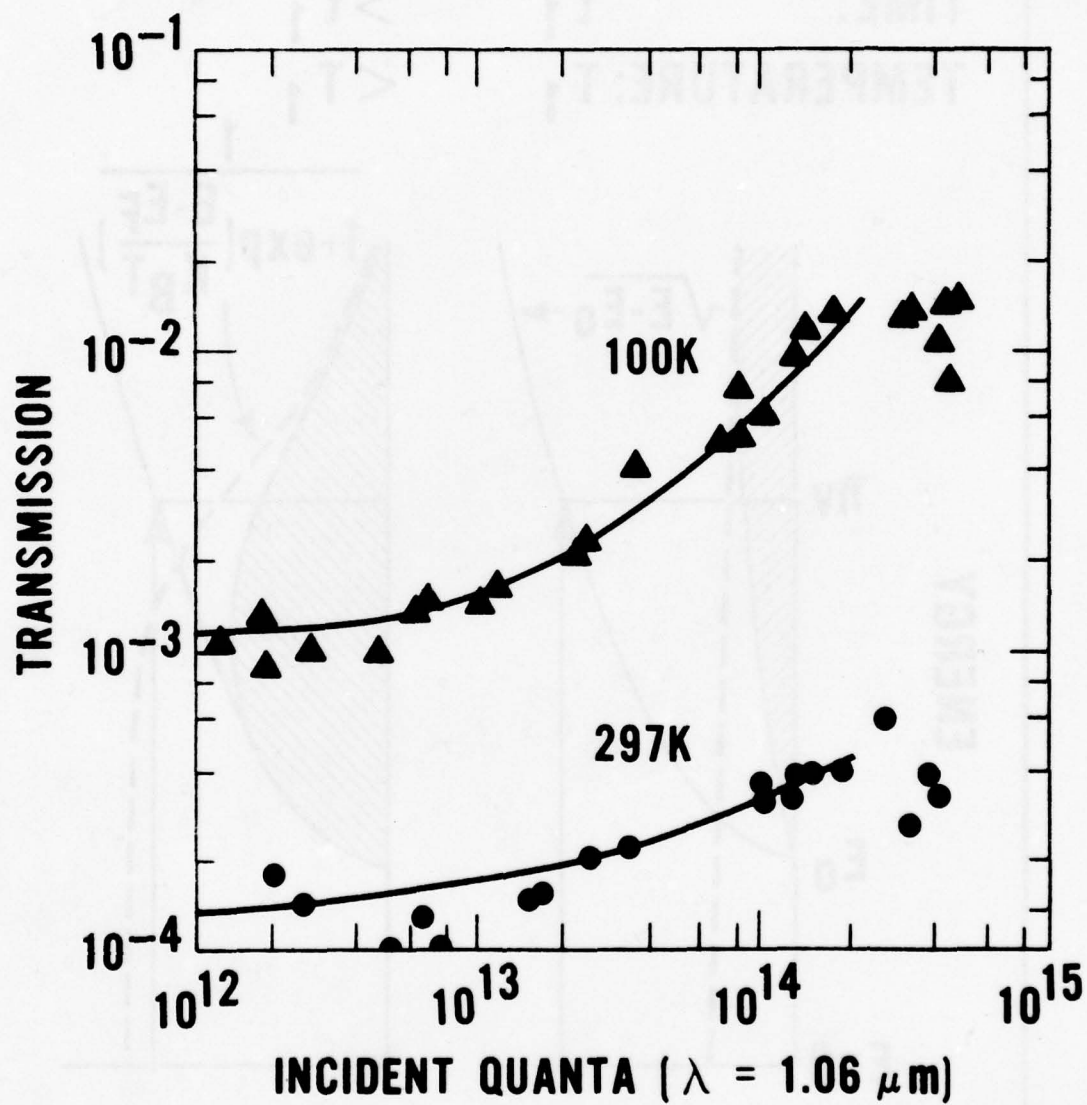


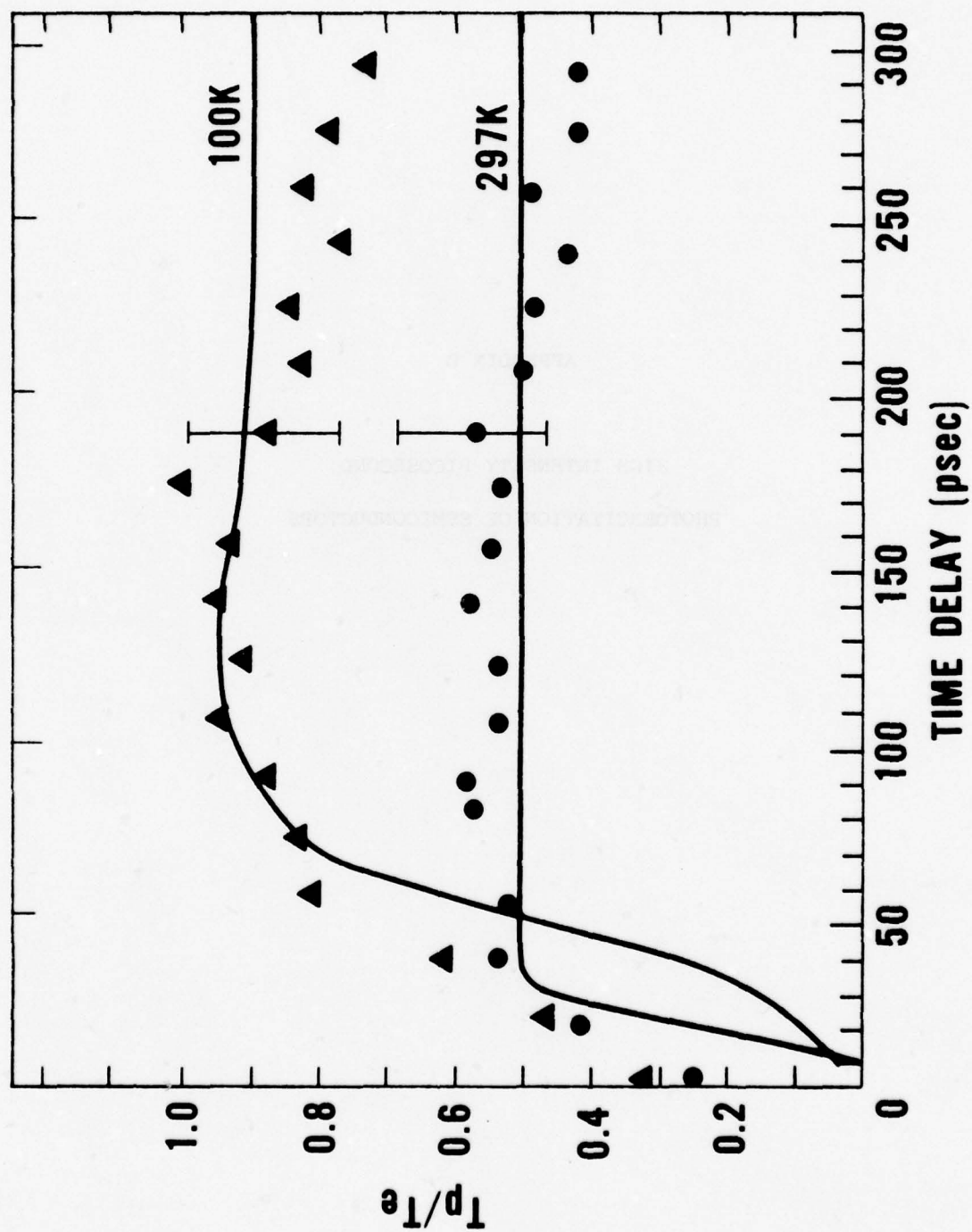




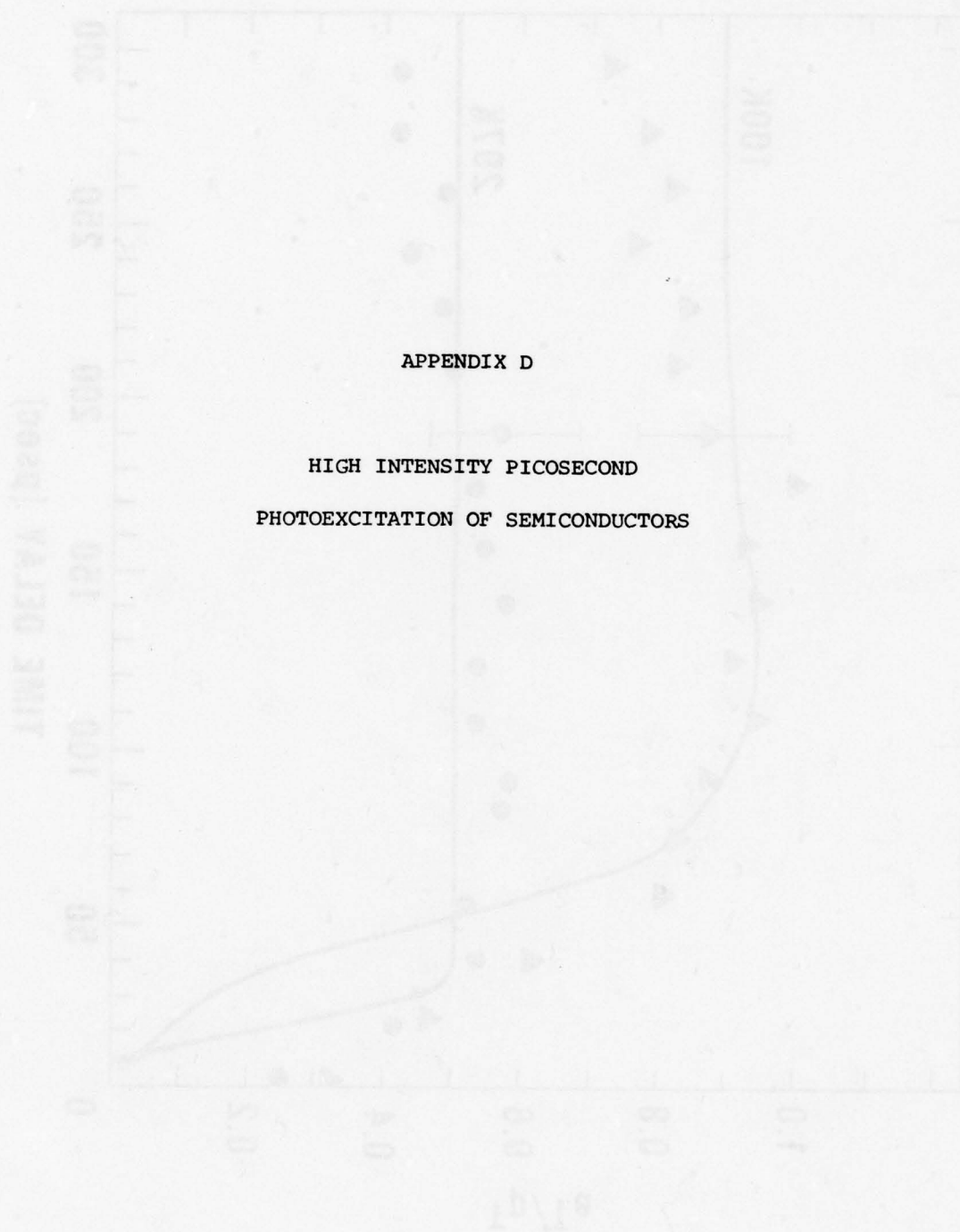
TIME: t_1 $> t_1$
 TEMPERATURE: T_1 $< T_1$







APPENDIX D

HIGH INTENSITY PICOSECOND
PHOTOEXCITATION OF SEMICONDUCTORS

ABSTRACT

Recently, studies of the optical properties of high-density electron-hole plasmas generated in germanium by intense, ultrashort pulses from mode-locked lasers have provided direct information concerning ultrafast electronic processes. As a rule, the experimental investigators have used a variation of the excite and probe technique. Here, the sample is first irradiated with an intense optical pulse (excite pulse) that causes a change in the transmission or reflection properties of the semiconductors. This initial pulse is followed, at various time delays, by a weak probe pulse that measures the change in the transmission or reflectivity of the semiconductor as it returns to its equilibrium condition. We shall review picosecond time-resolved measurements of the optically induced changes in the transmission and reflection spectrum of Ge. These experiments have directly monitored diffusion, Auger recombination, and intervalence band absorption on a picosecond time scale.

I. INTRODUCTION

In the past half decade, studies of the optical properties of high-density electron-hole plasmas generated in undoped semiconductors by the direct absorption of intense, ultrashort pulses from mode-locked lasers have provided direct information concerning ultrafast electronic processes.¹⁻²² Generally, early experimental studies in this area employed mode-locked pulses from a Nd-glass laser as an excitation source to generate the electron-hole plasma. This source produces optical pulses that are approximately 10 psec in duration and that often have peak powers in excess of 10^8 watts at a wavelength of 1.06 μm . These pulses when focused on the surface of a thin semiconductor sample can produce a measured irradiance of 10^{-2} J/cm^2 . Direct absorption of such an optical pulse can create carrier densities of approximately 10^{20} cm^{-3} . Germanium was chosen as a candidate for study in many of these early investigations primarily because it is a readily-available well-characterized semiconductor whose bandgap energy is comparable to but less than the energy of a photon at a wavelength of 1.06 μm (1.17 eV).

As a rule, in such studies, investigators have used a variation of the excite and probe technique. Here, the semiconductor sample is first irradiated with an intense optical pulse (excite pulse) that causes a change in the transmission or reflection properties of the germanium. This initial pulse is followed, at some later time, by a weak pulse (probe pulse) that monitors the change in transmission or reflectivity of the germanium as it returns to its equilibrium condition. (A more detailed description of this measurement technique is contained in lecture L14 of this ASI). There are any number of variations on this technique; some of these will be discussed in this seminar.

This excite and probe technique is embarrassingly simple in concept. In practice, quite the opposite is often true. Some of the experimental difficulties can be attributed to the statistical, nonlinear evolution of the optical pulse within the Nd-glass laser cavity. Typically, this laser produces a mode-locked train of 10 - 50 optical pulses in a single firing; however, the pulses vary in energy and in duration from the first pulse to the last. Moreover, the pulse train envelope usually varies from one laser firing to the next. This irreproducible and random nature of the pulse evolution within the laser cavity precludes the continued selection of identical excite pulses. In addition to the uncertainty in pulse energy and width from data point to data point, the transverse mode structure of the laser is also of questionable spatial quality. Deviations of the transverse mode structure from the TEM_{00} mode lead to "hot" spots on the surface of the semiconductor sample when the pulse is focused. Variations in the positions of these "hot" spots, caused by irreproducible day to day alignment or change in laser mode structure, will result in variations in the degree and quality of overlap between the excite and probe beams. Keep in mind, as well, that one is trying to maintain spatial overlap of the excite and probe pulses on the sample surface (each focused to a diameter of a millimeter or less) and that one is often irradiating the sample surface with optical intensities close to the damage threshold. Another frustration is the low repetition rate of Nd-glass laser systems: typically less than 10 firings per minute. Furthermore, if a probe wavelength different from $1.06 \mu m$ is desired, then it must be generated by some nonlinear process such as frequency doubling, tripling, or stimulated Raman scattering. Thus, data acquisition can be a tedious and exasperating procedure.

Because of the huge carrier densities generated and the complex nature of the germanium band structure, interpretation of these experiments has been

difficult as well. By its very nature (as we have seen in L14), the problem is a complex many-body problem, involving the simultaneous interaction of many processes. As a result of these experimental and theoretical problems (and others not discussed), progress in this field has been painstaking and tedious. None-the-less, progress has been, and is being, slowly and steadily achieved.

In lecture L14 of this ASI, we have provided the reader with an introduction to the physics of ultrafast relaxation processes in semiconductors. There, we discussed one of the early excite and probe experiments in germanium, we enumerated and discussed the important physical processes that could occur during such studies on picosecond time scales and at high carrier densities, and we presented an early interpretation of this experiment. We assume that the reader is familiar with that material.

In this seminar, we provide a semi-chronological account of our progress in understanding the temporal evolution of photogenerated electron-hole plasmas in germanium on a picosecond time scale. We believe such a review will be useful in providing insight into why certain investigations were undertaken and in providing a prospective of our progress in this area. It also allows us, in light of more recent studies, to make a few arbitrary comments concerning some of the earlier work. Throughout, we shall again (as in our previous lecture) emphasize the recent excite and probe studies in germanium. The remainder of this seminar is organized as follows. In Sec. II, we review experiments in which picosecond optical pulses are used to measure the saturation and the decay of the optical absorption of germanium at $1.06\text{ }\mu\text{m}$. We then, in Sec. III, describe investigations that attempt to isolate and measure the effects of diffusion, Auger recombination, free carrier absorption, intervalence band absorption, and Coulomb-assisted indirect absorption. In the next section

(Sec. IV), we discuss the possible contributions of hot phonon distributions to the picosecond optical response of germanium, and, in Sec. V, we outline a recent modification of the original ESSM model (discussed in L14) that includes Auger recombination and intervalence band absorption, as well as accounting for spatially inhomogeneous effects such as diffusion. Finally, in Sec. VI, we make some concluding remarks concerning the present status of our understanding of picosecond optical interactions in germanium and concerning remaining problems.

II. DYNAMIC SATURATION OF THE OPTICAL ABSORPTION

The direct absorption of a quantum of light of energy greater than the direct bandgap energy in germanium induces an electron to make a transition from the valence band to a state high in the conduction band, leaving behind a hole in the valence band. If a large enough number of such electron-hole pairs can be created on a short enough time scale, we can partially fill the states that are resonant with the optical transition, and the transmission of the germanium should be enhanced. As we discussed earlier in lecture L14, the narrow set of optically-coupled states that are resonant with the approximately monochromatic light from a mode-locked laser can be partially filled or saturated in two ways. If the optical generation rate into the optically-coupled states exceeds the scattering rate out, the states will be partially filled and the transmission of the germanium will increase. This process is known as state-filling. A condition of increased transparency will also be observed if the optical pulse generates enough electron-hole pairs to fill all of the states in either the valence or conduction band up to and including those required for the direct optical transition - a process called band filling. In this section, we review the techniques and results of experiments that measure the degree and duration of this bleaching of the optical transmission of germanium on a picosecond time scale.

The first observations of a saturation of the germanium transmission were reported by Kennedy et al.¹ They observed a decrease in the absorption of 1.06 μm picosecond pulses in thin germanium wafers at high optical intensities. They performed two experiments. In the first, they irradiated an 8 μm -thick single crystal germanium sample with picosecond pulses of varying intensity at 1.06 μm , and they measured the transmission of each pulse. A plot of germanium transmission

versus incident optical pulse energy (Fig. 1) showed that the germanium transmission was bleached or enhanced by a factor of approximately 20 over its linear value at low intensities. Second, these authors employed the excite and probe technique in an attempt to measure the decay of this enhanced transmission in the following manner. They irradiated the sample with an excite pulse intense enough to bleach the sample transmission by a factor of approximately 20. This excite pulse was then followed, at some later time, by a probe pulse that monitored the decay of the enhanced transmission. The authors observed (Fig. 2) a narrow spike in the probe transmission located near zero delay. The width of the spike was approximately 2 psec. No further structure in probe transmission was seen at this time due to problems related to experimental configuration and laser performance. Further structure would later be reported by Shank and Auston³ and Smirl *et al.*⁵, as we shall discuss. In the absence of further structure, however, the authors erroneously interpreted this narrow spike near zero delay as evidence of an intraband relaxation time for hot electrons of less than 5 psec.

Shank and Auston³ repeated the 1.06 μm excite and 1.06 μm probe measurements of Kennedy *et al.*¹ In addition to the narrow spike in the probe transmission near zero delay, the measurements revealed a slower, broader structure in the probe transmission (Fig. 3). The probe transmission exhibited a slow rise lasting approximately 20 to 30 psec followed by a gradual decrease lasting hundreds of psec. In view of this additional structure, Shank and Auston reinterpreted the narrow spike in probe transmission near zero delay as a parametric scattering of the strong excite beam into the direction of the probe beam by an index grating produced by the interference of the two beams in the germanium sample (for details, see L14). In addition, they attributed the slower rise in probe transmission to band-filling. That is, they attributed it to a filling

of conduction (valence) band states by electrons (holes) to the point where the electron (hole) Fermi energy approached the optically coupled states. As a result, the buildup of this effect should be proportional to the total number of carriers created, i.e. it should follow the integrated optical pulse energy. Notice that this interpretation does not involve hot electron effects. According to this interpretation, the correlation spike and rise in probe transmission contain little physics. They are merely artifacts of the measurement techniques: one being a correlation between the excite pulse and probe pulse, and the other, the integral of the intensity correlation function. These conclusions were based on observations performed only at room temperature.

Later, Smirl *et al.*⁵ independently extended the 1.06 μm excite and probe measurements of Kennedy *et al.*¹ to include probe structure at longer delays. In addition, they determined the dependence of the excite and probe measurements on sample temperature and excite pulse energy levels. Specifically, the nonlinear germanium transmission was measured as a function of incident optical pulse energy at sample temperatures of 105 K and 297 K (Fig. 4). In addition, the normalized transmission of the probe pulse as a function of time delay after an excite pulse was measured for the same two temperatures (Fig. 5) and for three different excite pulse energy levels (not shown). The temperature dependence of the probe transmission measurements contained surprising new information: the rise in probe transmission at 100 K was too slow (~ 100 psec) to be attributed to an integration effect (i.e. it did not appear to follow the integral optical energy of the excite pulse). The authors suggested that this slow rise in probe transmission might be attributed to a cooling of the energetic electrons (holes) created in the conduction (valence) band by the direct absorption of the excite pulse. Thus, the rise in probe transmission was taken to be an indication of the carrier energy relaxation time.

At this point, Elci et al.⁷ presented the first detailed theoretical treatment of these problems. Their model (hereafter referred to as the ESSM model) attempts to account for the nonlinear transmission and the excite and probe response of germanium in terms of: (1) direct band-to-band absorption, (2) free-carrier absorption, (3) long wavevector phonon-assisted intervalley carrier scattering, (4) phonon-assisted carrier relaxation, (5) carrier-carrier Coulomb collisions, and (6) plasmon-assisted recombination. We have presented a detailed overview of the ESSM model in L14, we will not repeat those discussions here. However, in short, the authors attributed the rise in the probe transmission with the delay after an intense excite pulse to a cooling of the hot electron-hole plasma created by the absorption of the excite pulse. The results of these calculations are presented as solid lines in Fig. 4 and Fig. 5; as we have stated, the theoretical fit to the nonlinear transmission data and the probe transmission data can be regarded as satisfactory, given the complexity of the problem. Subsequently, van Driel et al.⁸ conducted further nonlinear transmission studies, in which the energy band gap of the germanium sample was tuned by hydrostatic pressure, that seemed to corroborate the proposed model.

One of the interesting features of the ESSM model was that it predicted that the nonlinear transmission of the thin germanium sample should depend on the width of the optical pulses. In fact, Elci et al.⁷ had suggested that, as a test for their model, the transmission of the germanium be measured as a function of incident optical pulse energy for pulses of various widths. Initial measurements by Bessey et al.⁹ were found to differ substantially from the predictions of the ESSM model. This was the first disagreement between experiment and a heretofore successful model.

As a result of the disagreement between theory and experiment reported by Bessey et al.⁹, Latham et al.¹⁰ initiated numerical studies to determine whether

the differences between model and experiment could be attributed to assumptions made in the calculations, experimental uncertainties in the physical constants used in the calculations, or the limited number of physical processes included in the model. The results of these studies indicated that, due to uncertainties in the optical phonon-electron coupling constant in germanium, the optical pulsewidth experiments did not provide a definitive test of the ESSM model. This investigation of the uncertainties in the known values of the physical coupling constants produced an important and a disquieting result: accepted values of the optical phonon-electron coupling constant ranged from $6.4 \times 10^{-4} \text{ erg-cm}^{-1}$ to $18.5 \times 10^{-4} \text{ erg-cm}^{-1}$. An average of the eight values listed by Latham *et al.*¹⁰ is $1 \times 10^{-3} \text{ erg-cm}^{-1}$. Elci *et al.*⁷ had originally used constants of $6 \times 10^{-4} \text{ erg-cm}^{-1}$ at a lattice temperature of 297 K and $2 \times 10^{-4} \text{ erg-cm}^{-1}$ at 100 K. These values result in carrier cooling rates that are 3 and 25 times slower than that obtained by using the average value. In fact, if the average value for the optical phonon-electron coupling constant is substituted into the ESSM model, the energy relaxation rate for the hot carriers is too rapid to account for the rise in probe transmission. The theoretical probe transmission is plotted as a function of time delay for several values of optical phonon-electron coupling constant in Fig. 6. Consequently, the rise in probe transmission with delay time after excitation can, or can not, be accounted for by carrier cooling, depending on the value chosen for the coupling constant. As we shall discuss later, the cooling rate for the photogenerated hot carriers can be further complicated by hot phonon effects.

In view of the experimental uncertainties in key physical constants used in the original ESSM calculations (as discussed above), the magnitude of the energy relaxation rate and the origin of the rise of the probe transmission are

in doubt. These, however, were not the only indications that the model was incomplete. Other problems were related to certain major assumptions made in performing the calculations and to the limited number of physical processes included. We shall review these complications in the following section.

III. HIGH PHOTOGENERATED CARRIER DENSITIES

Studies to be discussed in this section indicate that processes other than those included in the original ESSM model can be important. Most of these effects, such as intervalence-band absorption, Auger recombination, and Coulomb-assisted indirect absorption, are only significant at large carrier densities. Other processes, such as diffusion, are enhanced at high carrier densities. The possible importance of including these processes in any theoretical model is discussed in this section. Previously, most information concerning these high-density phenomena has been obtained from measurements on highly-doped samples, in the presence of large donor and/or acceptor concentrations. One advantage of intense, picosecond excitation is the opportunity to study these processes in the absence of impurity effects.

Diffusion

One of the more drastic assumptions of the ESSM model was that the parameters that characterize the electron and hole distributions (i.e. Fermi energies, temperatures, and carrier densities) were taken to depend only on time, rather than on both space and time. The linear absorption coefficient α_0 for germanium at $1.06 \mu\text{m}$ is approximately $1.4 \times 10^4 \text{ cm}^{-1}$. Consequently, most of the excite pulse will be absorbed within a micron ($\sim 1/\alpha_0$) of the sample surface, creating a dense photogenerated electron-hole plasma localized to this region. Thus, neglect of the spatial variation of these parameters is not a reasonable assumption for typical sample thickness ($\sim 5 \mu\text{m}$) used in recent excite and probe experiments. Elci *et al.*⁷ recognized this problem, but, in order to simplify their initial calculations, they chose to view the parameters describing the electron-hole plasma as spatial averages throughout the sample volume.

Recent studies performed by Auston and Shank² indicate that longitudinal diffusion (that is, diffusion along the direction of light propagation) can be important on picosecond time scales. In these experiments, the authors first irradiated a germanium sample near normal incidence with an intense 1.06 μm picosecond pulse that produced a large carrier density near the sample surface. This excite pulse was then followed by a weak, circularly polarized probe pulse of the same wavelength. The change in polarization of the reflected probe light was monitored by ellipsometric techniques as shown in Fig. 7. The transmission of the ellipsometer as a function of time delay between excite and probe pulses is shown in Fig. 8. The transmission of the ellipsometer is proportional to the square of the fractional change in the index of refraction $|\delta n/n|^2$ induced by the absorption of the excite pulse, where δn is the change in index and n the index of refraction. The index change $\delta n/n$, in turn, is proportional to the photogenerated carrier density. As a result, we can see from Fig. 8, that the photogenerated carrier density at the sample surface is reduced to half its initial value in 30 psec following excitation. Auston and Shank attributed this decay of the surface density to a diffusion of the carriers into the sample bulk, and they deduced a diffusivity of $230 \text{ cm}^2 \text{ sec}^{-1}$ at estimated surface carrier densities of approximately 10^{20} cm^{-3} . This value is 3.5 times larger than the low density ambipolar diffusion constant in germanium. Using this value, we would expect the initial optically-created carrier layer to double its thickness in 75 to 100 psec. Recombination effects were considered to be negligible during these measurements.

Auger Recombination

In another novel application of the excite and probe technique, Auston et al.⁴ demonstrated the importance of Auger recombination at these densities

as well. They first illuminated a 300 μm -thick slab of germanium with a 1.06 μm excite pulse creating a large carrier density. The decay of this carrier density was then probed by a second pulse at 1.55 μm , generated by stimulated Raman scattering in benzene, as shown in Fig. 9. A quantum of the excite pulse (1.17 eV) is energetic enough to excite direct band-to-band transitions. The energy of a probe quantum (0.8 eV), on the other hand, is less than the direct band-gap energy but larger than the indirect gap at L. Thus, the probe pulse can be absorbed as a result of both indirect, and free-carrier transitions. At the carrier densities encountered in their experiments, these authors judged the indirect absorption coefficient to be negligible compared to the free-carrier coefficient. A plot of the change in absorbance of the 1.55 μm probe pulse as a function of time delay after the 1.06 μm excite pulse is shown in Fig. 10 for two optically-created carrier densities. Since the change in absorbance of the probe is taken to be a measure of the change in the free carrier absorbance and since the free carrier absorption coefficient is proportional to carrier number, Fig. 10 directly displays the decay of the carrier density. The probe absorbance decays significantly in the first 100 psec following excitation, indicating the importance of carrier recombination on a picosecond time scale. Auston *et al.*⁴ attribute this decay to an Auger process and extracted an Auger rate constant of approximately $10^{-31} \text{ cm}^6 \text{ sec}^{-1}$. The reader should note that the carrier recombination rate exhibits a cubic dependence on the carrier density, that is,

$$\frac{dn}{dt} = -\gamma_A n^3,$$

where n is the carrier density and γ_A is the rate constant. A sensitive estimate of the rate constant requires a precise knowledge of the carrier density.

Indirect, Intervalence-Band, and Free-Carrier

Absorption and Auger Recombination

At this point, perhaps we should pause to summarize the state of our understanding of the origin of the slow rise in probe transmission observed in the early excite and probe studies as discussed in Sec. III and displayed in Fig. 5. Originally, Shank and Auston³, attributed this rise in probe transmission to a saturation of the direct absorption as a result of band filling. We remind the reader, again, that this interpretation was based on measurements performed only at room temperature. Subsequently, Elci *et al.*⁷ attributed this rise in probe transmission to a cooling of a hot electron-hole plasma created by direct absorption of the excite pulse. Although the original calculations by Elci *et al.*⁷ are sound, time has shown that the proposed model (ESSM model) has several objectionable features as detailed in the last two sections: (1) uncertainties in the optical phonon-electron coupling constant, (2) neglect of the spatially inhomogeneous nature of the parameters that characterize the carrier distributions, and (3) the omission of important processes such as diffusion and Auger recombination from the model. The authors realized and stated at the outset that their model contained serious assumptions and approximations that warranted further study and that the model contained only a few of the many possible processes. It was hoped, however, that the model would serve as a basis for further study and development.

In sharp contrast to the interpretation by Elci *et al.*⁷, Auston *et al.*¹² stated that they expected the energy relaxation time in germanium to be too short to account for the rise in probe transmission shown in Fig. 5. This suggestion is, of course, consistent with the more detailed numerical studies presented by Latham *et al.*¹⁰, as discussed in Sec. II and shown in Fig. 6.

More importantly, in the spirit of suggesting plausible alternative models for evaluation, Auston et al.¹² stated that enhanced intervalence-band and Coulomb-assisted indirect absorption effects might be important at the high photogenerated carrier densities encountered in these excite and probe experiments. Furthermore, they suggested that these processes might introduce a minimum in the absorption versus carrier density curve in germanium in the following way: The direct absorption coefficient will remain approximately constant as a function of photogenerated carrier density until the density reaches the point where the electrons (holes) clog the states needed for direct electronic transitions in the conduction (valence) band. At this point, the direct absorption coefficient rapidly decreases. On the other hand, Coulomb-assisted indirect, intervalence-band, and free-carrier absorption coefficients monotonically increase with carrier density. Thus, the absorption coefficient could initially decrease with increasing density, as the direct absorption coefficient saturates, then increase with increasing density as the free-carrier, intervalence-band and indirect absorption coefficients become large enough to dominate. In a private communication, S. McAfee and D. H. Auston further explained how an absorption curve containing a minimum could be combined with Auger recombination to account for the rise in probe transmission of Fig. 5. Briefly, the absorption of the excite pulse creates an initial carrier density greater than n_{\min} , where n_{\min} denotes the density at which the minimum total absorption coefficient occurs. As the initial photogenerated carrier density is decreased in time by Auger recombination, the absorption coefficient of the germanium will decrease in time until the carrier density reaches n_{\min} , then increase. Thus, the probe transmission will increase then decrease, if the initial optically-created carrier density is greater than n_{\min} . In direct contrast to the ESSM model, this interpretation

does not require hot electron effects. This model does, however, require a minimum in the absorption versus carrier density curve.

Consequently, we summarize and emphasize that there were at this point in time at least three possible explanations for the rise in probe transmission with delay (see Fig. 5): (1) the rise is caused by band-filling and is, as a result, an integration effect that follows the integrated optical energy of our excite pulse, (2) the rise is due to a cooling of a hot carrier distribution created by direct absorption of the excite pulse, or (3) the rise can be attributed to Auger recombination combined with an absorption versus carrier density relationship containing a minimum.

In a recent work, Smirl *et al.*¹⁴ have attempted to test the first and third possibilities listed above and have attempted to ascertain the importance of free-carrier, intervalence-band, and indirect absorption effects in excite and probe experiments at 1.06 μm . The experimental configuration used in these studies is similar to that used by Auston *et al.*⁴ and is shown in Fig. 11. The excite pulses used here were approximately 10 psec in duration and had peak powers of approximately 10^8 W at a wavelength of 1.06 μm , and they produced a measured irradiance of approximately 10^{-2} J/cm² when focused on the crystal surface. The plasma produced by the absorption of the excite pulse was probed using weak pulses of two types: one at 1.06 μm had a photon energy greater than the direct band-gap energy for germanium, and the other at 1.55 μm had an energy less than the direct gap but greater than the indirect gap. The latter probe, at a wavelength of 1.55 μm , was generated by stimulated Raman scattering in benzene. We emphasize that the energy of a quantum at 1.06 μm (1.17 eV) is sufficient to excite direct band-to-band transitions in germanium as well as free-carrier, intervalence band, and indirect transitions; whereas, the energy of a quantum at 1.55 μm (0.08 eV) falls below the direct gap and is only a measure of the combined free-carrier, intervalence-band and indirect processes.

Smirl et al.¹⁴ performed three separate measurements. In the first of these, they carefully repeated the measurements by Smirl et al.⁵ (Fig. 5) of the transmission of a 1.06 μm probe pulse as a function of time delay after an intense 1.06 μm excite pulse for sample temperatures of 100 K and 295 K. The original measurements of Smirl et al.⁵ were repeated so that the authors could more carefully investigate the possibility that the rise in probe transmission follows the integrated excite pulse autocorrelation function. The rises in probe transmissions for the two sample temperatures are carefully compared to a calculated integration curve in Fig. 12, assuming an optical pulsewidth of 10 psec. The authors concluded from this comparison that the experimental rise in probe transmission at 295 K was indistinguishable from an integration effect, in agreement with the original interpretation of room temperature data by Shank and Auston.³ However, the rise at 100 K is much slower than the integration curve or the rise at 295 K and cannot be attributed to such artifacts; it represents a physical effect. For the remainder of this seminar, the rise in probe transmission at 100 K will be the object of our discussion.

Next, the authors measured the transmission of a thin germanium sample at 1.55 and 1.06 μm as a function of optically-created carrier densities as shown in Fig. 13. The data were obtained in the following manner. The crystal was illuminated by variable energy pulses with a wavelength of 1.06 μm . Each pulse at 1.06 μm was followed immediately at a fixed delay by pulses that monitored the absorbance of the crystal at wavelengths of 1.55 μm and 1.06 μm . The optical absorbance at 1.17 eV is seen to decrease by approximately 3.5 as the carrier number increases. By contrast the absorbance at 0.8 eV increases roughly by 2.3. Over the range of densities encountered in these experiments, the absorption versus density relationship at 1.17 eV does not exhibit a minimum.

Thus, a temporal decay of the carrier density alone cannot be combined with this absorption versus density relationship to account for the rise in probe transmission at $1.06\ \mu\text{m}$ exactly as we discussed earlier. In addition, these measurements indicate that the combined free-carrier, intervalence-band, and indirect absorbance changes are opposite in sign and smaller in magnitude than changes caused by saturation of the direct absorption. As a result, the authors concluded that the decrease in absorbance at $1.06\ \mu\text{m}$ with increasing carrier number is dominated by a saturation of the direct absorption coefficient; however, the rate of this decrease in absorbance is slowed by the contributions of these "other" processes that are opposite in sign. Note that, when comparing the data discussed here (Fig. 13) with the earlier data by Smirl et al.⁵ (Fig. 4), one must realize that the sample thickness and focused optical spot sizes are not identical.

Finally, Smirl et al.¹⁴ measured the temporal evolution of the absorbance of a $1.55\ \mu\text{m}$ probe pulse as a function of time delay after an intense excite pulse at $1.06\ \mu\text{m}$. In this experiment, the sample was irradiated by an optical pulse at $1.06\ \mu\text{m}$ containing roughly 2×10^{15} quanta (corresponding to surface energy density of $\sim 10^{-2}\ \text{J}/\text{cm}^2$) and was probed by a weak pulse having a wavelength of $1.55\ \mu\text{m}$ (See Fig. 14). The results of these probe measurements are similar to those obtained by Auston et al.⁴ However, Auston et al.⁴ stated that they performed their measurements at excite intensities such that the absorption of the excite pulse was linear. These experiments were clearly performed in the nonlinear region. In addition, the measurements of Auston et al.⁴ were performed on a $300\ \mu\text{m}$ -thick sample, our sample was $6\ \mu\text{m}$ thick. The measurements presented in Fig. 14 indicate that free-carrier, intervalence-band, and indirect absorption can be significant at the carrier densities encountered during excite and probe experiments described here. Recall that Auston et al.⁴

attributed the decrease in probe pulse absorbance at $1.55\text{ }\mu\text{m}$ shown in Fig. 10 to a decrease in free-carrier absorption caused by a temporal decay in carrier density due to Auger recombination. The experiments that we have just described only allow the measurement of the change in the combined free-carrier, intervalence-band and indirect absorbance, and they do not provide for a convenient separation of the individual contributions.

Summarizing the results of the measurements described in the previous three paragraphs, we conclude that the rise in probe transmission during the $1.06\text{ }\mu\text{m}$ excite and $1.06\text{ }\mu\text{m}$ probe experiments at 100 K is not an integration effect (i.e. not a simple band filling) and that it cannot be attributed to free-carrier, intervalence-band, and Coulomb-assisted transitions combined with Auger recombination. The contributions of these latter processes are significant, however, and they must be accounted for by any successful model. Unfortunately, the measurements described here yielded no direct information concerning carrier distribution temperatures or energy relaxation rates, and the question of attributing the rise in $1.06\text{ }\mu\text{m}$ probe transmission to a cooling of a hot carrier plasma created by the excite pulse remains unresolved.

Having rejected two of the three possible explanations for the probe transmission listed earlier and with the other explanation all but rejected, to what do we attribute this rise in probe transmission? Recent suggestions are reviewed in the next two sections.

IV. HOT PHONONS

As we recall from our discussion of the work of Latham *et al.*¹⁰, the physical constants for germanium are not well enough known to allow a precise calculation of the energy relaxation rate. For theoretical fits to experiment by Elci *et al.*⁷ (Fig. 5), the optical phonon-electron coupling constants were chosen as $6 \times 10^{-4} \text{ erg-cm}^{-1}$ for a lattice temperature of 297 K and $2 \times 10^{-4} \text{ erg-cm}^{-1}$ at 100 K. These values are within the accepted theoretically and experimentally determined values listed by Latham *et al.*¹⁰; however, they are much lower than the mean value of $1 \times 10^{-3} \text{ erg-cm}^{-1}$ as obtained from an average of the eight values listed. In fact, as we have seen (Fig. 6), a repetition of the original calculations substituting the average phonon-electron coupling constant shows that carrier cooling is too rapid to account for the rise in probe transmission, in complete agreement with the statements of Auston *et al.*¹²

However, van Driel¹⁶ has recently calculated the influence of hot phonons on the carrier energy-relaxation rate in these problems. In his calculations, van Driel adopted the ESSM model and extended it to include optical phonon heating effects. Briefly, the modified picture for the probe transmission is as follows. Just as in the ESSM model, the carriers generated by the absorption of the excite pulse cool by emitting optical phonons with a characteristic relaxation time τ_e , where τ_e is determined by using the average phonon-electron coupling constant. Since these phonon-assisted electronic transitions are intraband, they occur between states separated by small wavevectors. Consequently, the optical phonons emitted during these transitions also have a short wavevector and are located near the center of

the Brillouin zone. Van Driel¹⁶ estimated that approximately 10^{-2} of the volume of the Brillouin zone is involved in hot carrier relaxation. As 10^{19} carriers/cm³ relax within the conduction bands (each one emitting approximately 15 optical phonons), an enormous number of these short wavevector optical phonons is created. These short wavevector optical phonons are believed to decay into two long wavevector acoustic phonons in a characteristic time τ_p . This decay brings the optical phonons into equilibrium with the lattice. This simplified picture is illustrated in Fig. 15. The optically-created carriers give their excess energy to the optical phonon reservoir with a characteristic time τ_e ; the optical phonon reservoir, in turn, gives its excess energy to the lattice with a time constant τ_p . As we discussed in L14, the optical phonon lifetime for germanium at 77 K is 10 psec. This lifetime is relatively long compared to τ_e when a single average temperature-independent optical phonon-electron coupling constant is employed. This results in a relaxation bottleneck for the hot carriers due to the buildup of the optical phonon population on a picosecond time scale.

The results of these calculations, taking into account optical phonon heating and using the average phonon-electron coupling constant, are shown as solid curves in Fig. 16. Note that the inclusion of hot phonons accounts for one of the major discrepancies between the original theory and experiment. Namely, in contrast to the original theory that predicted a delayed, steep rise (dotted curve, Fig. 16), the present theory shows a steep rise with gradual leveling off in agreement with the data. The solid curves in Fig. 16 were taken from van Driel.¹⁶ The agreement between the modified theory and experiment is remarkable; however, this should be regarded as somewhat fortuitous in view of the simplifications of the model, the limited number of processes included, and the uncertainty in some of the physical constants.

V. THE RELAXATION-DIFFUSION-RECOMBINATION MODEL

In previous sections, we have reviewed evidence that some of the assumptions included in the early ESSM model are not well justified. For example, the experiments by Auston and Shank² (Fig. 8) clearly indicate that the carrier density is inhomogeneously distributed throughout the interaction volume of the germanium sample and that diffusion is important on picosecond time scales. By contrast, the ESSM model had assumed that all parameters characterizing the electron and hole distributions were functions of time only, independent of spatial coordinates, and all diffusion effects were neglected. In addition, studies by Auston *et al.*⁴ and Smirl *et al.*¹⁴ have demonstrated that processes originally omitted from the ESSM model such as Auger recombination and intervalence band absorption are important. And, finally, studies by Latham *et al.*¹⁰ have shown that the values chosen by Elci *et al.*⁷ for the optical phonon-electron coupling constant were extreme.

Recently, Leung¹⁷ has modified and extended the original ESSM model to remove most of these objections. In this model, he (1) allowed all parameters characterizing the electron and hole distributions to depend on both spatial coordinates and time, (2) used an optical phonon-electron coupling constant approximately equal to the mean value determined by averaging the values listed by Latham *et al.*¹⁰, and (3) included the effects of intervalence band absorption and Auger recombination. Hot phonon effects were, however, neglected. As we shall now discuss, this model leads to a radically different interpretation for the rise in probe transmission from that proposed by Elci *et al.*⁷ This model is briefly reviewed in the following paragraphs.

Just as in the ESSM model, the direct absorption of the excite pulse creates a large density of electrons (holes) in the central valley of the

conduction (valence) band. The electrons are rapidly scattered to the conduction band side valleys by long wavevector phonons. Carrier-carrier scattering events, which occur at a rate comparable to the direct absorption rate, ensure that the carrier distributions are Fermi-like. Since the excite pulse photon energy (1.17 eV) is greater than either the direct-gap energy (0.8 eV) or the indirect gap energy (0.7 eV), such a direct absorption event followed by the scattering of an electron to the side valleys results in the electron giving an excess energy of approximately 0.5 eV to thermal agitation. As a result, absorption of the excite pulse results in the generation of a huge carrier distribution with an initial distribution temperature greater than the lattice temperature. Other processes such as free-carrier absorption and nonradiative recombination can raise the carrier temperature during passage of the excite pulse, while phonon-assisted carrier relaxation processes can reduce the carrier temperature. So far, the description of the carrier evolution during the period the excite pulse is present in the sample is identical to that given in L14 for the ESSM model. The present model differs in two respects. First, the inclusion of intervalence band absorption results in additional carrier heating effects as electrons are induced to make transitions from the split-off valence band to the light-hole and heavy-hole bands. Second, the carrier density, temperature, and Fermi energies are strongly dependent on longitudinal position within the semiconductor sample. For example, a typical plot of the carrier density as a function of longitudinal position immediately following excitation is shown as a solid line in Fig. 17.

Immediately following the passage of the excite pulse, the interaction region of the sample contains a large number of carriers with a high distribution temperature. The final number and temperature are complicated functions

of position as determined by the relative strengths of direct absorption, nonradiative recombination, intervalence band absorption and phonon-assisted relaxation rates. Experimentally, the probe pulse interrogates the evolution of the distribution after the passage of the excite pulse, and its transmission is a sensitive measure of whether the optically-coupled states are available for absorption or are occupied. The probe pulse transmission versus time delay (Fig. 5) can be understood in the following way. Initially, after the passage of the excite pulse, the probe transmission is small since the electrons (holes) are located high (low) in the conduction (valence) bands because of the high distribution temperature, leaving the states that are optically coupled available for direct absorption. As the carrier distribution temperature cools and carriers fill the states needed for absorption, the transmission increases. In contrast to the ESSM model, however, here the phonon-assisted relaxation is extremely rapid. For an optical phonon-electron coupling constant of $10^{-3} \text{ erg-cm}^{-1}$, the energy relaxation time of the carrier distribution is estimated to be less than 10 psec. Consequently, the electron and hole distributions, while still spatially inhomogeneous, have cooled to lattice temperatures within 5 to 10 psec following excitation. As a result, any initial rise in probe transmission as a result of hot carrier relaxation will be too rapid to account for the protracted rise displayed in Fig. 5. Diffusion is a slow process on a time scale of 10 psec.

For longer delay times (greater than 10 psec), longitudinal carrier diffusion is a dominant process in determining the evolution of the probe pulse transmission. Specifically, for large carrier densities, according to Leung's calculations¹⁷, longitudinal diffusion can cause a rise in the probe transmission. This may seem surprising at first, but it can be understood by considering a simple schematic of the diffusion process, such as the one shown in

Fig. 18. Since the carrier number remains constant, the probe pulse "sees" the same total number of carriers regardless of time delay. As time progresses, however, the carriers diffuse into the sample bulk as illustrated in Fig. 17. At first one might guess that this would reduce the carrier density and, thereby, free the states near the front surface of the sample for direct absorption of the probe. However, recall that the states that are resonant with the probe transmission are localized to narrow regions in the conduction and valence bands. As a result, not all carriers are effective in filling these optically-coupled states and preventing absorption. The total number of carriers effective in preventing absorption can be altered by diffusion as illustrated in Fig. 18. If the carrier density near the front sample surface is large, as the carriers migrate from this region, they can fill the states needed for absorption away from the front surface without depleting the optically-coupled states near the surface. The number of carriers in the sample effective in preventing absorption increases and the probe transmission will rise. Note, however, that if the initial density is small in the front region, diffusion will decrease the carriers effective in preventing absorption in the front region without significantly increasing the effective density in the back; probe transmission will decrease. Thus, depending on the initial carrier density, longitudinal (along the direction of light propagation) diffusion can cause a rise or fall in probe transmission. In this model, then, the slow rise in probe transmission is attributed to a diffusion of the photogenerated carriers from the front sample surface into the sample bulk, in direct contrast to the original interpretation of the ESSM model. Note, however, that the high carrier temperature still plays a key role during the generation of the carrier distribution as a result of the absorption of the excite pulse. In this model the slow fall in probe

transmission for much longer delays is attributed to a reduction in carrier density as a result of Auger recombination.

A comparison of the calculations of Leung to the probe pulse transmission data of Smirl *et al.*⁵ is shown in Fig. 19. Again, as with the hot phonon model of the last section, the agreement between theory and experiment is excellent. And, again, we feel that, given the complexity of the model, the agreement must be considered somewhat fortuitous. Measurements that attempt to determine which, if either, of these two proposed models is correct are in progress.

VI. SUMMARY

In this seminar, we have described experiments that attempt to measure the evolution of electronic processes in germanium with a time resolution approaching 10^{-12} sec. In Sec. II, we surveyed experiments that measured the saturation and relaxation of the germanium transmission at high photo-generated carrier densities. These measurements are important because they have the potential of yielding direct information on the ultrafast relaxation of optically-created hot carriers. However, as we have stressed throughout, investigators have been unable to provide a clear, unique interpretation of these experiments, since so many competing processes are simultaneously active. For example, workers have been unable to unambiguously attribute the rise in probe transmission to a single process.

In Sec. III, we reviewed experiments that provided information on diffusion, nonradiative recombination, and the combined effects of free carrier, intervalence-band, and Coulomb-assisted indirect absorption at high carrier densities. These measurements are interesting in two respects. First, they illustrate that by proper choice of the experimental configuration one can isolate and identify the contributions of single processes, and, second, they provide the opportunity to study these processes on a picosecond time scale and in the absence of impurity effects. The studies reviewed here clearly indicate that picosecond techniques have matured to the point of providing precise quantitative information concerning ultrafast processes in semiconductors.

In Sec. IV and Sec. V, we summarized recent attempts to assemble the information provided by the experimental studies of Sec. II and Sec. III into

a single theoretical model that describes the generation and evolution of the electron-hole plasma during and following excitation with a single picosecond pulse at $1.06\text{ }\mu\text{m}$. To date no single, palatable description of the evolution of the carrier distributions has emerged. Further experimental studies are needed to substantiate or reject the two models reviewed here.

In conclusion, the reader should note that we have made no effort to provide a complete review of picosecond studies in semiconductors. Further information concerning this subject can be found in a recent review article by von der Linde¹⁹ and in the Proceedings of the First International Conference on Picosecond Phenomena.²⁰ In particular, the reader should be aware of the recent work performed by Shank et al.²¹ and von der Linde and Lambrich²² in GaAs. These studies provide picosecond time-resolved measurement of hot-carrier relaxation, band-gap narrowing, and screening effects in GaAs, and they represent, in our opinion, some of the best experimental picosecond semiconductor studies to date. Finally, we comment that the recent development of continuous subpicosecond mode-locked dye laser systems has eliminated many of the data acquisition problems detailed in the introduction of this seminar. However, because these systems are relatively new and because high intensity systems are presently expensive to construct, Nd-glass and Nd-YAG systems are still, at this point, the most readily available to workers in the field.

This work was supported by the Office of Naval Research and the North Texas State University Faculty Research Fund.

REFERENCES

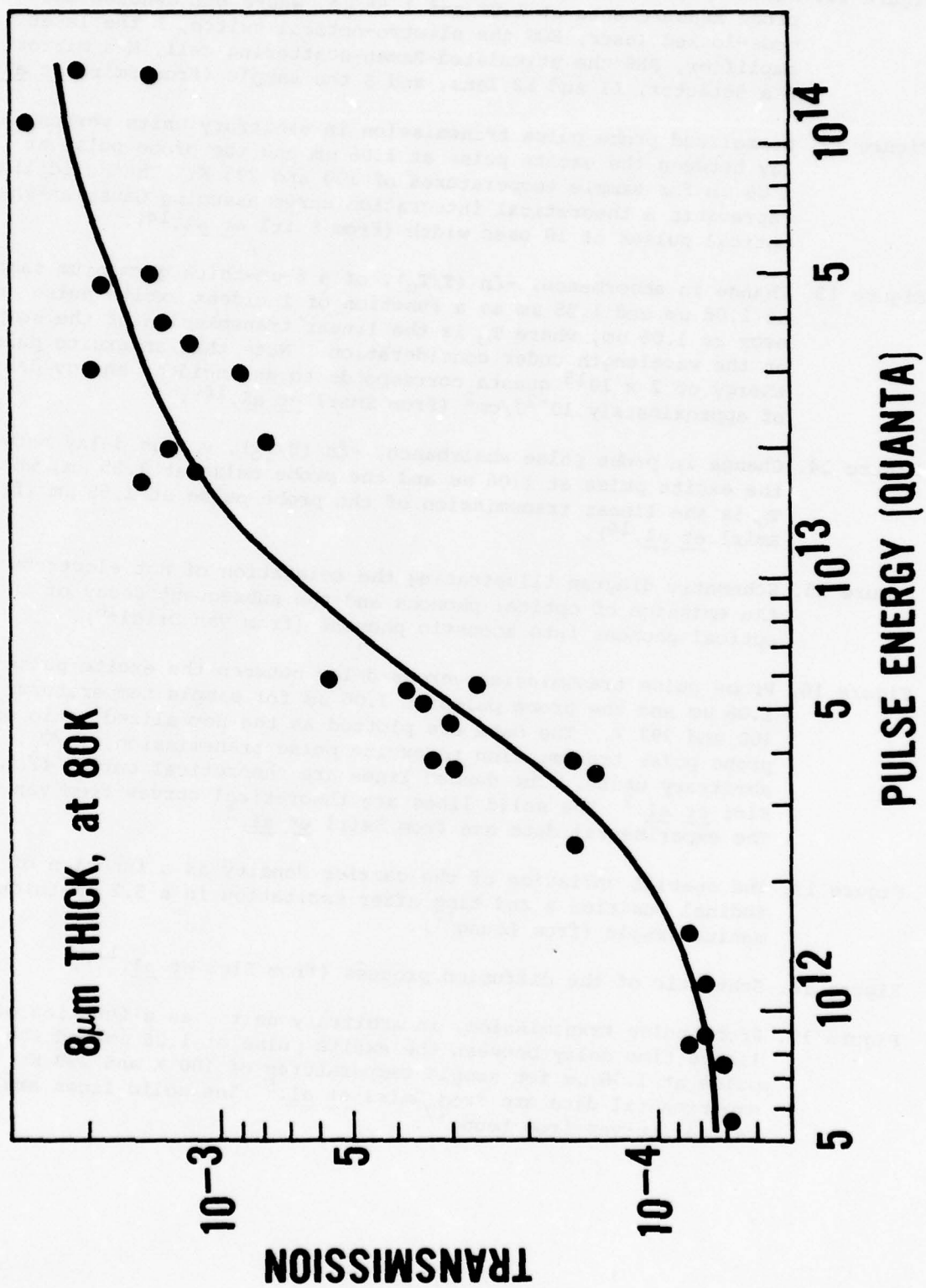
1. C. J. Kennedy, J. C. Matter, A. L. Smirl, H. Weichel, F. A. Hopf, S. V. Pappu, and M. O. Scully, "Nonlinear absorption and ultrashort carrier relaxation times in germanium under irradiation by picosecond pulses," *Phys. Rev. Lett.* 32, 419 (1974).
2. D. H. Auston and C. V. Shank, "Picosecond ellipsometry of transient electron-hole plasmas in germanium," *Phys. Rev. Lett.* 32, 1120 (1974).
3. C. V. Shank and D. H. Auston, "Parametric coupling in an optically excited plasma in Ge," *Phys. Rev. Lett.* 34, 479 (1975).
4. D. H. Auston, C. V. Shank, and P. LeFur, "Picosecond optical measurements of band-to-band Auger recombination of high-density plasmas in germanium," *Phys. Rev. Lett.* 35, 1022 (1975).
5. A. L. Smirl, J. C. Matter, A. Elci, and M. O. Scully, "Ultrafast relaxation of optically excited nonequilibrium electron-hole distributions in germanium," *Opt. Commun.* 16, 118 (1976).
6. J. C. Matter, A. L. Smirl, and M. O. Scully, "Saturable transmission in mercury cadmium telluride," *Appl. Phys. Lett.* 28, 507 (1976).
7. A. Elci, M. O. Scully, A. L. Smirl, and J. C. Matter, "Ultrafast transient response of solid-state plasmas. I. germanium: theory, and experiment," *Phys. Rev. B* 16, 191 (1977).
8. H. M. van Driel, J. S. Bessey, and R. C. Hanson, "Pressure tuning of picosecond pulse transmission in germanium," *Opt. Commun.* 22, 346 (1977).
9. J. S. Bessey, B. Bosacchi, H. M. van Driel, and A. L. Smirl, "Pulsewidth dependence of the transmission of ultrashort optical pulses in germanium," *Phys. Rev. B* 17, 2782 (1978).
10. W. P. Latham, Jr., A. L. Smirl, and A. Elci, "The role of phonons and plasmons in describing the pulsewidth dependence of the transmission of ultrashort optical pulses through germanium," *Solid-State Electron.* 21, 151 (1978).
11. A. Elci, A. L. Smirl, C. Y. Leung, and M. O. Scully, "Physics of ultrafast phenomena in solid-state plasmas," *Solid-State Electron.* 21, 151 (1978).
12. D. H. Auston, S. McAfee, C. V. Shank, E. P. Ippen, and O. Teschke, "Picosecond spectroscopy of semiconductors," *Solid-State Electron.* 21, 147 (1978), and S. McAfee and D. H. Auston, private communication.
13. A. L. Smirl, J. R. Lindle, and S. C. Moss, "Picosecond optical absorption at 1.06 μm and 1.55 μm in thin germanium samples at high optically-created carrier densities," *Proceedings of the Conference on Picosecond Phenomena*, 174, Springer-Verlag (1978).

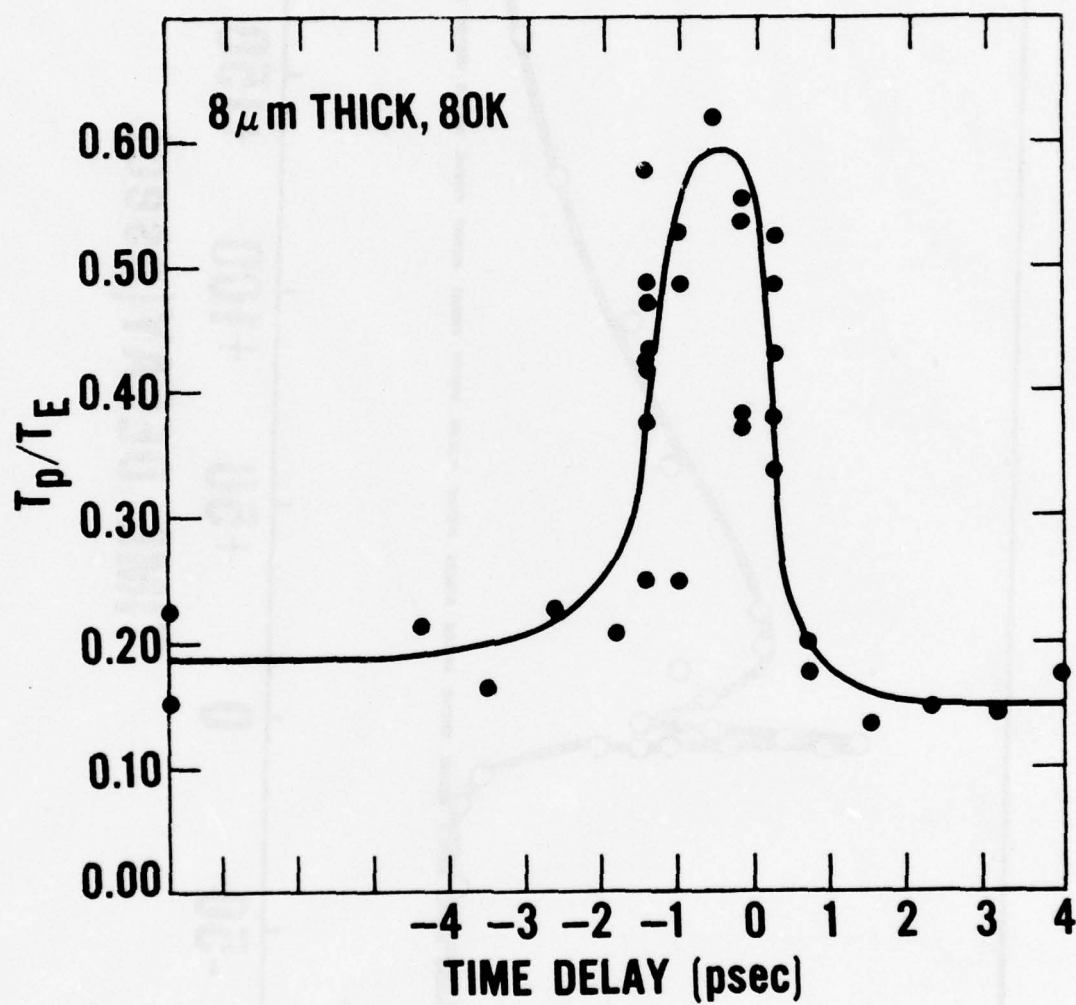
14. A. L. Smirl, J. R. Lindle, and S. C. Moss, "Picosecond optical measurement of free-carrier, intervalence-band, and indirect absorption in germanium at high optically-created carrier densities," *Phys. Rev. B* 18, 5489 (1978).
15. D. K. Ferry, "Energy-gap narrowing and state filling in semiconductors under intense laser irradiation," *Phys. Rev. B* 18, 7033 (1978).
16. H. M. van Driel, "Influence of hot phonons on carrier energy relaxation in semiconductors," to be published.
17. T. C. Y. Leung, Ph.D. dissertation, University of Arizona, 1978.
18. J. Ryan Lindle, Steven C. Moss, and Arthur L. Smirl, "The effects of parametric scattering, energy-gap narrowing, and state filling on the picosecond optical response of germanium," to be published.
19. D. von der Linde, "Ultrashort light pulses: picosecond techniques and applications," *Topics in Applied Physics*, Vol. 18, (Edited by S. L. Shapiro), Springer-Verlag, Berlin (1977).
20. C. V. Shank, E. P. Ippen, and S. L. Shapiro, "Picosecond phenomena," *Springer Series in Chemical Physics*, Vol. 4, Springer-Verlag, Berlin (1978).
21. C. V. Shank, R. L. Fork, R. F. Leheny, and Jagdeep Shah, "Dynamics of photoexcited GaAs band edge absorption with subpicosecond resolution," *Phys. Rev. Lett.* 42, 112 (1979).
22. D. von der Linde, and R. Lambrich, "Direct measurement of hot electron relaxation by picosecond spectroscopy,"

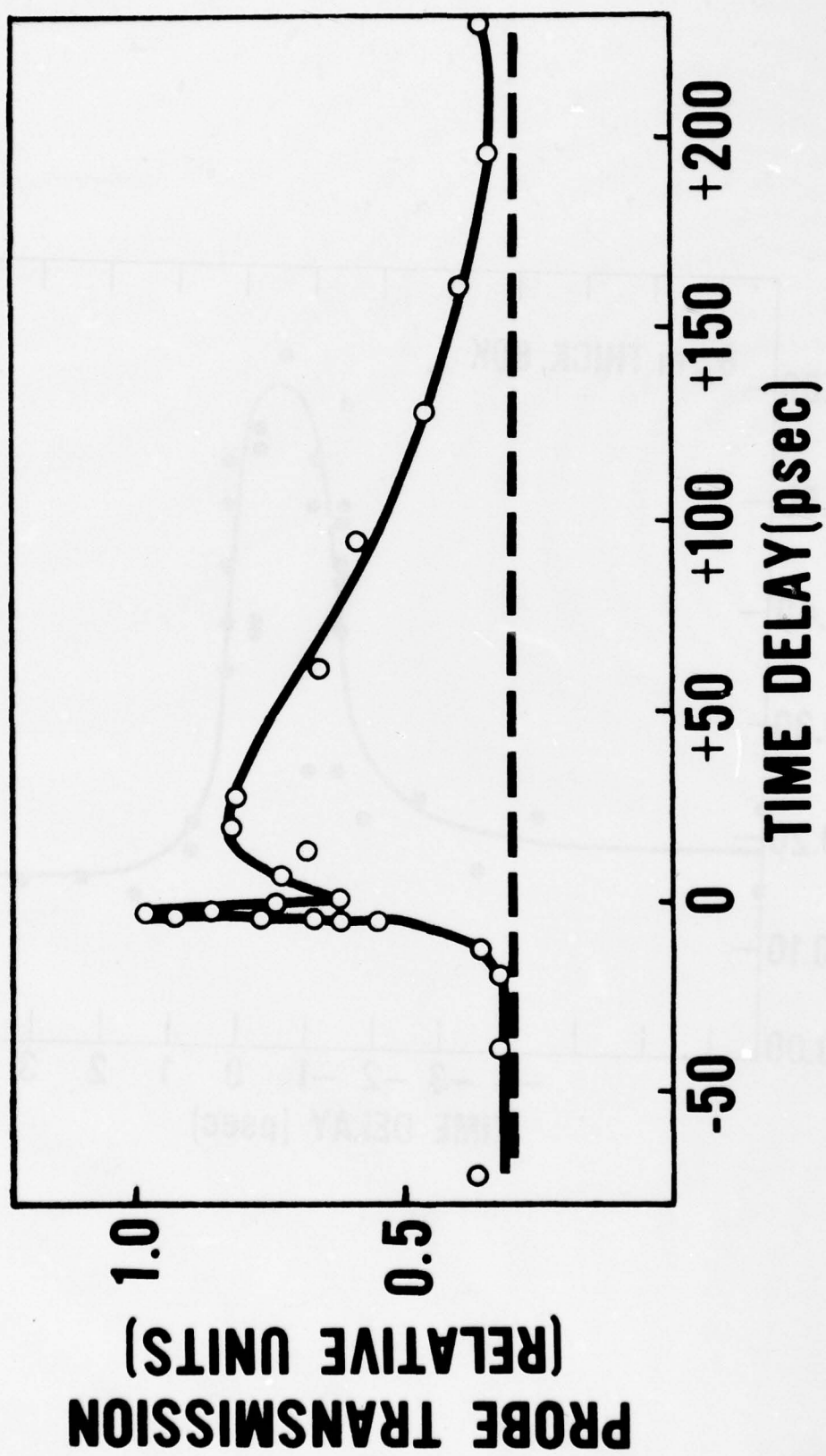
FIGURE CAPTIONS

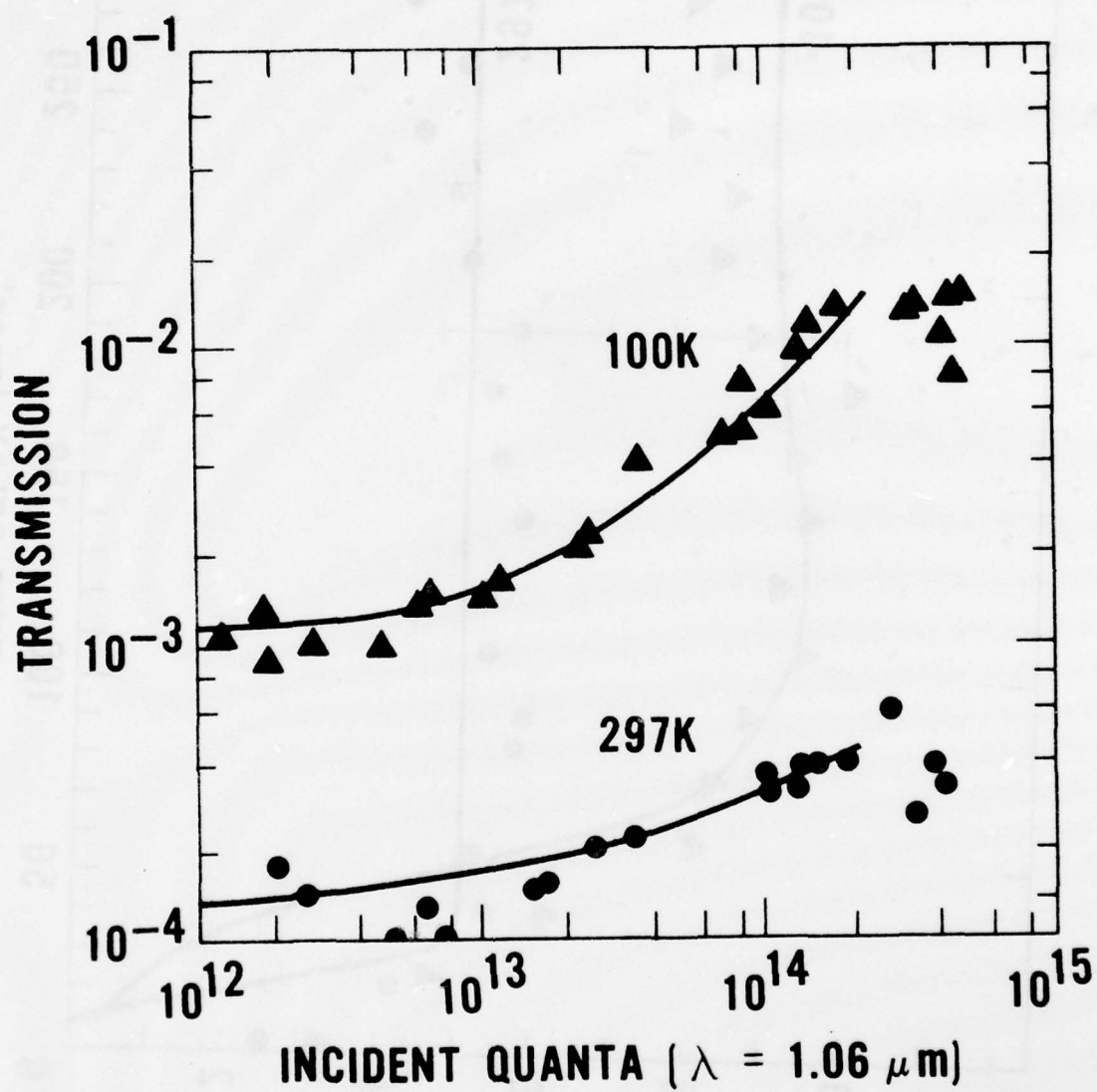
- Figure 1. Nonlinear transmission of an 8- μm -thick germanium wafer versus incident optical pulse energy at a wavelength of 1.06 μm in units of quanta (from Kennedy *et al.*¹).
- Figure 2. Probe pulse transmission versus time delay between the excite pulse at 1.06 μm and the probe pulse at 1.06 μm for a sample temperature of 80 K. The data are plotted as the normalized ratio of probe pulse transmission to excite pulse transmission T_P/T_E , in arbitrary units (from Kennedy *et al.*¹).
- Figure 3. Probe pulse transmission as a function of relative time delay between excite and probe pulses at room temperature (from Shank and Auston³).
- Figure 4. Transmission of a 5.2- μm -thick germanium sample as a function of incident quanta at 1.06 μm for sample temperatures of 100 K and 297 K. The solid lines are theoretical curves from Elci *et al.*⁷ The data are from Smirl *et al.*⁵
- Figure 5. Probe pulse transmission versus delay between the excite pulse at 1.06 μm and the probe pulse at 1.06 μm for sample temperatures of 100 and 297 K. The data are plotted as the normalized ratio of probe pulse transmission to excite pulse transmission, T_P/T_E , in arbitrary units. The solid lines are theoretical curves from Elci *et al.*⁷ The experimental data are from Smirl *et al.*⁵
- Figure 6. Instantaneous probe transmission as a function of relative time delay between probe and excite pulses for several values of the optical phonon-electron coupling constant, Q_0 (from Latham *et al.*¹⁰).
- Figure 7. Picosecond ellipsometer used to measure the time evolution of optically generated electron-hole plasmas in germanium, where PP denotes a polarizing prism, $\lambda/4$ a quarter waveplate (from Auston and Shank⁹).
- Figure 8. Ellipsometer transmission, $\Delta T_\alpha |\delta n/n|^2$, versus time delay between carrier generation by absorption of the excite pulse and probe pulse (from Auston and Shank²).
- Figure 9. Schematic diagram of experimental apparatus used for the measurement of Auger recombination. The excite pulse was at 1.06 μm and the probe, generated by stimulated Raman scattering in Benzene, was at 1.55 μm (from Auston *et al.*⁴).
- Figure 10. The change in free-carrier absorbance as a function of time delay between the excite pulse at 1.06 μm and the probe pulse at 1.55 μm for two carrier densities n_0 . Here, T_0 represents the sample transmission before excitation (from Auston *et al.*⁴).

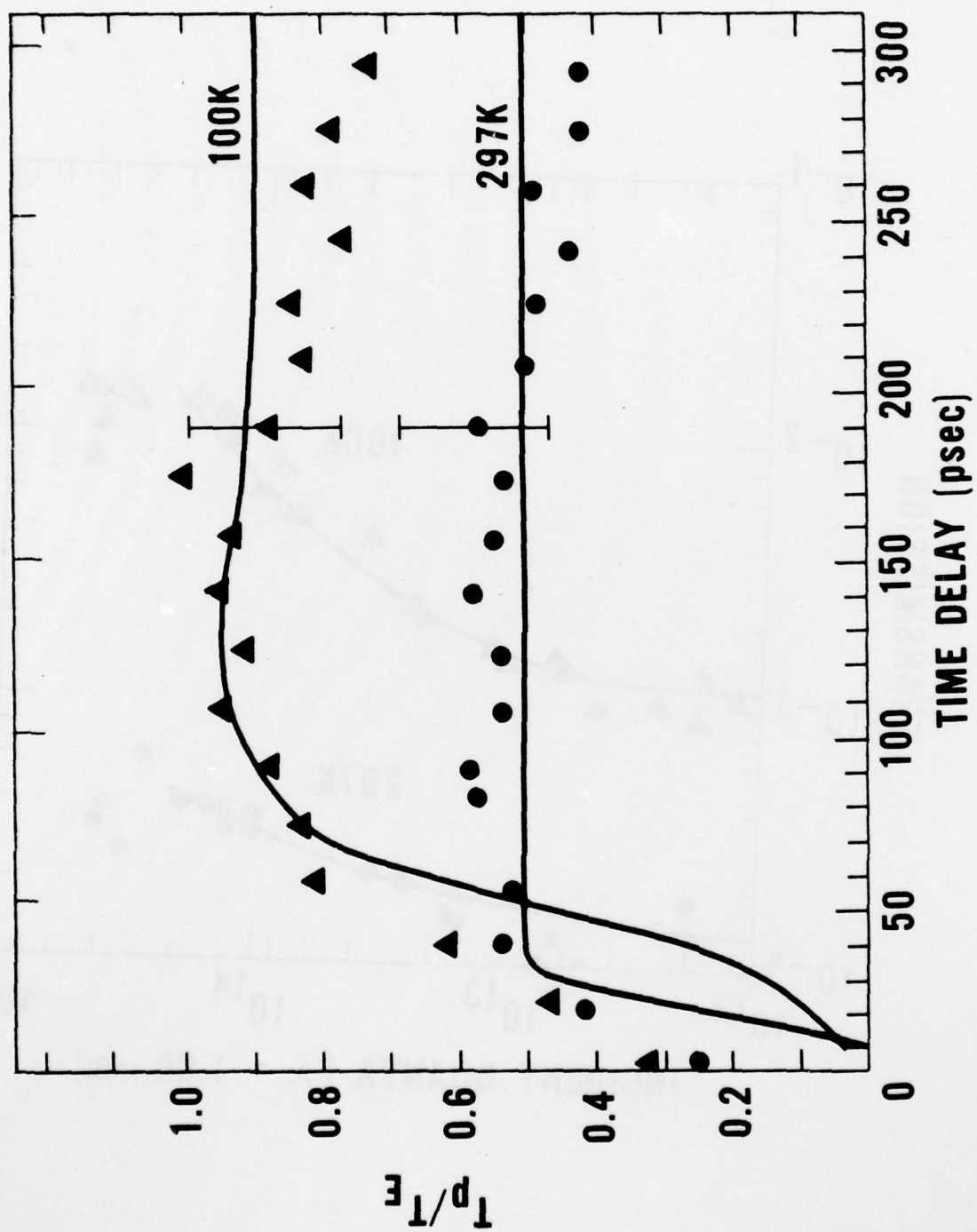
- Figure 11. Block diagram of the experimental configuration for excite and probe measurements at 1.06 and 1.55 μm , where MLL denotes the mode-locked laser, EOS the electro-optical switch, A the laser amplifier, SRS the stimulated-Raman-scattering cell, M a mirror, D a detector, L1 and L2 lens, and S the sample (from Smirl *et al.*¹⁴).
- Figure 12. Normalized probe pulse transmission in arbitrary units versus delay between the excite pulse at 1.06 μm and the probe pulse at 1.06 μm for sample temperatures of 100 and 295 K. The solid line represents a theoretical integration curve assuming Gaussian-shaped optical pulses of 10 psec width (from Smirl *et al.*¹⁴).
- Figure 13. Change in absorbance, $-\ln(T/T_0)$, of a 6- μm -thick germanium sample at 1.06 μm and 1.55 μm as a function of incident excite pulse energy at 1.06 μm , where T_0 is the linear transmission of the sample at the wavelength under consideration. Note that an excite pulse energy of 2×10^{15} quanta corresponds to an incident energy density of approximately 10^{-2}J/cm^2 (from Smirl *et al.*¹⁴).
- Figure 14. Change in probe pulse absorbance, $-\ln(T/T_0)$, versus delay between the excite pulse at 1.06 μm and the probe pulse at 1.55 μm , where T_0 is the linear transmission of the probe pulse at 1.55 μm (from Smirl *et al.*¹⁴).
- Figure 15. Schematic diagram illustrating the relaxation of hot electrons by the emission of optical phonons and the subsequent decay of the optical phonons into acoustic phonons (from van Driel¹⁶).
- Figure 16. Probe pulse transmission versus delay between the excite pulse at 1.06 μm and the probe pulse at 1.06 μm for sample temperatures of 100 and 297 K. The data are plotted as the normalized ratio of probe pulse transmission to excite pulse transmission, T_p/T_e , in arbitrary units. The dashed lines are theoretical curves from Elci *et al.*⁷ The solid lines are theoretical curves from van Driel¹⁶. The experimental data are from Smirl *et al.*⁵
- Figure 17. The spatial variation of the carrier density as a function of longitudinal position z and time after excitation in a 5.2 μm -thick germanium sample (from Leung¹⁷).
- Figure 18. Schematic of the diffusion process (from Elci *et al.*¹¹).
- Figure 19. Probe pulse transmission, in arbitrary units, as a function of relative time delay between the excite pulse at 1.06 μm and the probe pulse at 1.06 μm for sample temperatures of 100 K and 298 K. The experimental data are from Smirl *et al.*⁵ The solid lines are theoretical curves from Leung¹⁷.

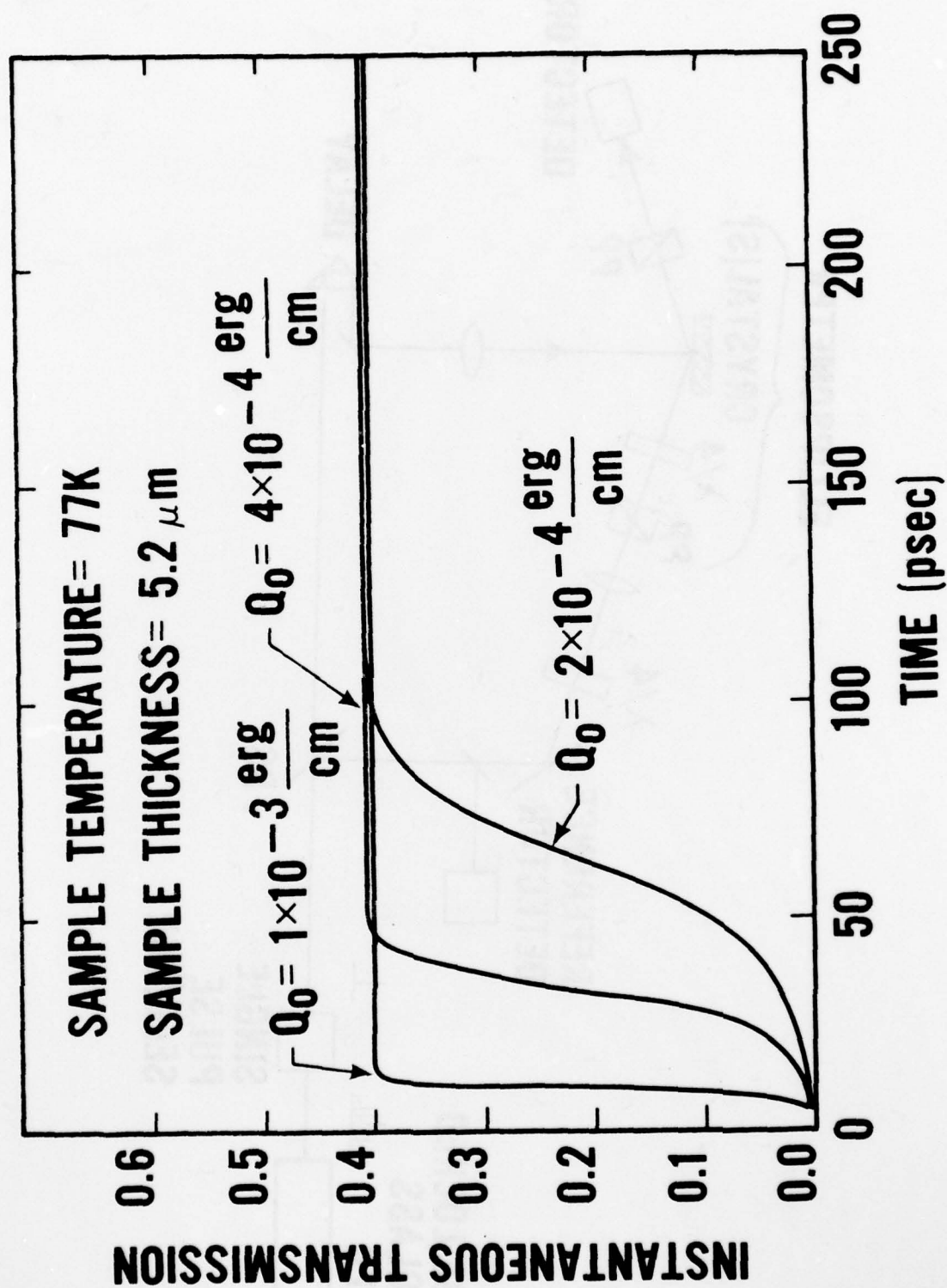


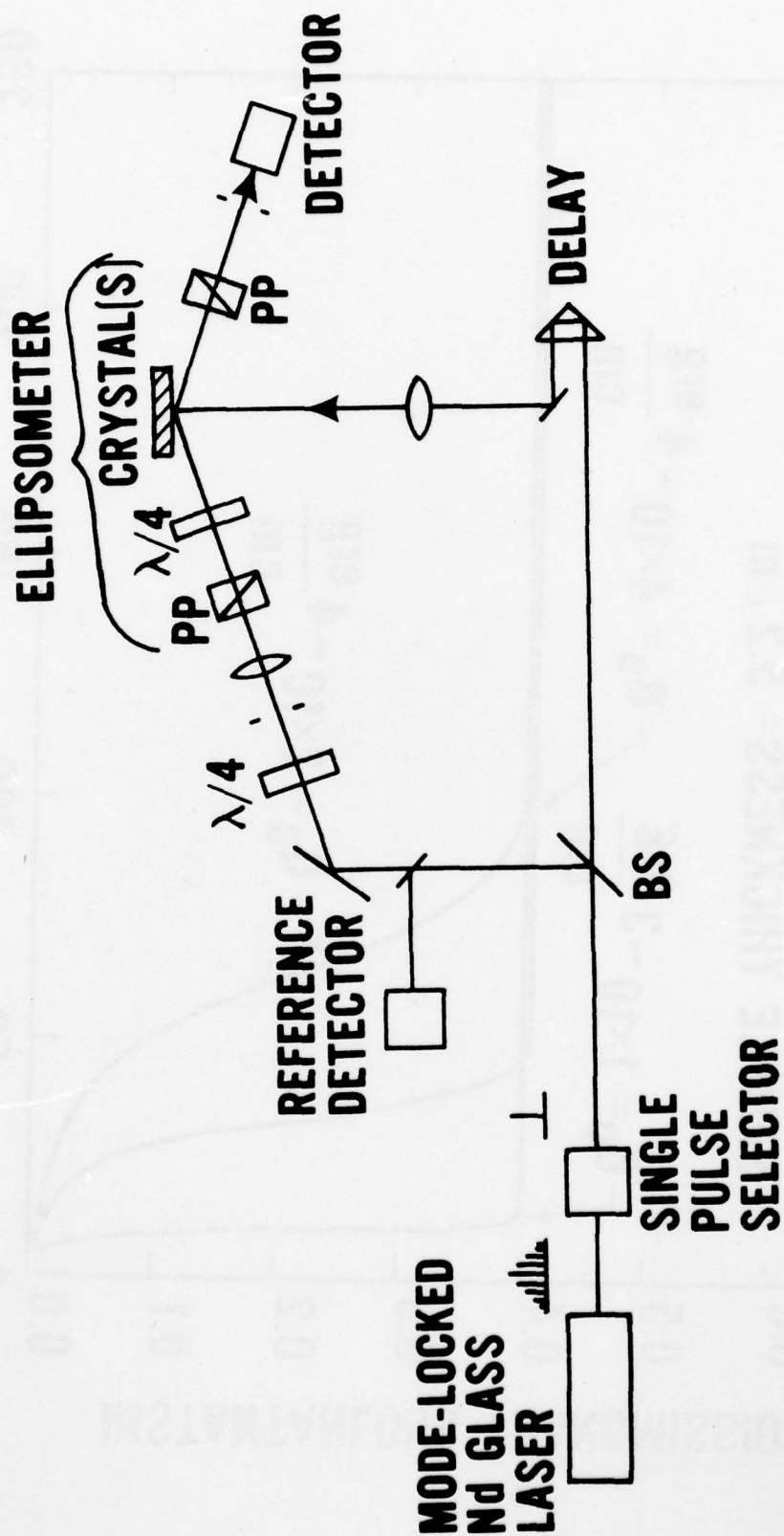


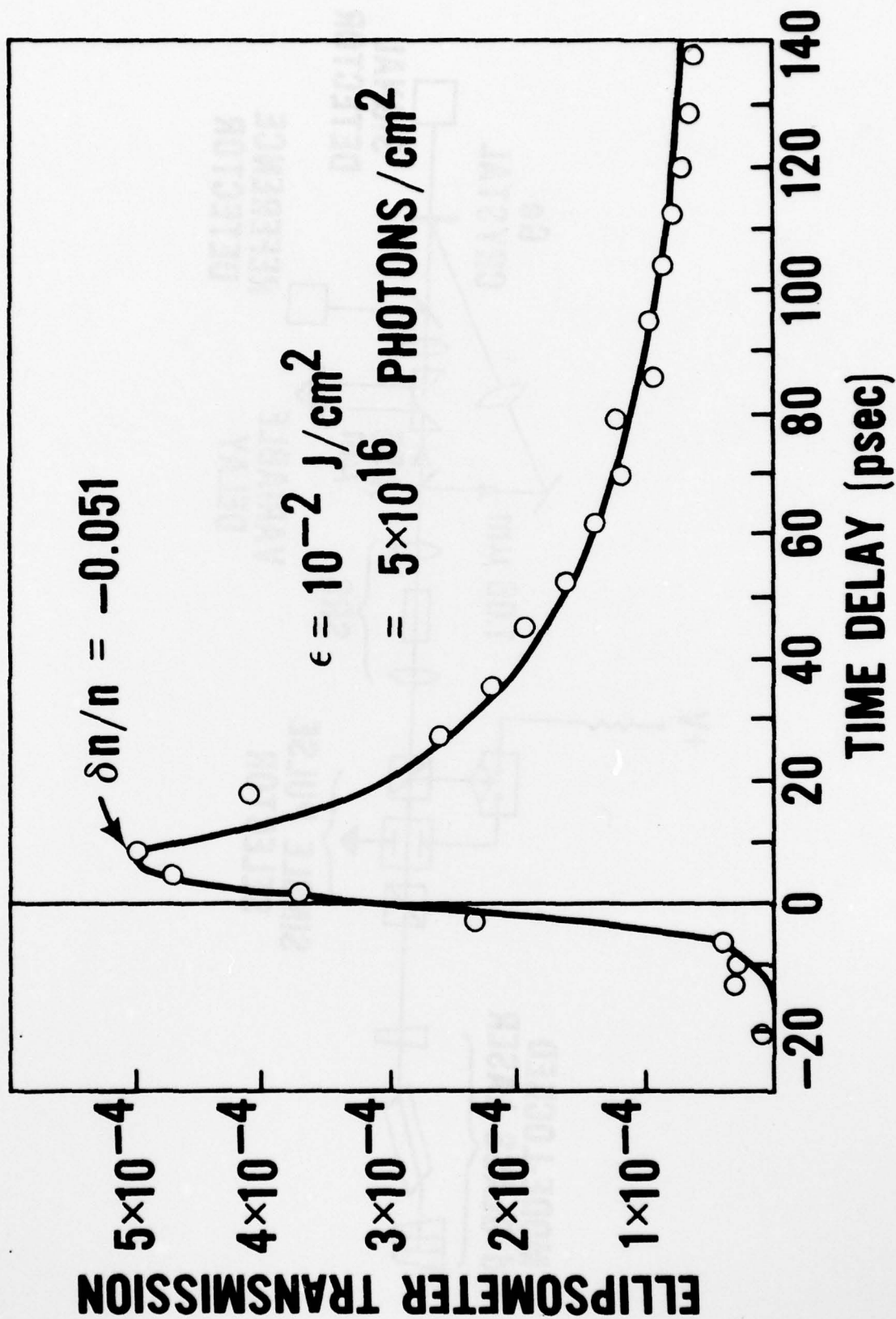


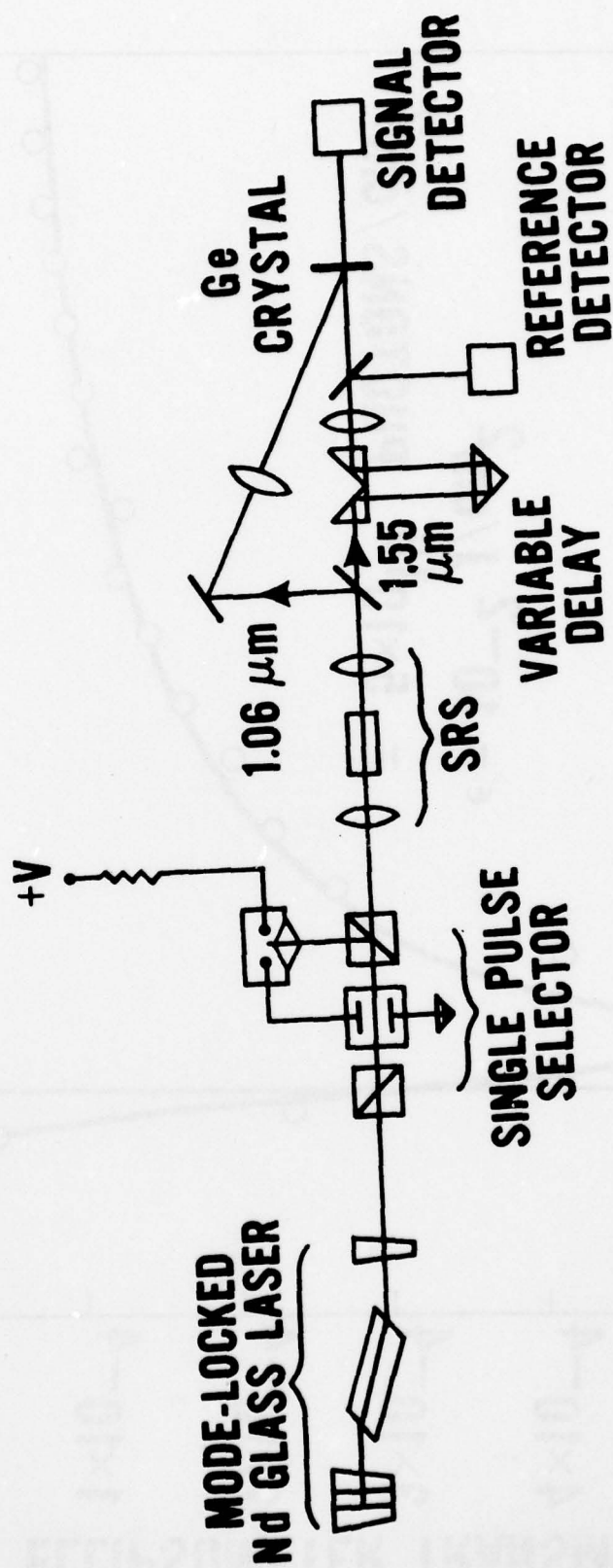


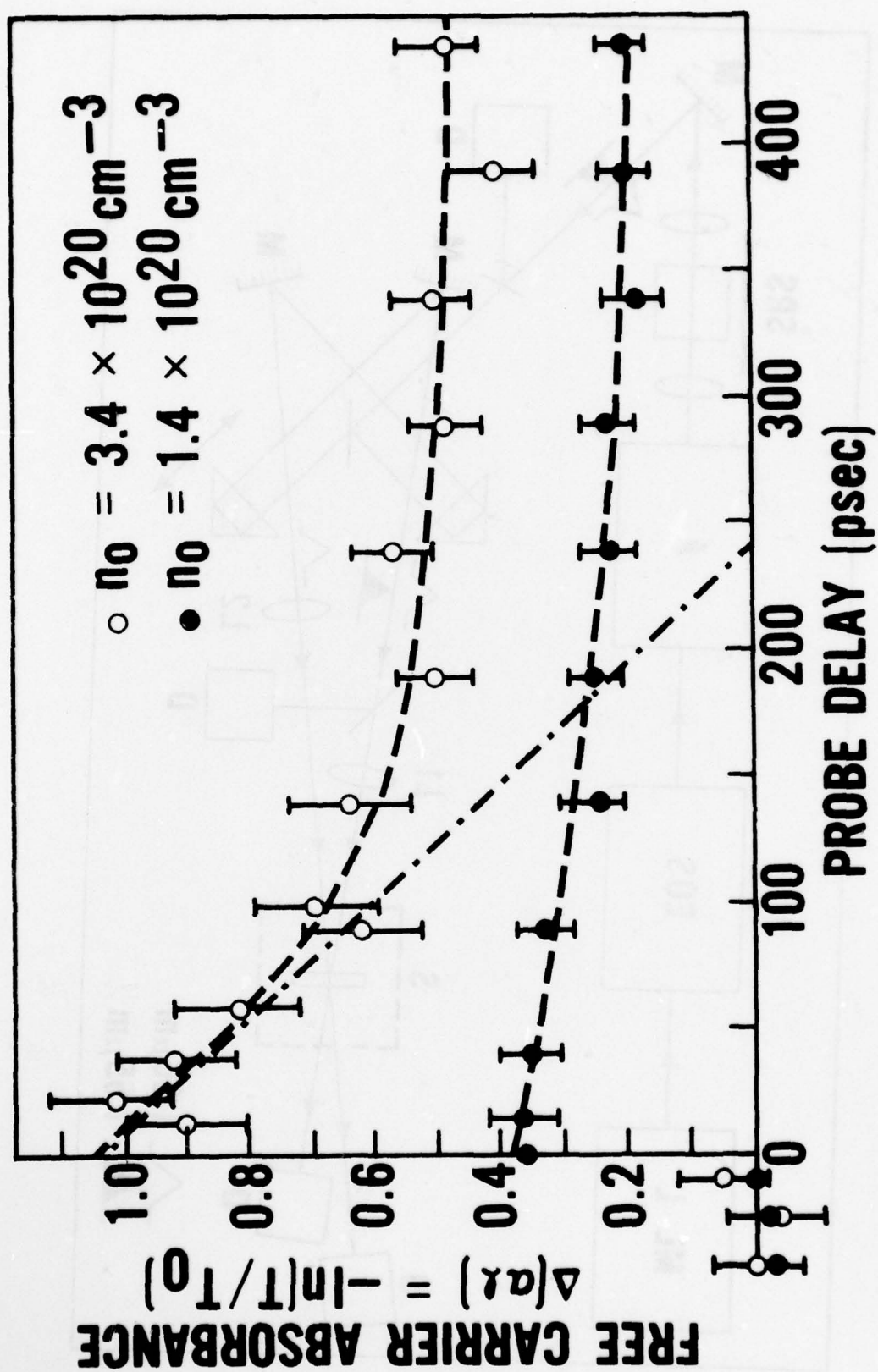


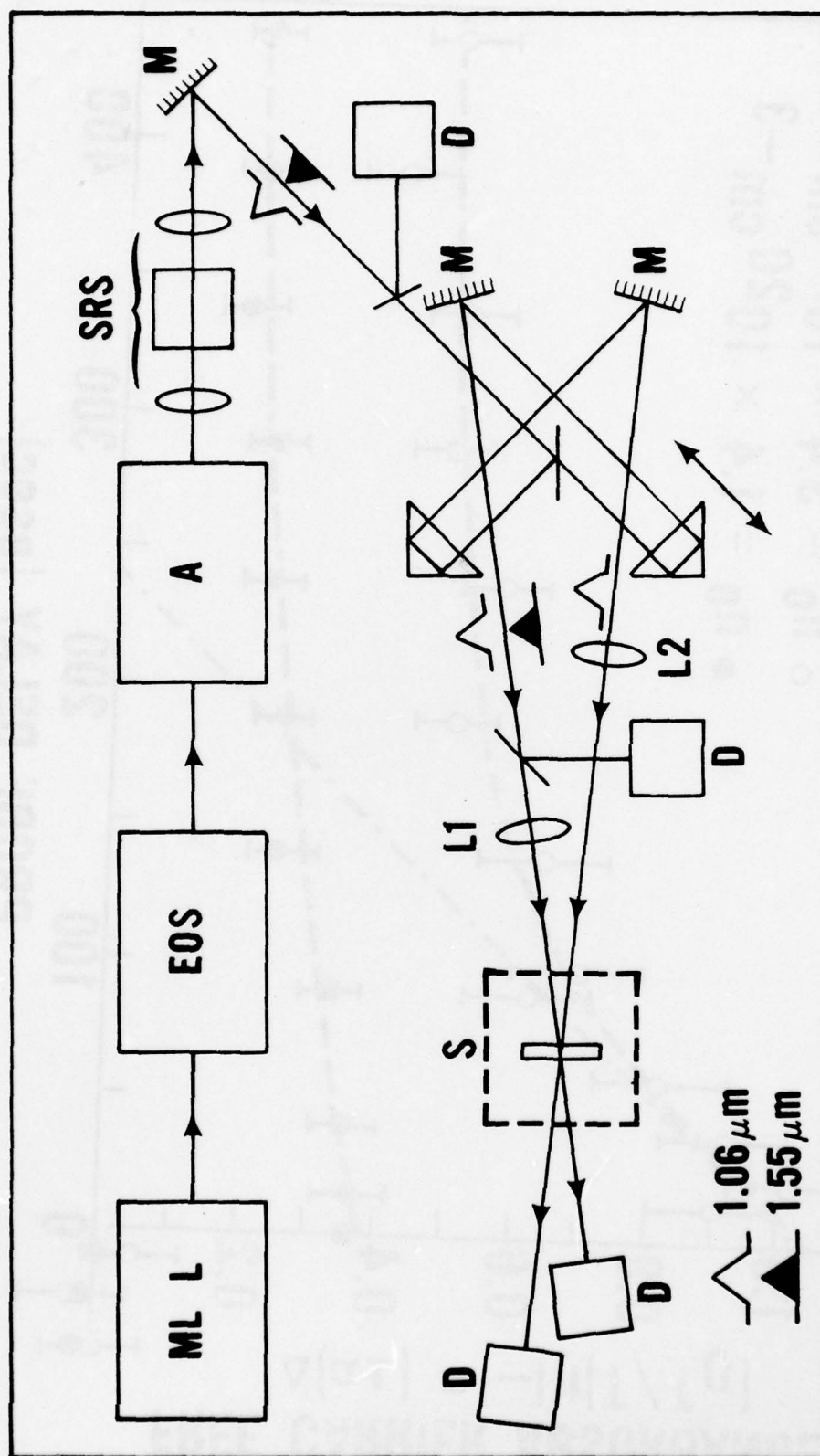


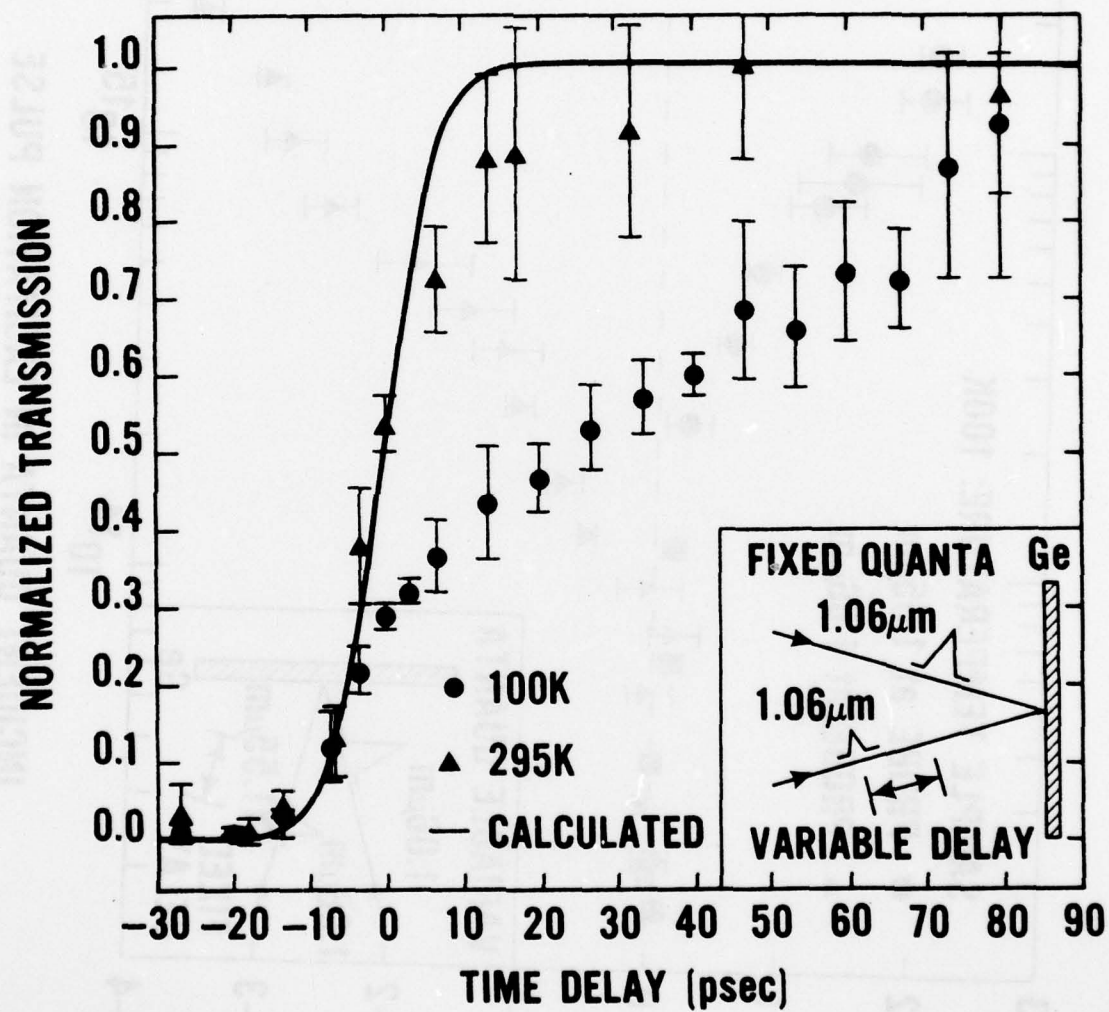


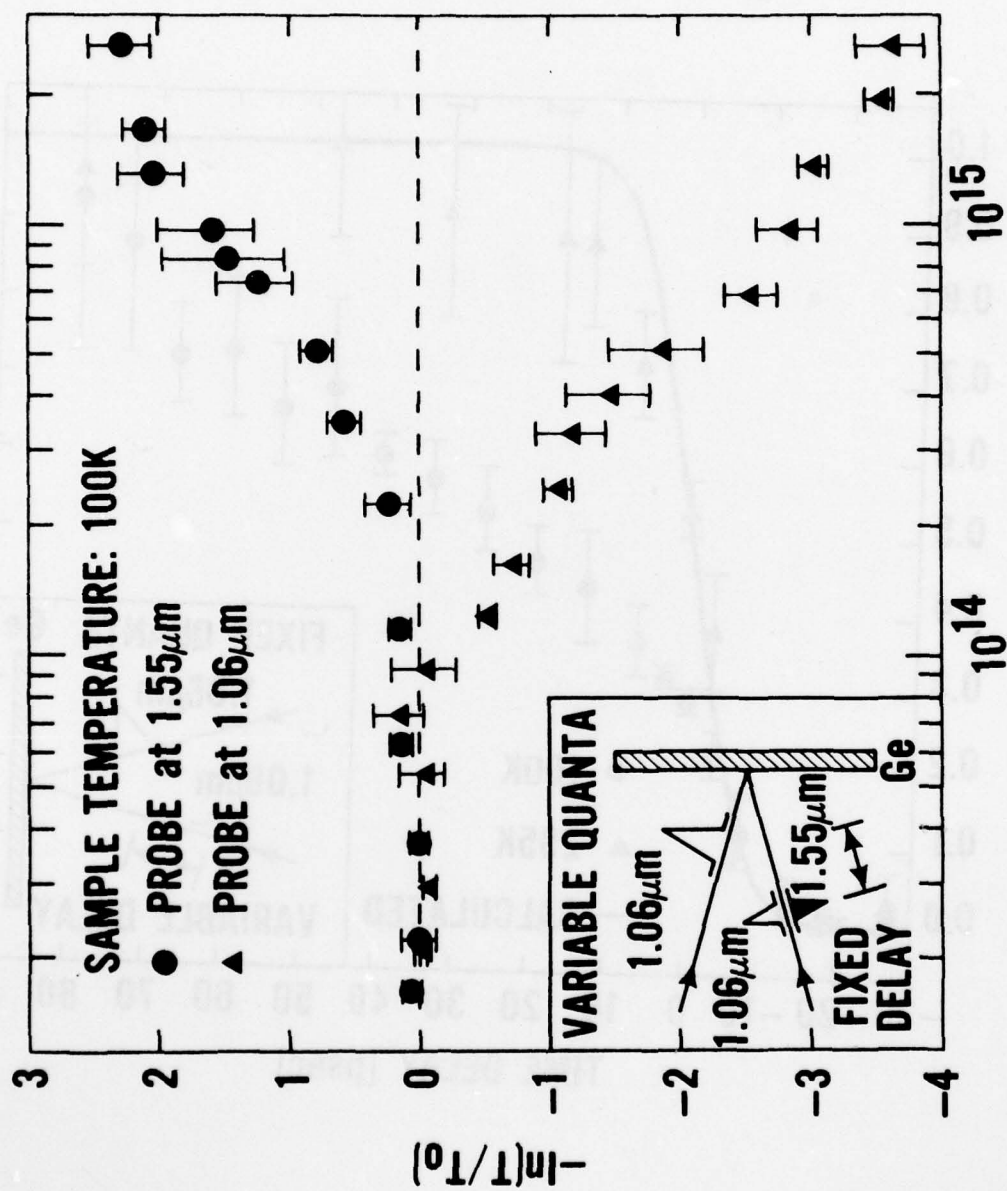


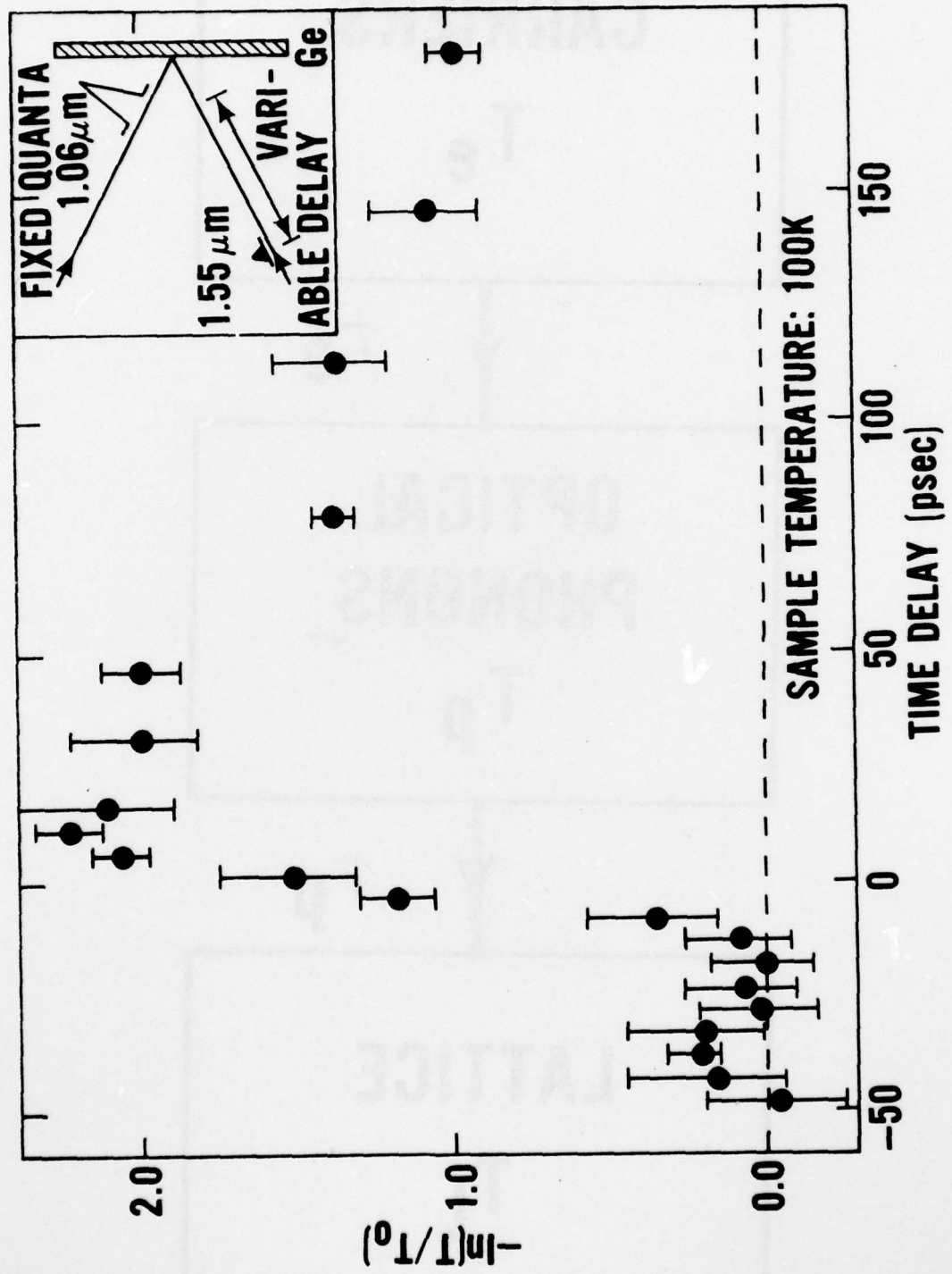


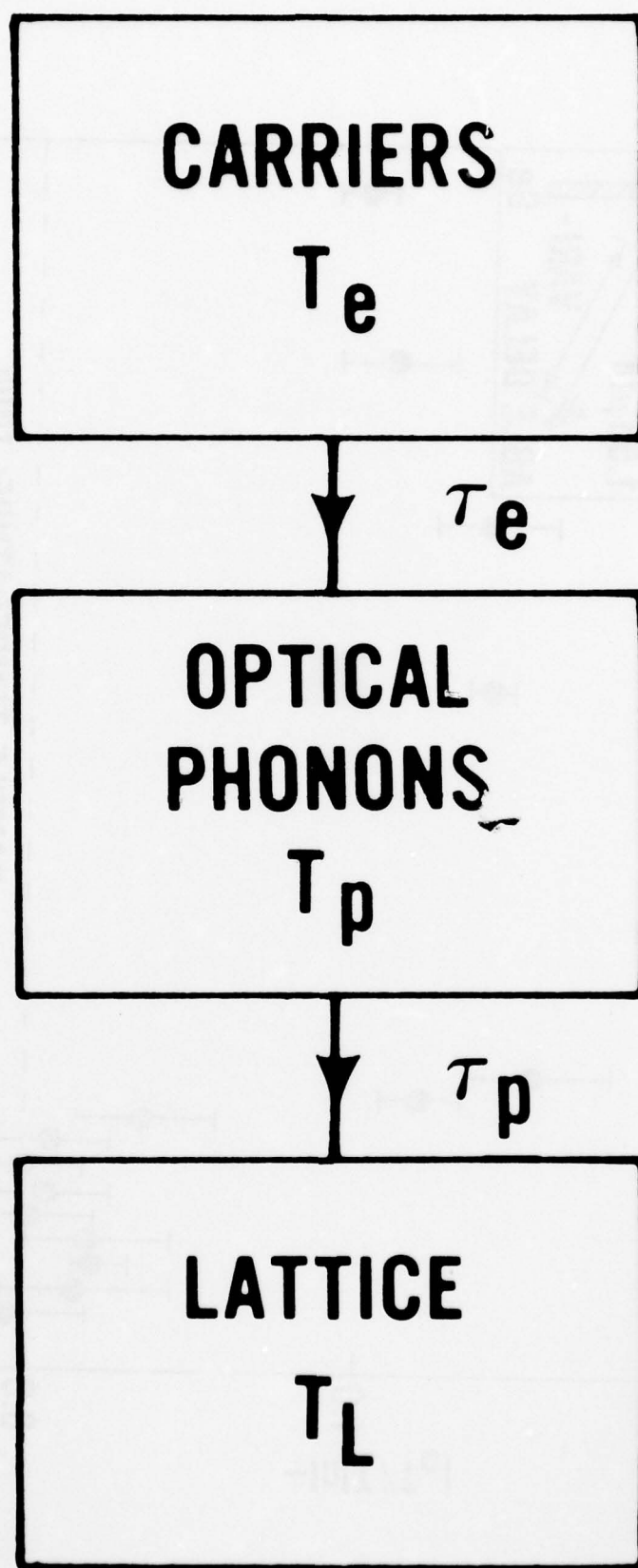


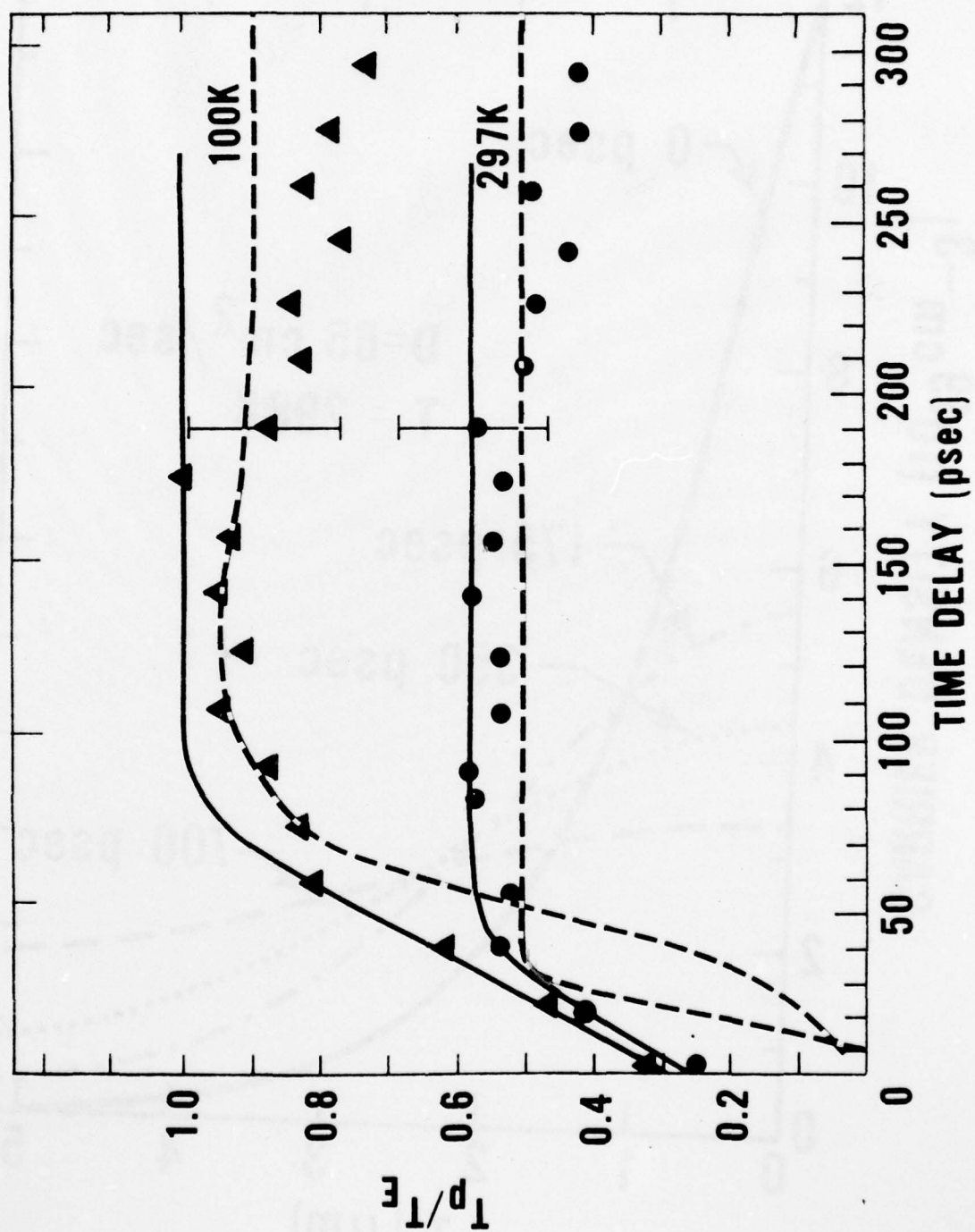


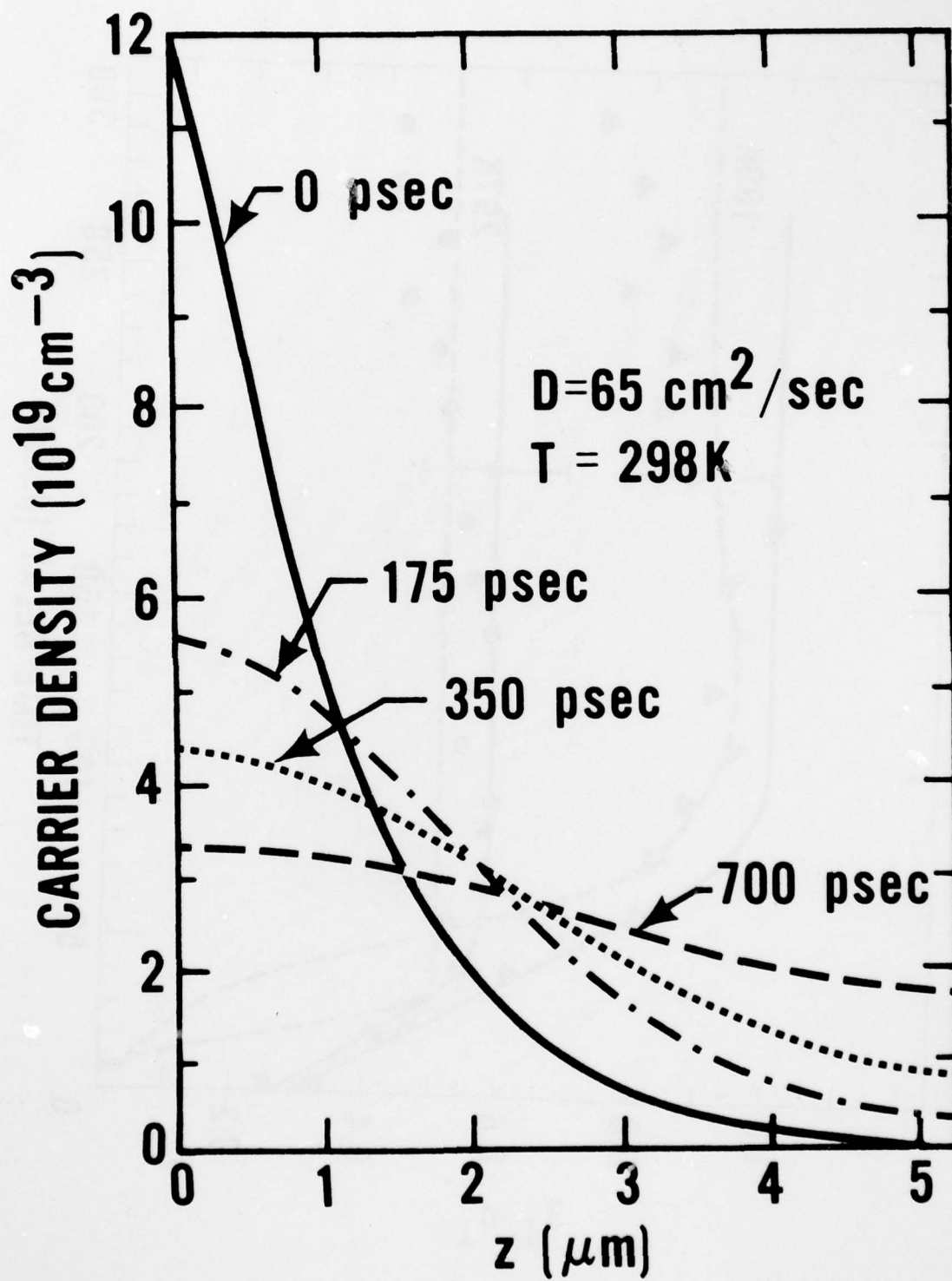












AD-A073 920

NORTH TEXAS STATE UNIV DENTON DEPT OF PHYSICS
OPTICALLY INDUCED HOT ELECTRON EFFECTS IN SEMICONDUCTORS.(U)
JUN 78 A L SMIRL

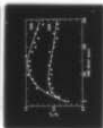
F/G 20/12

N00014-76-C-1077

UNCLASSIFIED

3 of 3

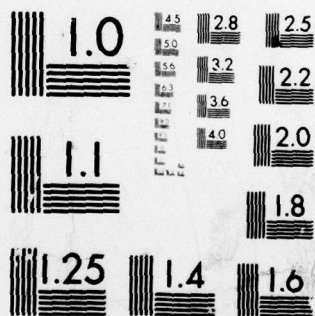
AD
A073920



END
DATE
FILMED

10-19

DDC



MICROCOPY RESOLUTION TEST CHART
NATIONAL BUREAU OF STANDARDS-1963-A

BACK SURFACE

FRONT SURFACE

